Comparative phylogeography of small mammals across the Great Plains Suture Zone highlights repeated processes of speciation and community assembly coincident with the 100th meridian

by

Thomas M. Herrera

B.S., Kansas State University, 2021

A THESIS

submitted in partial fulfillment of the requirements for the degree

MASTER OF SCIENCE

Division of Biology
College of Arts and Sciences

KANSAS STATE UNIVERSITY
Manhattan, Kansas

2022

Approved by:

Major Professor
Andrew Hope

Copyright

Abstract

Accelerating anthropogenetic environmental change is globally impacting species' distributions, resulting in altered eco-evolutionary trajectories with the potential to cause severe disruption to ecosystem stability and human health. Ameliorating impacts of biotic turnover requires management of species as well as their interactions. Therefore, it is crucial to understand how past environmental change influenced the evolutionary history of species and regional assemblages. The Great Plains presents a novel system for diagnosing both evolutionary histories and community assembly of North American mammals.

By encompassing the middle third of North America, the Great Plains supports mammal faunas from both western and eastern communities, which meet at the peripheries of their ranges, providing insight towardsinto the ecological history of multiple communities through evolutionary time. With no physical barriers and geographic complexity, it is an unexplored but ideal region for understanding evolutionary and ecological histories driven almost solely by environmental change. I couple comparative phylogeography with ecological niche models to investigate the evolutionary history of ten small mammal species that belong to eastern, central, and western assemblages co-distributed across the Great Plains. I assess (1) intraspecific diversification across the Great Plains, (2) congruence of species histories considering regional origins, and (3) the location of regional biodiversity hotspots for both historic and emerging eco-evolutionary interactions. Bayesian phylogenies were estimated from mitochondrial DNA, and Last Glacial Maximum (LGM) niche models were estimated using bioclimatic layers. Given the diverse number of biogeographic contact zones associated with the Great Plains suture zone, I hypothesized species would possess a shared history across the Great Plains regardless of regional and ecological associations. Intra-specific phylogeographic breaks based on current

distributions showed broad-scale clustering in the southern Great Plains for eastern, central, and western species. LGM niche models showed that Great Plains small mammals with different regional origins occupied distinct refugia but with a region of contact between assemblages maintained in the southern Great Plains. The combined evidence suggests the southern Great Plains is a hotspot for both diversification within species and long-term interactions among distinct communities and points towards repeatable environmental processes across the Great Plains Suture Zone reciprocally driving diversification and assembly through time.

Tables of Contents

List of Figures

List of Tables

Acknowledgments

I would like to start by acknowledging the Indigenous peoples who once resided across the lands used in this project for field sampling. Sampling sites across Kansas were on land belonging to the Arapahoe, Comanche, Kaw, Kickapoo, Kiowa, and Pawnee peoples. Sites used across Manitoba were on land belonging to the Cree, Ojibway, and Dakota peoples. Finally, locations across the Rio Grande Valley of southern Texas were on land belonging to the Lipan Apache and Coahuiltecan peoples.

I would not have gotten here without the support of my advisor, Dr. Andrew Hope. When I was an undergraduate, he introduced me to the work I now hold a deep passion for. And during my four years under his guidance, Dr. Hope provided me with the experience and capability to pursue that passion as a career. Words cannot describe my gratitude for what he has given me. I want to thank both members of my graduate committee, Michi Tobler and Sean Maher. Their guidance and insight have been crucial to developing this thesis and my growth as an evolutionary and environmental biologist. Additionally, I want to thank Dr. Fraser Combe, who guided me through the realm of bioinformatics and programming languages.

I would like to thank the Hope Lab for all their hard work in both the field and the lab. And for being the best group of friends, someone could ask for. Thank you, Litsa, Mary, Kailey, Ben, and Tommy for all the beautiful memories you have given me.

The multi-species framework of this thesis was made possible by the countless contributions of others towards field sampling and genetic assessment of each of the ten species included. Thank you to all for your pioneering work. Also, a special thank you to Dr. Robert Wrigley and the pivotal role he played in getting access to field sites across Manitoba, Canada.

Sampling across Kansas was funded by the Kansas Department of Wildlife and Parks through the Chickadee Checkoff Small Grant Program. Financial support for my project was also provided by the American Society of Mammalogists, the Central Plains Society of Mammalogists, and the Konza Prarie Long Term Ecological Research Program.

A warm thanks to the McNair Scholars Program and the Developing Scholars Program for supporting me during my time as both an undergraduate and graduate student at Kansas State University and for accelerating my growth as an academic.

Lastly, thank you to my family for always supporting me in everything I do. I owe all accomplishments to my parents, who worked tirelessly to provide the opportunities that have gotten me where I am.

Introduction

Given that ongoing environmental changes are globally impacting the evolutionary trajectories and ecological interactions of biodiversity (Parmesan, 2006; Rosenzweig et al., 2007; Walther et al., 2002), pushing towards a multi-species framework for managing ecological stability across broad spatial scales as opposed to individual taxa is a mechanism for keeping pace with rapid rates of change and corresponding responses of millions of species, many of which are undescribed (Berg et al., 2010; Brooks & Hoberg, 2007; Grumbine, 1994; Kareiva et al., 1993; Montoya & Raffaelli, 2010; Ricklefs, 1987; Ricklefs & Jenkins, 2011; Schmitz et al., 2003; Tylianakis et al., 2008). However, a crucial prerequisite for up-scaling management efforts to entire assemblages and ecosystems still lacking is knowledge of the responses that species both collectively and individualistically exhibit to broad-scale environmental changes (Mooney, 1991; Violle et al., 2014). Historical biogeography (changing spatial associations of species across evolutionary timescales) offers the opportunity to assess past responses of biota to long-term global environmental change and test whether current community structure represents a stable state or ephemeral dynamics through time (Gerhold et al., 2015; Parmesan & Yohe, 2003).

Temperate grassland is the biome most heavily impacted by habitat fragmentation and habitat loss (Jacobson et al., 2019), and the biota native to these regions have experienced more decline than any other (Newbold et al., 2016). The Great Plains of North America has in recent timeframes (Holocene; the last several thousand years) been a vast system of temperate grasslands that separates western arid and eastern mesic ecosystems across a significant longitudinal gradient of precipitation (Ricketts et al., 1999; Rosenberg, 1987) expected to dramatically shift in future decades (Kunkel et al., 2013). The Great Plains currently represents the largest terrestrial region on the earth experiencing a critical loss of native biota concerning

both species abundance and richness (Newbold et al., 2016). Unlike other biomes across North America, which often possess regionally and ecologically distinct assemblages of fauna and flora, the Great Plains is a region of multi-assemblage interaction as its continentally centralized location often signifies the range periphery for inhabiting biotas that are otherwise associated with neighboring ecosystems (Ricketts et al., 1999). The eco-evolutionary history of these modern interactions has significant implications for predicting responses to global change. For instance, through the central Great Plains of Kansas, small mammals experience contact between northern, southern, western, and eastern assemblages, and this region is recognized as a global epicenter for emerging zoonotic diseases from rodent reservoirs (Han et al., 2015). However, climatic and landscape drivers of faunal community assembly across the Great Plains remain poorly understood. In part, this is due to widespread anthropogenic habitat changes that include extensive changes in the dominant habitat types, including fragmentation of native grassland habitats and expansion of woody habitats, the latter especially from the east (Coppedge et al., 2001; Symstad & Leis, 2017). Part of the reason for such complexity stems from 1) that the Great Plains are relatively homogeneous with respect to physical geography and yet the distributional extent of prevailing grassland habitats have fluctuated dramatically through the Pleistocene (the last ~2.6 million years [Myr]; Cotton et al., 2016; Fox & Koch, 2003; Koch et al., 2004; Still et al., 2019), and 2) much of the eastern Great Plains represents a region of alternative stable states, meaning that multiple distinct vegetative communities (and their associated faunal communities) might exist within the same climatic envelope, depending on environmental contingencies (Collins et al., 2021; Epstein et al., 1996; Epstein et al., 1997; Hargrove & Hoffman, 2004; Klemm et al., 2020; Küchler, 1970; Martin & Hoffmann, 1987; Ratajczak et al. 2014; Wang et al., 2013). As such, this raises the question: Does a snapshot of

faunal communities across the Great Plains reflect long-term assembly (even given multiple alternative vegetative communities) or recent and fluctuating associations among previously discrete assemblages?

For my thesis, I investigate how Pleistocene environmental change has shaped the intra-specific diversification and community assembly of North American small mammals across the Great Plains. In so doing, I establish a predictive framework for emerging eco-evolutionary interactions of North American biodiversity. My research integrates a phylogeographic toolset in order to perform both hindcast ecological niche modeling and comparative evolutionary analyses across deep timescales to 1) assess congruence of responses, including both repeated intra-specific diversification and inter-specific biogeographic responses to long-term climate fluctuations, among multiple co-distributed species and 2) identify regions of particular importance that might be considered as hotspots of eco-evolutionary interactions between species. Ultimately, my research provides the first detailed historical biogeographic assessment of Great Plains terrestrial mammal responses to changing environments that may inform both future conservation and more in-depth assessment of modern community dynamics from both ecological and evolutionary perspectives.

The Pleistocene is an epoch defined by rapid shifts in global temperatures cycling between glacial and interglacial climate phases (with a periodicity of ~100 thousand years [kyr] through the last 800 kyr) exceeding 10°C shifts in temperate regions (Dansgaard et al., 1993; Petit et al., 1999), with a global impact on the distribution and diversity of species (Davis et al., 2013; Dupont et al., 2001; G. Hewitt, 1996; Hope et al., 2010; Pandolfi, 1999; Vuilleumier, 1971). In comparison, we are now within an interglacial warm phase, and global temperatures are forecast to experience a further 1.9-8.5°C increase expected by the year 2100 (*IPCC Sixth*

Assessment Report, 2021). The upper extreme of these predictions would surpass all global temperature records through the entire Pleistocene, and current rates of change are potentially faster than many species' ability to respond, through either distributional change or adaptive change (Berg et al., 2010; Davis & Shaw, 2001; Hoffmann & Sgrò, 2011).

If we assume niche conservatism (that the Grinnellian ecological niche remains constant for species across evolutionary time-scales), then we would expect a distributional change in response to global climate trends to be concordant across species within a given regional community (Bruno et al., 2003; Freestone, 2006; Walther et al., 2002). Alternatively, differences in natural histories suggest species may respond independently to different combinations of climatic variables coupled with species-specific ecological associations to a myriad of other potential abiotic and biotic factors (Gleason, 1939; Le Roux & McGeoch, 2008; Lurgi et al., 2012; Williams & Jackson, 2007). Yet, given ecological variation across both spatial and temporal scales, acknowledging individual species responses to shared processes across a continuum of collective and individualistic responses can help characterize the complexity of historic community dynamics and elucidate the eco-evolutionary context of current biogeographic patterns (Brooker et al., 2008; Goodall, 1963). Similarly, in distinguishing between the role of climatic and geographic drivers of current biogeographic patterns, phylogeographic history is best perceived acting across a continuum of 'hard' and 'soft' allopatric processes (Pyron & Burbrink, 2010). Hard allopatry refers to strict vicariance facilitated by physical landscape features that pose a discrete barrier to otherwise suitable areas (e.g., mountain range, Soltis et al., 2006), whereas, soft allopatry refers to vicariance facilitated by shifts in ecologically suitable areas where fragmentation results from species' intrinsic physiological and ecological responses to dynamic environmental gradients. Distributional shifts

resulting from both historic and future changes are inherently associated with evolutionary change within species and ecological differences between species (Avise, 1998). Such changes may include homogenization of biodiversity, new ecological interactions of lineages within species, between species of a given community, or between species of different communities, and likely will result in altered evolutionary trajectories (Breshears et al., 2005; Dornelas et al., 2014; McKinney & Lockwood, 1999; Woolhouse et al., 2005).

During the Pleistocene, North American biodiversity experienced periodic range shifts accompanied by fragmentation into distinct refugia and subsequent expansion as physical geography was dramatically altered by continental ice sheets, fluctuating sea-levels, and diverse barriers to dispersal (Brant & Ortí, 2003; Petit et al., 1999); The cyclic nature of Pleistocene climate regimes repeatedly acting on biotic distributions in the same manner through time resulted in regional hotspots of secondary contact and novel intra- and interspecific interactions (particularly with respect to gene flow) called suture zones (Remington, 1968; Rissler & Smith, 2010; Swenson, 2006; Swenson & Howard, 2005). In the absence of isolating barriers, biodiversity should have maintained the ability to track climate through distributional change, whereas more complex geography such as through the intermountain west of North America would have led to more pronounced signals of biogeographic concordance (Lanier et al., 2015; Schmitt, 2007; Soltis et al., 2006). In both situations, there should be potential for shared responses among co-distributed species, but with different evolutionary outcomes associated with geographic complexity and species-specific traits. However, regions defined by discrete geographic barriers, where biogeographic patterns are often more discernable, have classically received more attention, from a comparative perspective, than regions positioned across environmental gradients and ecotones (Swenson, 2013). The Great Plains Suture Zone is one of

the first established and supported suture zones in North America (Remington, 1968; Swenson & Howard, 2005), and despite occurring across an otherwise topographically homogenous region, it continues to represent one of the most pervasive zones of contact among North American biodiversity.

The 100th meridian signifies the western limit of the zone of alternate stable states for major biomes in North America (Hargrove & Hoffman, 2004; Salley et al., 2016b). John Wesley Powell's report on the arid regions of the U.S. declared the 100th meridian as the transition from eastern temperate to western arid conditions based on the 20-inch (50.8cm) longitudinal isohyet (Powell et al., 1879). While the "Powell Line" failed to consider factors such as temperature and seasonality (Hoerling et al., 2014), it is still geographically coincident with the westward extent of moist air from the Gulf (Cook et al., 2007; Forman et al., 2001; Kunkel et al., 2013; Rosenberg, 1987), and the transition between major soil types (Marbut, 1935). Nearly a century passed until the 100th meridian environmental transition's impact on North American biodiversity was evaluated. Remington (1968) identified what he called the Central Texas suture zone based on the clustering of faunal and floral hybrid zones in the southern Great Plains. Küchler (1970) identified what he called the Tatschl Line after observing a concordant east and west contact zone between flora and mammal communities across Kansas that was spatially conserved across mammalian fauna through the Pleistocene (Martin & Hoffmann, 1987). While little attention was placed on the Central Texas suture zone and Tatschl Line as major components of North America biogeography following their delineation, numerous intraspecific contact zones (García et al., 2017; McDonough & Ferguson, 2020; Reding et al., 2012, 2021; Swenson & Howard, 2005), interspecific contact zones (Allen, 1990; Bock et al., 1977; E. R. (Eugene R. Hall, 1981; Lovette, 2005; Martin & Hoffmann, 1987; Mengel, 1970; Rising, 1983;

Root et al., 1981), and hybrid zones (Carling et al., 2011; Dixon, 1989; Emlen et al., 1975; Remington, 1968; Rising, 1969, 1970; Swenson, 2006; Swenson & Howard, 2005; Szijj, 1966) among both continentally and regionally distributed flora and fauna have been identified to be coincident with the 100th meridian, supporting its formal distinction as the Great Plains Suture Zone.

Empirical isotope data of megafaunal mammal grazers, coupled with hindcast niche models of C4 plants that dominate the Great Plains today, suggests that Last Glacial Maximum (LGM; ~18 kya) conditions pushed grassland habitats southward during glacial phases to occupy a more limited distribution in southwestern, -central, and -eastern refugia coincident with latitudes of western Mexico, southern Texas, and Florida, with additional isolated refugia further south in Mexico (Still et al., 2019). The question remains whether fauna associated with the Great Plains Suture Zone (associated with the peripheries of both grasslands and eastern forests) were shunted southward in concert, maintaining at least partial connections between different ecological assemblages, or if grassland and eastern forest species were repeatedly isolated and reconnected through the Pleistocene, with implications for shared versus allopatric evolutionary histories.

The relationship of ecological and evolutionary processes and their reciprocal impacts on community dynamics have classically been a point of contingency (Johnson & Stinchcombe, 2007) as the environmental factors that best describe observed patterns in biodiversity are largely scale dependent (Dansgaard et al., 1993). Evolutionary mechanisms of differentiation include drift, selection, and gene flow (Ottenburghs et al., 2019). Ecological interactions, including competition and resource partitioning, drive levels of co-occurrence across fine spatial scales, and where local adaptation may also be a factor over relatively short timeframes 7/31/2022

6:08:00 AM. Ecological niches reflect regional and continental co-distribution among species through shared physiological tolerances to biotic and abiotic factors with niches more or less conserved over extended timeframes (Peterson, 2011). As such, through my thesis, I do not explicitly consider adaptive responses to historic changes and assume that observed evolutionary differentiation within species is a result of broad scale distributional shifts accompanied by prevailing neutral differentiation. I nonetheless acknowledge that species-specific ecological and life-history traits may have large impacts on biogeographic inconsistencies with meaningful implications for explaining seemingly discordant signals across broad spatial scales and environmental gradients (Riddle, 2016).

Most comparative phylogeographic studies to date have focused on biogeographic responses of single regional dynamics due to a persistent lack of sampling of broad rangewide distributions across many species (e.g., Carstens & Richards 2007; Hope et al. 2015). However, holistic sampling of biodiversity through comprehensive regional field surveys can provide insight into whole regional communities as modern assemblages, greatly expanding the potential for comparative analyses (Hope et al. 2018; Galbreath et al. 2019). A more comprehensive perspective of regional communities allows us to ultimately ask whether observed communities are a result of recent or long-term community assembly. Recent assembly would provide strong implications towards increased novel species interactions in response to current environmental turnover whereas historic long-term interactions maintained through time has strong implications towards shared evolutionary histories and shared responses to current environmental change. Given we now have multiple decades of phylogeographic single-species inference along with sufficient sampling across the distribution of many respective species, detailed georeferenced locality data of species occurrence is now much more available and

combined with climate data can provide more accurate estimates of changes in distribution, again assuming niche conservatism.

Comparative phylogeography, often considered in parallel with historical biogeography (Arbogast & Kenagy, 2001; Zink, 2002), integrates ecological and evolutionary processes to test for shared histories among co-distributed species and to assess climatic and geographic drivers of community assembly. Assessment of a given species' evolutionary history generally reveals the multiple intra-specific lineages and the geographic transitions between these lineages frequently cluster across multiple species. Much like using multiple loci for increasing lines of phylogenetic evidence, comparative assessment of co-distributed species provides increased lines of evidence for biogeographically meaningful landscape features that drive spatial and temporal concordance among assemblages, and for identifying regional suture zones and historic refugia (Arbogast & Kenagy, 2001; Dawson, 2014). However, reconstruction of community assembly based on current phylogeographic patterns (i.e., the current distribution of genetic diversity) alone is often insufficient to capture the full complexity of biotic responses to dynamic environmental processes through time, particularly under potential soft allopatry where lineage breaks may be spatially removed from the geography associated with their formation (Gerhold et al., 2015; Peterson, 2009). Use of coalescent methods can help with determining degree of concordance among histories. Coalescent methods can estimate the timing of divergence events and infer the existence of multiple historic refugia, based on estimated phylogenies. However, from a comparative perspective, we often lack comprehensive sampling coverage and genetic data across all study species that would enable more accurate assessment of coalescence dating and demographic history at the level of community analyses. In the face of shortcomings from any

given aspect of my work, the power of these comparative phylogeographic analyses comes from a capacity to integrate perspectives and tools across disciplines (Avise, 2000).

Evolutionary differentiation in response to fluctuating climate conditions was accompanied by fauna and flora repeatedly responding from an ecological perspective through time (such as distributional change) (Hope et al., 2019; Svenning & Skov, 2004). As such, integrating ecological niche modeling (ENM) with analyses of lineage diversification provides a strengthened analytical framework for assessing community complexity through time (Knowles et al., 2007; Richards et al., 2007; J. Soberón & Peterson, 2004; Willis & Whittaker, 2002).

Given that the current Holocene epoch is in effect the most recent interglacial phase of the Pleistocene "ice age", modern communities are responding to continuing climatic changes (a general warming trend) dated to the LGM (Blonder et al., 2015). Hindcast ENMs provide independent lines of evidence for historical assembly (Carstens & Richards, 2007; Cheddadi et al., 2006; Kozak et al., 2008; Morrone & Crisci, 1995; Wiens & Donoghue, 2004), by using empirical occurrence data and the associated climatic variables of temperature and precipitation to project species distributions assuming niche conservatism (Peterson et al., 1999). Ecological niche conservatism has been supported for many species over the latter part of the Pleistocene (Banks et al., 2008; Martínez-Meyer et al., 2004; Martínez-Meyer & Peterson, 2006; Peterson, 2011) and ENMs have also exhibited strong predictive ability concerning phylogeographic structure and endemic assemblages (Barrow et al., 2017; Bigg et al., 2008; Peterson & Nyári, 2008; Waltari et al., 2007; Waltari & Guralnick, 2009) . Assessment of predictability of these responses across regions, and within species of a given community can significantly improve our understanding of the impacts of recent environmental perturbations and provide new insights into

the processes that create and maintain suture zones (Hewitt, 2011; Lawing & Polly, 2011; Parmesan & Yohe, 2003; Swenson, 2013).

Prior to the advent of computational toolsets for phylogeographic reconstruction and ENMs, processes of community assembly and regional hotspots of assemblage interactions were inferred through broad-scale biogeographic frameworks such as the "faunal element hypothesis" (Udvardy, 1969) and "biotic suture zones hypothesis" (Remington, 1968). Faunal elements are regional or continent-wide assemblages of vertebrates with geographically coincident species-wide ranges with respect to shape and centroid. The faunal elements hypothesis follows that if species ranges spatially reflect the climatic and landscape factors driving broad-scale occurrence and ecological associations (Hengeveld, 1992; G. Peterson et al., 1998), then faunal elements are a product of historical ecological associations maintained through evolutionary time among species (Armstrong, 1972). Therefore, a group of species co-distributed across a broad area should represent assemblages with characteristic ecology and shared evolutionary histories. Alternatively, co-distributed taxa may represent localized and geographically novel communities formed by species with different historical origins, and should reflect varying ecological and evolutionary histories that co-exist through fine-scaled resource partitioning across landscapes subject to change. A third alternative explanation may be that localized communities, including species interacting at the periphery of broader distributions, indeed represent endemic assemblages with long-term continuous parapatry or sympatry, and the ecological complexity of a temporally continuous ecotone. In this latter case, the faunal element hypothesis of shared histories acts across a continuum from discrete ecological communities (to west [grassland] and east [woodland] in the case of North America) through a central shared zone of alternate stable states and increased community complexity. This situation would be contingent upon taxon-

specific traits allowing for stable geographic associations among peripheral/transitional populations. In this case, persistence of such communities would likely be a consequence of long-term environmental gradients.

Remington's suture zones were defined as narrow to broad zones of geographic overlap between distinct biotic assemblages where multiple zones of both interspecific and intraspecific hybridization occur and were hypothesized to be a result of secondary contact between analogous biotic assemblages previously isolated in refugia with subsequent genetic drift leading to differentiation in sister taxa (1968). Recent revisions of Remington's suture zone hypothesis produced new insights into the environmental mechanisms driving divergence, interaction, and community assembly, particularly from the perspective and application of phylogeography (Avise, 1998, 2000; Avise et al., 1987). Recognition of a species' intra-specific lineages was accompanied by the realization that geographic transitions between these lineages frequently coincide with identified suture zones, 7/31/2022 6:08:00 AMAs such, the original emphasis of hybridization as the defining eco-evolutionary interaction across suture zones failed to fully explain the evolutionary and ecological complexity of biodiversity interactions (Swenson & Howard, 2004). A revised and more holistic definition of suture zones recognizes these regions as clusters of contact zones (where multiple communities experience secondary contact), hybrid zones (where multiple species or intra-specific lineages experience gene flow), and phylogeographic breaks (regions of spatial turnover between intra-specific lineages), given that spatial clustering of each likely results from a combination of macro- to micro-evolutionary responses to the same processes (Swenson & Howard, 2004). This definition better acknowledges other, more functionally consequential, eco-evolutionary interactions across suture zones such as competition, host-parasite co-evolution, and disease transmission, all of which can

be spatially predicted by testing for the presence of suture zones (Swenson, 2013). A remaining gap in the definition of suture zones concerns their importance for regional assemblages that are distributed across environmental gradients, where the cyclic nature of the Pleistocene environmental change and the global distribution of biomes has resulted in regions of long-term (continuous) interaction of otherwise ecologically distinct species assemblages. I hypothesize that the Great Plains Suture Zone is one such region, and if so, would represent a critical focus for future analysis at the intersection of ecological and evolutionary relevance.

Here, I address this remaining gap concerning the definition of suture zones as a significant driver for maintaining long-term community complexity between regional assemblages that are otherwise separated across increasingly divergent abiotic gradients (Swenson, 2013). I hypothesize a further concept to describe suture zones, in addition to those criteria mentioned above, as *regional ecotones and zones of alternative stable ecological states where otherwise ecologically and evolutionarily distinct assemblages suture to comprise a single complex community that interacts continuously across both ecological and evolutionary timescales, without the prerequisite need for hard allopatry followed by secondary contact, but instead embracing the importance of soft allopatry in driving cyclic environmental dynamics*. Importantly, the cyclical nature of Pleistocene climate, coupled with high environmental heterogeneity across North America has also maintained the functional consequences previously attributed to suture zones, that has led repeated episodes of intra-specific differentiation, inter-specific divergence (potentially accompanied by gene flow), and maintenance of regionally distinct assemblages. As such, this mid-continental suture zone may be a significant driver of North American biodiversity.

For my thesis, I selected ten small mammal species currently exhibiting broad distributions across the Great Plains to assess the current intraspecific phylogeographic structure and historic distributions during the LGM. Small mammals are ideal proxies for community dynamics as they possess fast rates of population turnover, respond quickly to changing conditions, and are ecologically diverse, occurring in all terrestrial ecosystems (Hope et al. 2016). I have selected four "eastern" woodland-associated species belonging to the described Eastern faunal element, three "central" species belonging to the described Campestrian faunal element, and three "western" grassland-associated species belonging to the described Chihuahuan faunal element (Armstrong, 1972). Species belonging to the Eastern faunal element include the North American least shrew (*Cryptotis parvus*), eastern woodrat (*Neotoma floridana*), and hispid cotton-rat (*Sigmodon hispidus*), and white-footed mouse (*Peromyscus leocopus*). Species belonging to the Campestrian faunal element include the prairie vole (*Microtus ochrogaster*), Elliot's short-tailed shrew (*Blarina hylophaga*), and the hispid pocket mouse (*Chaetodipus hispidus*). Lastly, species belonging the Chihuahuan faunal element include the western harvest mouse (*Reithrodontomys megalotis*), the southern plains woodrat (*Neotoma micropus*), and the fulvous harvest mouse (*Reithrodontomys fulvescens*). I use the cytochrome b gene (*Cytb*) of mitochondrial DNA (mtDNA), regarded as the workhorse of comparative phylogeography (Avise et al. 1987), to assess intraspecific diversity and lineage structure through Bayesian coalescent models and ENMs to hindcast species distributions to the LGM. I use this combined toolset to test if the Great Plains Suture Zone can be considered a complex center of shared intra-specific differentiation, a region of transition between assemblage associated with different habitat types, a long-term zone of community interaction as a result of co-occurring alternate stable states, and a hotspot for ongoing eco-evolutionary interactions. I

hypothesize that community assembly and processes shaping shared histories act across a continuum dependent upon species-specific traits and that, as a consequence, idiosyncratic responses among species may impact resolution of potentially concordant responses to ecological gradients. I predict that western, eastern, and central associated species across the Great Plains will display evolutionary histories that reflect both regional geographic ranges and shared biogeographic responses, potentially negating the validity of faunal elements as biologically meaningful units of analysis.

Methods

North American terrestrial biodiversity has been regionalized into faunal elements based on species ranges and distinctly corresponding to continental biomes and ecoregions across North America (Armstrong, 1972; Ricketts et al., 1999). However, species broadly distributed across the Great Plains fall into the Eastern, Campestrian, and Chihuahuan faunal elements reflecting the longitudinal ecotone from woodland to grassland. Eastern fauna is geographically coincident and ecologically associated with the eastern deciduous forest but possess western extents coincident with the Great Plains. Some eastern faunal species are distributed westward as far as the west coast; however, these taxa circumvent the southern extent of the Chihuahuan Desert and through the Cochise filter barrier to reach it (Riddle & Hafner, 2006). Campestrian faunal distributions are centered on the Great Plains but reflect ecological associations with mesic grasslands in the northern Great Plains and arid grasslands in the southern Great Plains. Chihuahuan fauna are geographically biased towards western aridlands reflecting ecological associations with arid scrubland and grassland. Species are listed according to faunal element identity from east to west regionalization, and species in each faunal element are organized

according to increasing phylogenetic complexity based on the number of supported intraspecific lineages and potential lineages.

Field Sampling

From 2019 to 2021, we performed collection-based field surveys of mammal diversity throughout the latitudinal extent of the Great Plains, including regional sampling across southern Manitoba (summer 2019), southernmost Texas (spring 2000), Kansas (summer 2020), South Dakota (summer 2021) and Minnesota (summer 2021). Field crews of four to six persons sampled general localities throughout each province and state for three nights per locality, collecting and salvaging all permitted mammal species. General trapping localities were chosen to broadly transect the ecotone between Great Plains prairie habitats and eastern deciduous forests. We set traps in the evening, including pitfall cups, Sherman live traps, "museum special" snap traps, gopher/mole traps, and firearms for medium-sized species such as squirrels and rabbits, all in accordance with approved IACUC protocols (KSU IACUC permits #4055, #4544) and following guidelines of the American Society of Mammlogists (Sikes et al., 2016). We checked traps every morning near sunrise and referenced the coordinates for each sample at trap localities to the World Geodetic System 1984 datum using Garmen hand-held GPS units. Directly after checking traps, we processed and preserved all specimen parts, including skin, skeleton, organ tissues, and ecto- and endo-parasites to maintain molecular quality and maximize the breadth of downstream research (Galbreath et al., 2019). We preserved molecular samples with one or more of 90% EtOH, Longmire buffer, -80°C cryopreservation (in a mobile nitrogen dewar), and dehydration. Voucher specimens and their associated parts have since been archived and accessioned at the Museum of Southwestern Biology at the University of New Mexico, and

all data is publicly available through the ARCTOS multi-institutional specimen database (http://arctos.database.museum/). Altogether, we collected over 50 species of mammal with our sampling efforts. Of them, ten species were chosen for my thesis project based on strong association with the Great Plains and sufficient geographic coverage of publicly available mitochondrial *Cytb* sequence data (archived in GenBank) from throughout the range of these species, which was coupled with data from my own sequencing efforts.

Species Accounts

Cryptotis parvus — Altogether, the phylogenetic analysis of the North American least shrew included 98 *Cytb* sequences, including 2 *Cryptotis berlandieri* and 11 *Cryptotis parvus floridanu*s which were previously recognized as *Cryptotis parvus* until recent revision (Galfano, 2021). Of the 85 sequences used, 6 were directly contributed through cooperative sampling and sequencing efforts for both this study and Galfano (2021), while I downloaded the rest from NCBI GenBank. I constructed current and hindcast ENMs of the North American least shrew with a total of 625 occurrence records after the original dataset, attained from GBIF, was filtered and thinned, and I set a buffer radius of 200 km around occurrence points for the study area. The North American least shrew is a member of the eastern faunal element (Armstrong, 1972) occurring across the eastern US. Its westward distribution spans across the central Great Plains with a western extent in the southern Great Plains coincident with the Edwards Plateau region of Texas, and High Plains of New Mexico (Fig. 1A). A recent taxonomic revision has resulted in samples from Mexico and Florida being recognized as two distinct species (Galfano, 2021). The North American least shrew is associated with mesic areas with underbrush coverage such as woodlands, marshes, and grassland riparians (Choate et al., 1994; Hamilton, 1944; Schwartz &

Schwartz, 1981). They are primarily insectivorous, feeding on various invertebrates but may also supplement diet with fungi and plants (Choate et al., 1994; Schwartz & Schwartz, 1981).

Neotoma floridana — Altogether, the phylogenetic analysis of the eastern woodrat included 24 *Cytb* sequences. Of the 24 sequences used, 10 were directly contributed through my study's sampling and sequencing efforts, and I downloaded the rest from NCBI GenBank. I constructed current and hindcast ENMs of the eastern woodrat with a total of 350 occurrence records after the original dataset, attained from GBIF, was filtered and thinned, and I set a buffer radius of 200 km around occurrence points for the study area. The eastern woodrat is a member of the eastern faunal element (Armstrong, 1972) occurring across the southeastern US. It has a westward distribution restricted to the eastern Great Plains except for its northwestern extent that reaches the western extent of the central Great Plains in Colorado. It also has a disjunct population across South Dakota and Nebraska (Fig. 2A). The eastern woodrat is primarily associated with mesic deciduous woodlands, shrubland, and marshes but can also occur across grasslands in proximity to shrubby and wooded areas (Webster et al., 1985; Wiley, 1980). They are generalists capable of attaining water from their diet which includes acorns, fruits, invertebrates, and agricultural grains (Palmer, 1957) and are known for caching food in large middens (Wiley, 1980).

Sigmodon hispidus — Altogether, the phylogenetic analysis of the hispid cotton rat included 141 *Cytb* sequences. Of the 141 sequences used, 18 were directly contributed through my study's sampling and sequencing efforts, and I downloaded the rest from NCBI GenBank. I constructed current and hindcast ENMs of the hispid cotton rat with a total of 1491 occurrence records after the original dataset, attained from GBIF, was filtered and thinned, and I set a buffer radius of 200 km around occurrence points for the study area. The hispid cotton rat is a member

of the eastern faunal element (Armstrong, 1972) occurring across the southcentral and eastern US, and across the entire central and southern Great Plains, with isolated populations in both southern California and Arizona (Fig. 3A). Historically, hispid cotton rats were considered rare at the northern range extent across Kansas (Hall, 1955), however, recent occurrences indicate a rapid northward expansion reaching as far as the Platt River in Nebraska (Frisch et al., 2015). The hispid cotton rat is common in dense grassy areas, such as roadside drainages and grassy fields, but is largely a habitat generalist that is broadly associated with mesic to dry shrublands, woodlands, grasslands, and agricultural fields (Cameron, 1999; Webster et al., 1985).

Peromyscus leucopus — Altogether, the phylogenetic analysis of the white-footed mouse included 76 *Cytb* sequences. Of these, 18 were directly contributed through my study's sampling and sequencing efforts, and I downloaded the rest from NCBI GenBank. I constructed current and hindcast ENMs of the white-footed mouse with 2626 occurrence records after the original dataset, attained from GBIF, was filtered and thinned, and I set a buffer radius of 250 km around occurrence points for the study area. The white-footed mouse is a member of the eastern faunal element (Armstrong, 1972). They are the most common small mammal species native to eastern forests (Wilson & Ruff, 1999) and occur across the entire Great Plains, into the warm deserts of the southwest, and southward into arid to mesic tropical forests of Mexico (Fig. 4A). In the east, they are most common in deciduous and mixed woodlands, building nests in tree cavities and abandoned birds' nests, but are highly adaptable to a range of environments including mesic to dry grasslands, dense to open shrubland, semi-desert scrub, agricultural fields, and urban areas (Lackey et al., 1985; Wilson & Ruff, 1999). The white-footed mouse is recognized as a primary reservoir for potentially zoonotic pathogens across North America, particularly hantavirus (Long et al., 2019; Tufts & Diuk-Wasser, 2018), as different strains of pathogens are associated with

different lineages of mice reflecting divergent evolutionary histories (Dragoo et al., 2006). Populations have rapidly expanded in recent decades in both density and distribution associated with woody encroachment (Dreier et al., 2015) and the displacement of grassland species (Swihart & Slade, 1990). Further, their expansion has facilitated the expansion of the black-legged tick and Lyme disease into southeastern Canada, severely impacting human health in local communities (Gasmi et al., 2017; Roy-Dufresne et al., 2013).

Blarina hylophaga — Altogether, the phylogenetic analysis of Elliot's short-tailed shrew included 35 *Cytb* sequences. Of the 35 sequences used, 2 were directly contributed through my study's sampling and sequencing efforts, and I downloaded the rest from NCBI GenBank. I constructed current and hindcast ENMs of Elliot's short-tailed shrew with a total of 185 occurrence records after the original dataset, attained from GBIF, was filtered and thinned, and I set a buffer radius of 200 km around occurrence points for the study area. Elliot's short-tailed shrew is a member of the Campestrian faunal element, occurring in the central US from southern Nebraska and Iowa to northeastern Texas and across Missouri, Arkansas, Oklahoma, and Kansas, and with isolated populations in Bastrop and Aransas counties of Texas (Thompson et al., 2011; Fig. 5A). They have relatively broad habitat preferences, preferring areas with damp soils, leaf litter, and underbrush cover for easy burrowing including deciduous woodlands, grasslands, and riparian areas (George, 1999; Thompson et al., 2011), and precipitation, among other factors, plays a key role in driving population densities (Kaufman et al., 2012). The Elliot's short-tailed shrew's diet consists primarily of earthworms, insects, and other invertebrates but they are also known to frequently take much larger prey such as mice and voles and supplement with plant material (Davis & Schmidly, 1994; The University of Kansas, 2001). While we consider Elliot's short-tailed shrew as a Campestrian species, it is a part of a complex of *Blarina*

shrews (including *Blarina brevicauda,* and *Blarina carolinensis*) that extend across the eastern forests and which collectively diversified during the Pliocene (Brant & Ortí, 2002). Further, mounting evidence suggests *Blarina* shrews may be one of the primary reservoirs of Hantavirus across North America (Arai et al., 2007; Dietrich et al., 1997; Liphardt et al., 2020).

Microtus ochrogaster — Altogether, the phylogenetic analysis of the prairie vole included 24 *Cytb* sequences. Of the 24 sequences used, 6 were directly contributed through my study's sampling and sequencing efforts, and I downloaded the rest from NCBI GenBank. I constructed current and hindcast ENMs of Elliot's short-tailed shrew with a total of 497 occurrence records after the original dataset, attained from GBIF, was filtered and thinned, and I set a buffer radius of 150 km around occurrence points for the study area. The prairie vole is a member of the Campestrian faunal element (Armstrong, 1972), occurring contiguously across the northern and central Great Plains and from Wyoming and northeast New Mexico to Virginia with disjunct populations in northwest and southeast Texas (Fig. 6A). The prairie vole prefers areas with a heavy buildup of plant debris including prairies, pastures, and weedy fields but is more strongly associated with dry upland areas, as opposed to mesic meadows (Clark & Kaufman, 1990; Miller, 1969; Stalling, 1990). Decreases in prairie voles abundance are strongly associated with increased woody encroachment (Hope, 2019). They cache food in their burrows and are primarily folivores feeding on grasses, roots, seeds, and occasionally insects and woody vegetation (Kurta, 1995).

Chaetodipus hispidus — Altogether, the phylogenetic analysis of the hispid pocket mouse included 56 *Cytb* sequences. Of the 56 sequences used, 2 were directly contributed through my study's sampling and sequencing efforts, and I downloaded the rest from NCBI GenBank. I constructed current and hindcast ENMs of the hispid pocket mouse with a total of 548

occurrence records after the original dataset, attained from GBIF, was filtered and thinned, and I set a buffer radius of 200 km around occurrence points for the study area. The hispid pocket mouse is a member of the Campestrian faunal element (Armstrong, 1972), occurring contiguously across the southern, central, and parts of the northern Great Plains, with a peripheral distribution across the southwest Chihuahuan dessert of Arizona and Mexico and a disjunct population in the southern semi-arid highlands of Mexico (Fig. 7A). The hispid pocket mouse prefers areas with sandy soils including shortgrass prairies, grasslands, and along fence lines (Davis & Schmidly, 1994). They generally feed on seeds but will also consume insects, cactus, and various herbaceous plants (Caire et al., 1989).

Reithrodontomys fulvescens — Altogether, the phylogenetic analysis of the fulvous harvest mouse included 18 *Cytb* sequences. Of the 18 sequences used, 4 were directly contributed through my study's sampling and sequencing efforts, and I downloaded the rest from NCBI GenBank. I constructed current and hindcast ENMs of the fulvous harvest mouse with a total of 878 occurrence records after the original dataset, attained from GBIF, was filtered and thinned, and I set a buffer radius of 200 km around occurrence points for the study area. The fulvous harvest mouse is a member of the Chihuahuan faunal element, occurring across Mexico and northward across the southeastern Great Plains into southern Kansas and Missouri and extending eastward as far as Mississippi (Fig. 8A). The fulvous harvest mouse is primarily associated with thick grassy areas in shrublands and grasslands but will generally occur in temperate to tropical open grasslands, meadows, and fields (Spencer & Cameron, 1982). Most of the fulvous harvest mouse's diet consists of insects during the spring and summer, but it will also feed on seeds, fruits, and other plant materials (Schmidly & Bradley, 2016).

Neotoma micropus — Altogether, the phylogenetic analysis of the southern plains woodrat included 41 *Cytb* sequences. Five of the 41 sequences used directly contributed through my study's sampling and sequencing efforts, and I downloaded the rest from NCBI GenBank. I constructed current and hindcast ENMs of the southern plains woodrat with 499 occurrence records after the original dataset, attained from GBIF, was filtered and thin. Id I set a buffer radius of 150 km around occurrence points for the study area. The southern plains woodrat is a member of the Chihuahuan faunal element (Armstrong, 1972), occurring across the southwestern Great Plains of New Mexico, Kansas, Oklahoma, Texas, and northern Mexico (Fig. 9A). The southern plains woodrat is primarily associated with arid cactus grasslands. Still, it is also common in mesquite grasslands, shrublands, rocky outcrops, semi-arid plains, and areas where cacti are present (Braun & Mares, 1989). Its diet consists of cactus materials, mesquite pods, berries, and other plant materials, which it will cache large amounts of in dens (Braun & Mares, 1989).

Reithrodontomys megalotis — Altogether, the phylogenetic analysis of the western harvest mouse included 91 *Cytb* sequences. Of the 91 sequences used, 6six were directly contributed through my study's sampling and sequencing efforts, and I downloaded the rest from NCBI GenBank. I constructed current and hindcast ENMs of the western harvest mouse with a total of 1539 occurrence records after the original dataset, attained from GBIF, was filtered and thinned. I set a buffer radius of 200 km around occurrence points for the study area. The western harvest mouse is a member of the Chihuahuan faunal element (Armstrong, 1972), occurring from the pacific coast to the eastern extent of the northern and central Great Plains, southerly circumventing the Western Cordillera and centered on North American deserts with the southern extent reaching the Tropical Wet Forests of Mexico (Fig. 10A). The western harvest mouse is

primarily associated with open grasslands but also occurs in meadows, marshes, and arid deserts and shrublands (Wilson & Ruff, 1999). They rely almost exclusively on grass seeds for their diet (Hope & Parmenter, 2007; Wilson & Ruff, 1999) .

Genetic Analyses

Cytb Sequencing

I attained DNA from muscle tissue using standard salt extraction methods for a subset of specimens of each of my study species obtained from field sampling efforts (Miller et al., 1988). Following extraction, I mixed 5µL of DNA with 3µL of loading dye containing Gel Red (biotium) to visually assess extraction quality on a 0.8% agarose gel (Huang et al., 2010). Extractions deemed low quality were re-extracted using additional tissue. However, since mtDNA possesses a high copy number, extractions were considered high-quality, assuming a faint band of DNA was present and then moved to PCR for amplification. The *Cytb* gene (1140-1143 bp) of the mitochondrial genome was amplified using universal mammalian *Cytb* primers MVZ05(Forward; Irwin et al., 1991)/MVZ14 (Reverse; Smith & Patton, 1993) and MSB05(Foward)/MSB014(Reverse) (Hope et al., 2010). PCR conditions were set to denaturation for 6 minutes at 94.0℃, followed by 40x cycles of denaturing at 94.0℃ for 25 seconds, annealing at 48.0℃ for 30 seconds, extending at 72.0℃ for 1 minute, and then held at 10.0℃ for 10 minutes once the 50x cycles finished. I visually evaluated PCR product quality on 0.8% agarose gels as described above. I then cleaned high-quality PCR products using the ExoSAP-it Cleanup Reagent (ThermoFisher) by adding 1µL of Exo-SAP to 5µL of PCR product and set in thermocycler conditions of 15 minutes at 37℃ and 15 minutes at 80℃ (Bell 2018). Depending on the quality, I loaded 3-4ul of cleaned PCR product into plate wells with water and

forward or reverse primers for Sanger sequencing by Genewiz LLC on an ABI 3730 (South Plainfield, NJ). Following sequencing, I mapped, cleaned, and visually inspected raw forward and reverse sequence reads through Geneious Prime (Kearse et al., 2012), then generated consensus sequences and alignments of all cleaned sequences by species. I then downloaded all publicly available *Cytb* sequences for each species from NCBI's GenBank and aligned them with the new consensus sequences using MUSCLE Alignment v3.8.425 with default parameters (Edgar, 2004). For each species one or more sequences of a known sister taxon were included in alignments as outgroup taxa for phylogenetic reconstructions.

Cytb Phylogenetic Trees

I used Bayesian coalescent models to estimate phylogenetic relationships from sequence sets for each species through BEAST version 2.6.6. (Bouckaert et al., 2019) to estimate intra-specific lineage divergence through time. Model parameters were set in BEAUti, a component of the BEAST software package. I estimated the nucleotide substitution model, range of site heterogeneity, and proportion of invariant sites during Markov Chain Monte Carlo (MCMC) analysis with the bModelTest Package (Bouckaert & Drummond, 2017), also part of the BEAST package, using the transition-transversion split option and empirical frequencies. I set tree priors to a Coalescent Constant Population size. I set the clock rate for all species to 5% per million years (Hope et al., 2010) for standardized comparison. I initially set a lognormal relaxed molecular clock but switched to a strict clock for the final model if the mean standard deviation of the clock model was maintained near zero. I ran MCMC chains for 10,000,000 generations sampling every 1,000 generations. I used Tracer v1.7.1 (Rambaut et al., 2018) to confirm chain convergence and TreeAnnotator v2.6.2 (Rambaut & Drummond, 2020) to set a burn-in of 10%

for annotating consensus trees. I visualized tree topology against a time axis in millions of years, and depicted branch labels as posterior probabilities with FigTree v1.4.4 (Rambaut & Drummond, 2012).

Phylogeographic Structure

I used the resulting coalescent models for each species to infer phylogeographic structure by identifying distinct monophyletic lineages based on robust posterior clade support (≥0.95). Geographic sampling coordinates associated with each sequence used for genetic analyses were either obtained directly from public specimen databases, including NCBI's Genbank, ARCTOS, Vertnet, and Gbif, or were georeferenced based on verbatim specific localities of specimens using Google Earth (accessed August 2021). I compiled all coordinate data into Microsoft Excel, with a separate file for each species and separate sheets within files for each intra-specific lineage. I used ArcMap Desktop v10.7.1 (ESRI, 2019) to estimate the genetic boundaries between intraspecific lineages by applying a similar approach to defining genetic populations as through analysis with SAMOVA 2.0. (Dupanloup et al., 2002). I transformed XY coordinate data into point shapefiles and projected occurrence points as symbols corresponding to clade assignment to visualize lineage regionalization and distributional extent. I used the Create Thiessen Polygons analysis tool and the Polygon-To-Line data management tool to calculate equidistant boundary lines around each point based on distance to the next nearest point. I selected boundary lines separating genetic populations to be exported as new shapefiles and used the Smooth tool to transform hard edges into softened lines while maintaining the overall spatial structure between groups of points. I clipped and extended genetic boundaries to match the maximum recognized extent of species ranges based on downloadable range map layers for each

species (IUCN, 2021). For all species, lineages were assumed to be parapatric (sharing range borders between lineages) or allopatric (spatially isolated lineages). For parapatric populations where two lineages were narrowly or broadly interspersed across their boundary, the phylogeographic transition was drawn by estimating the midline between the furthest interspersed points. For sympatric lineages, genetic populations were colored with different shades of the same color, and if points for one of the overlapping lineages were more spatially confined than the other then a spatial polygon of its distributions was estimated using the same method of equidistant lines. I omitted genetic boundaries between points separated by course landscape barriers on the scale of the Great Lakes. Still, I kept boundaries broadly coincident with finer barriers like the Mississippi River to maintain a conservative spatial structure. Final maps were transformed to US Atlas Equal Area projections.

Niche Modeling

Occurrence Data

I obtained and processed occurrence data, and calibrated and built niche models using R (v4.1.2; R Core Team, 2021). I downloaded modern species occurrence data using the rgbif package (v3.6.0; Chamberlain et al., 2021) which provides a direct connection to the Global Biodiversity Information Facility (GBIF) database. For each species, I filtered occurrences by first removing spatially duplicate records from datasets followed by removing spatially outlying points. Spatial outliers were defined in various ways and with great caution considering 1) GBIF relates data from various sources ranging from genetically verified museum specimens to geotagged photos shared by amateur naturalists (GBIF data sources) 2) the species in this assessment are categorized as being rarely to never distinguishable in photographs (Kays et al., 2022), and 3)

species ranges acknowledged by the International Union for Conservation and Nature (IUCN) are often skewed compared to species' true distributions due to both under- and overestimation of species occurrence (Hughes et al., 2021). While GBIF does provide some metrics of where occurrences came from for verification, false occurrences and misidentifications are still prevalent in datasets due to incomplete or inaccurate data. I employed IUCN ranges to visualize the accuracy of datasets. I calculated the maximum distance between neighboring points contained within continuous regions of IUCN range maps to be used as a buffer distance for considering points. To maximize true occurrences, I automatically kept occurrence records verified by genetic data and those falling within the calculated buffer, regardless if they agreed with IUCN range maps. Additionally, I added the buffer to each range map and kept all points falling within it after ensuring they came from reliable sources (i.e., museum voucher, verified by expert). To minimize misidentifications, I kept all points within the acknowledged range of a species unless recent literature suggested the occurrences were inaccurate. To reduce spatial bias among points, I spatially thinned occurrence data with spThin (v0.2.0; Aiello-Lammens et al., 2015) by setting the thin parameter to the expected mean distance between points assuming a random distribution, calculated with the Average Nearest Neighbor Index (Evans, 2021).

Environmental Data

I built ENMs using modern bioclimatic variables (1970-2000) at 2.5' spatial resolution from WorldClim (v2.1; Fick & Hijmans, 2017). I calibrated and estimated models with modern climate variables and made hindcast projections with three general circulation model (GCM) simulations, including Community Climate System Model (CCSM), Model for Interdisciplinary Research on Climate (MIROC), and Max Planck Institute for Meteorology Earth System Paleo Model (MPI-ESM-P) from WorldClim v1.4.

I based ENMs on 17 bioclimatic variables from the WorldClim dataset, excluding variables 3, 14, and 15 as these variables contain high variability between GCMs (Varela et al., 2015). All other 17 variables were included for modeling regardless of variable correlation as Maxent algorithm is robust against collinearity (Feng et al., 2019). I cropped bioclimatic variables to species-specific masks (M) based upon a 150–250 km buffer around occurrence points to represent availability and use (Soberón, 2010). To estimate M, a buffer of 150 km was set around points but was increased to 175, 200, 225, and 250 km until the M had the same number of contiguous polygons or less as species' distributions (Table 1.).

Models

For each species, I calibrated ENMs using the ENMeval package (v2.0.3; Kass et al., 2021) and applied the maxnet (Varela et al., 2015) implementation of the MaxEnt (Phillips et al., 2017). MaxEnt contrasts presence and pseudo-absence data to identify associations between conditions of occurrence and relative availability to produce an estimate of relative suitability. Within ENMeval, the I used the "block" method to partition occurrences into calibration and evaluation datasets into four geographically distinct bins with equal occurrences based the corners of the occurrences' spatial spread. This method then uses the same spatial partitions to split background points and trains the model by excluding the background points positioned in the same areas as the evaluation points at each step. Further, the 'block' method provides the best spatial independence between calibration and evaluation datasets and optimizes model performance when transferred to different spatial and temporal extents (Radosavljevic & Anderson, 2014; Roberts et al., 2017). I used the clamping option for model calibration to avoid the inflation of estimated suitability when projecting to conditions outside of the calibration area (Merow et al., 2013).

I evaluated models with a combination of feature class inputs, including linear, quadratic, product, threshold, and hinge, and regularization multipliers 1:10. I validated each model with a significance test of Partial ROC using the kuenm package (v. 1.0; Cobos et al., 2019; Table 1). Then, I selected models based on Akiake Information Criteria (AIC; Table 1) to maximize model simplicity when projecting to different timeframes (Cabos et al., 2019b) and provide increased discrimination between models (Escobar et al., 2018). If multiple models provided AICc values <2 I selected the model with the lowest 10% omission rate (Anderson, Lew, & Peterson, 2003; Table 1). I calculated the logistic output for final projections to current and past conditions. For converting continuous outputs of suitability to binary, I calculated the threshold (Table 1) by producing pseudoabsence data through dismo (v1.3-3; Real et al., 2006) across the projected study area to avoid discarding potentially valuable data. I used modEvA (v3.0; Liu et al., 2005) to compare predicted pseuodoabsence to observed occurrence points based on estimated prevalence to produce a threshold optimized for logistic outputs. For final maps of estimated areas of suitability during the LGM, I combined binary results from each GCM by only including areas where at least two of the three GCMs agreed and discarding areas of suitability that were only supported by a single GCM.

Fossil Occurrences

I gathered fossil occurrence data for a Late Wisconsin timeframe (29 – 11.8 kya; LGM) from FUANMAP II for visual comparison against LGM projections. I gathered two datasets, one including fossil occurrences dated to a temporal confidence that was completely contained within the Late Wisconsin timeframe representing occurrences dated to a strict temporal window. The second dataset included fossil occurrences dated to a temporal confidence that intersects the Late Wisconsin timeframe representing occurrences dated to a lenient temporal window. Datasets that

were dated to a lenient temporal window provide more occurrence points but they may have been deposited prior to or subsequent to the LGM.

Results

Cryptotis parvus — The *Cytb* phylogeny recovered two well-supported and geographically distinct lineages coincident with central and east regionalization (Fig 1A, B). The central and east lineages were reciprocally monophyletic, and coalescence between them was estimated to 0.42 Mya (95% HPD 0.30–0.55 Mya; Pre-Illinoian; MIS 9–14; Fig 1B). Representatives from the east lineage were restricted to Virginia and Maryland. The nearest representative from the central lineage was in Louisiana on the west side of the Mississippi River (Fig. 1A). However, phylogenetic assessment based on nuclear DNA assigned this sample to the east lineage and confirmed mito-nuclear discordance that strongly supports past or ongoing gene flow between east and central lineages across the Mississippi River (Galfano, 2021). There was also a sample from Missouri assigned to the east lineage (Galfano, 2021). Still, it was excluded in this analysis due to a lack of specific locality information past the state of occurrence. The ENM for current conditions estimated areas of suitability outside the range of the North America least shrew roughly coincident with tropical wet forests of eastern Mexico (Fig. 1C). The hindcast ENM for the North American least shrew estimated areas of suitability spanning the southeastern US and eastern Mexico. The northeastern extent was coincident with the Southern Texas Plains and stretches eastward into Florida. A disjunct area of suitability was estimated in west central Mexico in Nayarit. Only fossil records intersecting the Late Wisconsin timeframe are coincident with estimated areas of suitability in the area across Florida. All other fossil occurrences were located further north than estimated areas of suitability and two localities in

southwest and southeast New Mexico are both further northwest than estimated areas of predicted suitability (Fig. 2D).

Neotoma floridana — The *Cytb* phylogeny recovered two genetically and geographically discrete lineages coincident with a central and east regionalization (Figs. 2A, B). The central and east lineages were reciprocally monophyletic, and coalescence between them was estimated to 0.57 Mya (95% HPD 0.45–0.69 Mya; Pre-Illinoian; MIS 12–17; Fig. 2B). Phylogenetic structure estimated here agreed with prior designations based on *Cytb* (Edwards & Bradley, 2001). The closest points between individuals belonging to central and east lineages were >400 km apart, with the Mississippi river the only major barrier between lineages. There were no genetic representatives from the northwest disjunct population to confirm its lineage designation, and its unknown identity was expressed by the color gray (Fig. 2A). The ENM for current conditions estimated areas of suitability outside of the range of *N. floridana* in southern semi-arid highlands and the Pacific coast (Fig. 2C). The hindcast ENM of eastern woodrat recovered two primary areas of suitability stretching along the Gulf of Mexico. One area of predicted suitability was centered on the Southern Coastal Plain in Florida and extended northward to North Carolina along previously exposed Atlantic coast. The other area was centered in northwest and northeast Mexico with upper extents just north of the Rio Grande across southeast New Mexico, the Chihuahuan Desert, and Tamaulipas-Texas semiarid plain. There was also a small area of suitability across previously exposed coast south of Louisiana and west of the Mississippi River and an area across the northwest pacific coast of Oregon and California. No fossil records dated to a strict temporal window were coincident with estimated areas of suitability. Their location was positioned across the eastern-central US, much further northward than estimated areas of suitability (Fig. 2D).

Sigmodon hispidus — The *Cytb* phylogeny recovered three geographically distinct lineages supported by posterior probabilities >0.96 and generally coincident with southwest, central, and east regionalization (Fig 3A, B). Southwest and central lineages are reciprocally monophyletic and, combined, are reciprocally monophyletic with the east lineage. Coalescence of the southwest and central mitochondrial lineages was estimated to 0.20 Mya (95% Height Posterior Density [HPD] 0.15–0.26 Mya; Illinonian glacial–Pre-Illinoian; Marine Isotope Stage [MIS] 6–8; Fig. 3B), and the combined southwest and central clade were estimated to coalesce with the east lineage at 0.53 Mya (95% HPD 0.41–0.65 Mya; Pre-Illinoian; MIS 11–16; Fig. 3B), indicating two primary lineages consistent with prior designations (Bradley et al., 2008). A single locality in southwestern Kansas and four localities across northeastern, central, and eastern Texas all yielded individuals from both southwest and central lineages indicating a lineage contact running southeast across Kansas, Oklahoma, and Texas. In addition to supporting both southwest and central lineages, a locality in eastern Texas also supported individuals from both central and east lineages, indicating a contact zone between all three lineages in the area. A locality at the western extent of the species' contiguous distribution yielded an individual from the east lineage and a locality at the southern extent of the contiguous distribution yielded an individual from the southwest lineage (Fig. 3A). Both representatives were disjunct from their regional populations and may represent relictual populations (Bradley et al., 2012; Carroll et al., Unpublished). The ENM for current conditions estimated areas of suitability outside the range of the hispid cotton rat roughly coincident with tropical wet forests of eastern Mexico (Fig. 3C). The hindcast ENM for the hispid cotton rat estimated an area of suitability across the Gulf Coast of the US with large broader areas centered on southern Texas and Florida and disjunct areas across the Yucatán Peninsula. Fossil records dated to a strict temporal window were coincident

with hindcast estimates in northern and southern Florida. All other fossil records dated to a strict temporal window were located across the southern Great Plains of Texas and Oklahoma northward of hindcast estimates (Fig. 3D).

Peromyscus leocopus — The *Cytb* phylogeny recovered four geographically distinct lineages with southwest, central Great Plains, central North America, and east regionalization (Fig. 4A, B). The central Great Plains lineage was supported by a posterior probability of 0.91 with the remaining lineages supported by posterior probabilities of 1.0. The central Great Plains lineage was reciprocally monophyletic with respect to the central North America lineage and collectively these lineages were reciprocally monophyletic with respect to the east lineage. Finally, this clade, formed by the three lineages, was reciprocally monophyletic with respect to the southwest lineage. Coalescence between central Great Plains and central North America lineage was estimated to 0.18 Mya (95% HPD 0.12–0.22 Mya; Sangomonian–Pre-Illinoian; MIS 5e–7; Fig. 4B). Coalescence between the clade of central lineages and the east lineage was estimated to 0.20 Mya (95% HPD 0.14–0.24 Mya; Illinoian–Pre-Illinoian; MIS 6–7; Fig. 4B). Coalescence between the clade of three lineages and southwest lineage was estimated to 0.23 Mya (95% HPD 0.18–0.30 Mya; Illinoian–Pre-Illinoian; MIS 6–8; Fig. 4B). Phylogenetic structure generally agreed with *Cytb* prior designations (Rowe et al., 2006), however the samples provided from this study's survey efforts, particularly in Kansas, resulted in slight restructuring of lineage relationships. First, samples collected across Kansas allowed for identification of the newly described central Great Plains lineage, where it was previously represented by a single sample in Oklahoma assigned to the central North America lineage. Second, the previously reported *Cytb* genealogy estimated a sister relationship of central and southwest lineages as monophyletic, with this combined clade being reciprocally monophyletic with respect to the east

lineage (Rowe et al., 2006). The more comprehensive sampling included here resulted in placement of the southwest lineage as the most basal clade. Kansas was the only state confirmed to contain three of the four lineages. Montgomery and Barton counties have representatives of central Great Plains and central North America lineages, indicating lineage contact zones and potential sympatry of these lineages across Kansas. Southwestern Kansas also represents the northernmost record of the southwest lineage. Additional disjunct populations in Yucatan and Campeche, Mexico, and Nova Scotia, Canada had no samples available for genetic analysis, and the uncertainty of their genetic identity is represented by the color gray (Fig. 4A). The ENM for current conditions estimated areas of suitability outside the range of the white-footed mouse across Florida (Fig. 4C). The ENM for white-footed mouse projected to LGM conditions recovered a contiguous distribution spanning the southern US from Arizona to North Carolina and across the Gulf of Mexico to the Yucatán Peninsula. The only fossil occurrence dated to a strict temporal window was in the southern Great Plains of Texas, northward of hindcast estimates (Fig. 4D).

Blarina hylophaga — The *Cytb* phylogeny for recovered three geographically distinct lineages with central and south regionalization (Fig. 5A, B), in agreement with prior designations (Reilly et al., 2005). The central and south lineages formed a monophyletic clade and coalescence was estimated to 0.18 Mya (95% HPD 0.11–0.17 Mya; Sangamonian–Pre-Illinoian; MIS 5e–6; Fig. 5B). The south lineage was supported by a posterior probability of 0.98 and the central lineage was unresolved. Representatives from the south population (Fig. 5A). The ENM for current conditions estimated areas of suitability outside the range of Elliot short-tailed shrew across the Sierra Madre and Southern Coastal Plain region (Fig. 5C). The hindcast ENM for Elliot's short-tailed shrew estimated suitable conditions across the Gulf Coast of the US on

previously exposed coastal areas south of Texas and Louisiana, tangent to an area centered on Florida. Smaller disjunct areas were also estimated across areas in eastern, western, and southern Mexico. The only fossil occurrence dated to a strict temporal window was in Arkansas, far north of hindcast estimates. (Fig. 5D).

Microtus ochrogaster — The *Cytb* phylogeny for the prairie vole recovered two geographically distinct lineages with central and north regionalization in agreement with prior designations (Fig. 6A, B). Coalescence between the south and southwest lineage was estimated to 0.24 Mya (95% HPD 0.16–0.30 Mya; Sangamonian–Pre-Illinoian; MIS 6–8; Fig. 6A). The central lineage was supported by a posterior probability of 1.0 and the north lineage was only represented by one individual. The disjunct population of prairie vole in northern Texas was not genetically distinct from the central lineage. The disjunct population in southeastern Texas remains absent from genetic records (Fig. 6A). The ENM for current conditions estimated areas of suitability outside the range of the prairie vole across the cold deserts and northeastern deciduous forests plain region (Fig. 6C). The hindcast ENM for the prairie vole estimated a contiguous distribution spanning the southern US from Arizona to North Carolina with a southern extent generally coincident with the US and Mexico border and northern Florida. Two fossil occurrences dated to a strict temporal window were coincident with hindcast estimates in the southern Great Plains however five others were located in the central Great Plains outside the northern extent of hindcast estimates (Fig. 6D).

Chaetodipus hispidus — The *Cytb* phylogeny recovered four geographically distinct lineages all supported by posterior probabilities of 1.0 reflecting central, southwest, south, and south-central regionalization (Fig. 7A, B) The central lineage was reciprocally monophyletic to the southwest lineage. The clade formed by the central and southwest lineages was monophyletic

to the south lineage, and the clade formed by the three lineages was monophyletic to the south-central lineage. The posterior probability was 0.97 for the central lineage and 1.0 for the southwest lineage, and coalescence between them was estimated to 0.26 Mya (95% HPD 0.17–0.33 Mya; Pre-Illinoian–Illinonian; MIS 6–9; Fig. 7B). The clade formed by central and southwest lineages was supported by a posterior probability of 0.81 and the south lineage by a posterior probability of 0.97, and coalescence between them was estimated to 0.34 Mya (95% HPD 0.25–0.42 Mya; Pre-Illinoian; MIS 8–11; Fig. 7B). The clade formed by central, southwest, and south lineages was supported by a posterior probability of 0.8 and the south-central lineage by a posterior probability of 1.0, and coalescence between them was estimated to 0.45 Mya (95% HPD 0.30–0.62 Mya; Pre-Illinoian; MIS 9–15; Fig. 7B). Phylogenetic and phylogeographic structure for hispid pocket mouse agreed with prior mtDNA designations (Andersen & Light, 2012). There was at least one representative from both central and south lineages that overlap in their occurrence with the hypothesized zone of contact broadly coincident with the Tamaulipas-Texas semiarid plain. The closest points between the central and southwest lineage are >250 km apart and the hypothesized zone of contact or separation was coincident with the Deming plains (Andersen & Light, 2012; Fig 7A). The ENM for current conditions estimated areas of suitability in Fig. 7C. All representatives from the south-central lineage are from the same general locality so the extent of its range remains unclear. The hindcast ENM for the hispid pocket mouse estimated an area centered on the Rio Grande of Texas. Fossil occurrences dated to a strict temporal window were located outside of hindcast estimates norward in the central Great Plains (Fig. 7D).

Reithrodontomys fulvescens — The *Cytb* phylogeny for the fulvous harvest mouse recovered two geographically distinct lineages with southwest and central regionalization (Fig.

8A, B). The two lineages were not reciprocally monophyletic although the central clade was monophyletic with strong support. Coalescence between them was estimated to 0.13 Mya (95% HPD 0.08–0.18 Mya; Sangamonian - Illinoian; MIS 5–6; Fig. 8B). The closest points between individuals belonging to central and east lineages are >100 km away and the lineage contact zone was estimated from northwest Texas to southeast Texas (Fig. 8A). The ENM for current conditions estimated areas of suitability outside the range of the fulvous harvest mouse across Baja California, southeastern deciduous forests, and the Yucatán Peninsula (Fig. 8C). The hindcast ENM for the hispid pocket mouse estimated two primary areas of suitability. One spanning Mexico and another centered on the southern coastal plain of Florida. The fulvous harvest mouse lacked fossil occurrences dated to a strict temporal window but occurrences dated to a lenient temporal window were located in the southern Great Plains northward of hindcast estimates in Mexico (Fig. 8D).

Neotoma micropus — The *Cytb* phylogeny recovered three genetically distinct lineages but only two lineages are geographically distinct, coincident with southwest and south regionalization (Fig. 9A, B). The southwest population comprises two sympatric lineages referred to as southwest-1 and southwest-2 lineages. The southwest-1 lineage and south lineage were reciprocally monophyletic. The southwest-1 lineage was supported by a posterior probability of 1.0 and the south lineage by a posterior probability of 0.96, and coalescence between them was estimated to 0.11 Mya (95% HPD 0.06–0.14 Mya; Early Wisconsin–Illinoian; MIS 4–6; Fig. 9B). The resulting clade between the southwest-1 and south lineages was not well-supported, and the southwest-2 lineage was supported by a posterior probability of 0.99. Coalescence between the lineages was estimated to 0.12 Mya (95% HPD 0.07–0.17 Mya; Early Wisconsin–Illinoian; MIS 5; Fig. 9B). Phylogenetic structure agreed with prior designations

(Planz et al., 1996). The closest occurrence of the southwest population was ~100 km apart, indicating a zone of contact across southern Texas (Fig. 9A). The ENM for current conditions estimated areas of suitability outside the range of the southern woodrat across the Colorado Plateau and central basin (Fig. 9C). The hindcast ENM for *N. micropus* estimated an area centered on Rio Grande of southern Texas and two areas across the previously exposed Gulf coast in Florida. A single fossil occurrence dated to a strict temporal window was located in southeast New Mexico northward of hindcast estimates (Fig. 9D).

Reithrodontomys megalotis — The *Cytb* phylogeny for western harvest mouse recovered three geographically distinct lineages with central, southwest, and south regionalization in agreement with prior designations (Nava-García et al., 2016; Fig 10A, B). Coalescence between the south and southwest lineage was estimated to 0.24 Mya (95% HPD 0.16–0.30 Mya; Sangamonian–Pre-Illinoian; MIS 6–8; Fig. 10B). The south lineage was supported by a posterior probability of 1.0 and the southwest by 0.98. Coalescence between the south and southwest clade and the central linage was estimated to 0.27 Mya (95% HPD 0.20–0.36 Mya; Pre-Illinoian; MIS 7–10; Fig. 10B). The central lineage was supported by a posterior probability of 1.0. The central lineage was designated as central due to its regionalization across the central Great Plains, however, it appears to span across the entire western US. Prior to this study's sampling efforts, the genetic identity of the populations across the Great Plains was unknown. Representatives from both southwest and central lineage were sampled at the same locality in west-central Kansas, and representatives from the central lineage were sampled in southwest Kansas, indicating spatial overlap between the two populations across the central Great Plains. The western harvest mouse's distribution across the southwestern US is severely under-sampled with representatives between southwest and central lineages >1000 km apart across the area and no

clear zone of contact between lineages. The contact zone between the southwest and south lineage appeared to be roughly coincident with the southern extent of the Chihuahuan Desert. The ENM for current conditions is in Fig. 10C. The hindcast ENM for the western harvest mouse estimated a large area of suitability across the southwest US and Mexico from Coastal California to the coastal Gulf of Mexico, and a smaller area on previously exposed coast east of Florida. A single fossil record dated to a strict temporal window was located in north Texas, northward of hindcast estimates. (Fig. 10D).

Combined Faunal Distributions

Combined ENMs for all ten species under current conditions recovered the area of highest spatial overlap in the central Great Plains of Kansas and Oklahoma (Fig. 11).in agreement with distributional overlap of IUCN ranges (Supplemental material). Combined hindcast projections of all ten species estimated the highest areas of overlap in the southern Great Plains of Texas and northeast Mexico (Fig. 12).

The center of overlap for Eastern species under current conditions was estimated across the southeastern U.S. (Fig. 11), consistent with original geographic designations of the Eastern faunal element (Armstrong, 1972). Combined hindcast projections of Eastern species estimated three primary areas of overlap, including areas in south Texas, the coastal line extending from Louisiana, and the Florida peninsula (Fig 13).

The center of overlap for Campestrian species under current conditions was estimated in Kansas, spatially coincident with the northwestern extent of the Eastern faunal element (Fig. 11), and consistent with original faunal element designations (Armstrong, 1972). Combined hindcast

projections of Campestrian species estimated the primary area of overlap in southern Texas (Fig 14).

The center of overlap for Chihuahuan species under current conditions was estimated across the Chihuahua Desert (Fig. 11), consistent with original geographic designations of the Eastern faunal element (Armstrong, 1972). Combined hindcast projections of Chihuahuan species estimated the primary areas of overlap across the southern Great Plains of northeast Mexico (Fig 15).

Discussion

I demonstrate here that, through the Great Plains, the assemblage of species included in my work represents a fauna that experienced long-term sympatry between species with vastly different geographic and ecological range-wide associations. In addition, this region of sympatry forms a zone of shared mechanisms of differentiation despite a lack obvious isolating barriers. Given all the evidence, the southern Great Plains represents a novel suture zone that reciprocally facilitates ecological and evolutionary differentiation and interactions across intraspecific and interspecific levels of diversity and up to the level of regional community composition.

I used a comparative approach towards the spatial structure of lineages and the temporal timing of divergence among 10 species. Within all species, discrete evolutionary lineages recovered were well-supported. However, the basal support for groups of linages was low for most species, and consequently, the sequence of divergence was not considered in these analyses. This is reasonable given only a single locus and high potential for stochastic sorting of lineages, coupled with low support among them. But theory would suggest that if the spatial structure and estimated timing of divergence were the same across species, it would signal a

concerted response of all taxa to a single (or multiple) historical event across Great Plains mammals. Conversely, if the spatial structure of lineages showed no similarities but species lineages differentiated at coincident times, it would suggest that all species experienced the same evolutionary forces but responded differently. Similarly, if only the timing of divergence differed between species and the spatial structure of lineages formed congruent phylogeographic breaks, it would suggest a repeatable mechanism of differentiation acting across species through time as previously recorded across the Great Plains Suture Zone (Reding et al., 2021; Shaffer et al., 2018).

Evolution of Species Within Described Faunal Elements

Overall, the evolutionary history of species within their respective faunal elements supported the existing faunal element hypotheses to an extent. However, even though species within faunal elements tended to share an evolutionary history, there also appeared to be overlapping history between species from different faunal elements. This suggests that the traditional faunal elements could serve as baseline hypotheses for testing and interpreting history but that they cannot explain the full complexity of species histories from more nuanced ecological and evolutionary perspectives.

The eastern faunal element and previous conclusions of shared history among the eastern community's terrestrial flora and fauna are strongly supported by my data (Lyman & Edwards, 2022; Soltis et al., 2006). The four species belonging to the eastern faunal element, including the North American least shrew, eastern woodrat, hispid cotton rat, and white-footed mouse, all expressed phylogeographic signals reflecting shared histories. Unlike the Great Plains, community assembly and phylogeographic history of biodiversity occurring through eastern

North America have been well documented. During the Pleistocene, the Mississippi River was the primary source of outflow from glacial ice sheets covering much of northern North America (Blum et al., 2000; Rittenour et al., 2007). This river provided a strong and constant filter barrier to dispersal that resulted in a pattern of genetically distinct populations east and west of the river concordant across non-volant species (Lyman & Edwards, 2022; Soltis et al., 2006). Concerning ecological traits, the four eastern species are all broadly associated with eastern temperate climate. Still, the eastern woodrat relies on mesic forests for habitat.

The least shrew, hispid cotton rat, and white-footed mouse are more generalist and can persist in forested to open prairie ecosystems ranging from mesic to arid conditions, but generally are found at least in proximity to shrubby or woody habitats. The four eastern species supported divergences coincident with the Mid Pleistocene and are the only species in this assessment to possess intraspecific lineages, regionalized east and west of the Mississippi River.

The three species included in the Campestrian faunal element, Elliot's short-tail shrew, prairie vole, and hispid pocket mouse, also expressed biogeographic signals for shared histories. The hispid pocket mouse and Elliot's short-tailed shrew both expressed breaks between central and southern lineages. Due to Elliot's short-tailed shrew being more geographically restricted, the location of the break is much less apparent. Still, the south population for both species is located in the same area of the southern Great Plains in south Texas. The prairie vole is the only Campestrian species with no genetic signal of a north-south break. Still, this species is known from a disjunct population (which is considered in imminent threat of extirpation) with the same distribution in southern Texas as with Elliot's short-tailed shrew. Unfortunately, no genetic samples were available for analysis. Based on the other two species, samples of prairie vole from this region would likely reveal the same break between south and central lineages. The break

between central and south lineages strongly suggests a shared history for Campestrian species. Still, the southwest lineage in the hispid pocket mouse supports shared histories with the other faunal elements. The north lineage in the prairie vole indicates an individualistic response to pressures not experienced by other species with more southern distributions.

Species associated with North America's arid lands have responded to similar forces as the Great Plains, with the Cochise filter barrier representing the transition between Sonoran and Chihuahuan deserts and a primary driver of shared differentiation among species of the southwest deserts (McDonough & Ferguson, 2022; Morafka, 1977; Provost et al., 2021; Zink, 2002). The three species in the Chihuahuan faunal element expressed phylogeographic signals supporting shared histories. The western harvest mouse and southern plains woodrat supported two genetically distinct populations, and the fulvous harvest mouse supported three. The southern plains woodrat and western harvest possessed a phylogeographic break between southwest and southern lineages across the southern transition between the Great Plains, Chihuahua desert, and the tropical forest of Mexico, indicating a shared history between the two species. Alternatively, the fulvous harvest mouse possessed a southwest-northeast break across Texas with no signal of a southern lineage as found in the other two species. Given that the fulvous harvest mouse's southern distribution remains under-sampled, the evolutionary history linked to this area is still unclear. The southern plains woodrat and fulvous harvest mouse possess westward distribution limits associated with the Cochise filter barrier. The western harvest mouse expressed a phylogeographic break between central and southwest lineages estimated across this region. While the spatial error associated with this estimate is significant, it may suggest evolutionary responses to the Cochise filter barrier or refugia isolated in the Baja Peninsula. The fulvous harvest mouse possessed the most distinct phylogeographic structure that

closely resembles the structure of species from other faunal elements distributed across the Great Plains' longitudinal extent, further suggesting shared history between faunal elements.

Shared History of Mammals Across the Great Plains

Intraspecific contact zones between southwest, south, and central lineages clustered in the southern Great Plains region for seven species, including the hispid cotton rat, white-footed mouse, hispid pocket mouse, Elliot's short-tailed shrew, southern plains woodrat, western harvest mouse, and fulvous harvest mouse coincident with the Central Texas suture zone identified by Remington (1968). The prairie vole is likely an eighth species, but increased sampling and genetic resources from its southern distribution are needed to be sure. These breaks generally range between southwest-northwest, east-west, and north-south boundaries, agreeing with the variable orientation of hybrid zones in avifauna (Rising, 1983).

Possibly the most prevalent biogeographic contact zone between biota separates east and west populations. Specifically, it tends to orient northwest to southwest starting around southwest Kansas and continuing to the gulf coast of the southern Great Plains. This phylogeographic pattern is most evident between southwest and central lineages in the hispid cotton rat, white-footed mouse, and fulvous harvest mouse. It is coincident with phylogeographic breaks identified in widespread mammalian carnivores with east and west lineages that diverged at variable times during the Pleistocene (García et al., 2017; Loveless et al., 2016; McDonough et al., 2022; Reding et al., 2012, 2021; Sacks et al., 2021), suggesting a repeated process of differentiation. Species with this phylogeographic break also possess similar phylogeographic patterns of regionalization to other mammalian species with much broader distributions. For example, the phylogeographic structure of the white-footed mouse is strikingly similar to the

phylogeographic structure of spotted skunks (Genus: *Spilogale*; McDonough et al., 2022), with east, central, southwestern, and the Yucatán Peninsula intraspecific populations. This east-west break is also present between congeneric species, such as the southern plains woodrat and eastern woodrat, agreeing with identified hybrid and contact zones between both closely and distantly related taxa (Allen, 1990; Carling et al., 2011; Rising, 1983; Swenson, 2006; Swenson & Howard, 2005). Further, this zone also represents the distributional limit for species without both western and eastern regionalized lineages, such as the North American least shrew, Elliot's short-tailed shrew, and western harvest mouse, which also agree with the distribution of numerous east and west species including migratory avifauna (Bock et al., 1977; Hall, 1981; Remington, 1968; Rising, 1983; Root et al., 1981; Swenson & Howard, 2005), suggesting that it is not only playing a role in species differentiation but also the regionalization of east versus west assemblages.

The Great Plains east-west suture is broadly concordant with the westward extent of the central Great Plains, a region of alternative stable states between grassland and woodland (Ratajczak et al., 2014; Seager et al., 2018). As well as the eastern extent of southwest arid land communities (Ricketts et al., 1999; Rosenberg, 1987) and western extent of the North American Coastal Plain communities, both of which represent regions of endemism (Noss et al, 2015; Zink, 2002). Additionally, the upper quartile threshold of increasingly arid climate and soil conditions is also coincident with this area (Salley et al., 2016), along with a myriad of other environmental drivers (Hargrove & Hoffman, 2004). Environmental gradients with coincident east-west orientations in precipitation and vegetative community turnover across the southern Great Plains are spatially and compositionally steeper than the northern Great Plains (Klemm et al., 2020; Rosenberg, 1987), which may aid in maintaining east and west lineage regionalization

across the area. The strong environmental gradient also suggests that lineages coming into contact across the east-west suture may be ecologically distinct. Additionally, original taxonomic species accounts for these taxa hypothesized upwards of seven subspecies based on ecological and morphological differences (Hall, 1981), but the only phylogeographic break in agreement with subspecies boundaries was the southern Great Plains east-west break, corroborating the potential for ecological differentiation.

In proximity to the east-west southern Great Plains phylogeographic break was the north-south break between south lineages and central and southwestern lineages. The orientation of the north-south break can also vary and was not always distinct from the east-west break. For example, the south lineage in Elliot's short-tailed shrew is isolated in a similar area to south lineages in hispid pocket mouse, southern plains woodrat, and western harvest mouse. Still, the southwestern distributional limit for the Elliot's short-tailed shrew's central lineage strongly resembles the phylogeographic break between southwest and central lineages for the hispid cotton rat, white-footed mouse, and fulvous harvest mouse, suggesting that the mechanisms or responses driving these patterns are not mutually exclusive (Rising, 1983). However, species such as the hispid pocket mouse, which possessed a north-south break between the south lineage and central and southwest lineages, and an east-west break between southwest and central lineages, suggest there is some level of distinction between the processes resulting in east-west and north-south breaks. Similar to the spatial dynamics suturing biota observed in African ungulates (Lorenzen et al., 2012). Like the east-west break, the north-south break also extends to congeneric species, such as the North American least shrew and its sister species *Cryptotis berlandieri* (Fig. 2A).

Paleodistributions

Hindcast ENMs and fossil records supported the phylogeographic results in that species from different faunal elements may have a shared history and maintained interaction across the Great Plains. Although hindcast ENMs are consistently biased towards the south, with fossil records suggesting occurrences further north, consistent with previous paleodistribution models of mammals (Davis et al., 2014; Guralnick & Pearman, 2010; McGuire & Davis, 2013; Waltari et al., 2007). While fossil records from FAUNMAP II are biased towards the US, neglecting potential areas in Mexico predicted by models, this can only explain a portion of the observed disagreement between ENMs and fossil records. Spatial discordance among ENMs and fossils could be due to 1) erroneous model assumptions, 2) a lack of niche conservatism, 3) underlying issues in GCMs or 4) Eltonian (biotic) and other drivers that cannot be predicted by climate alone (Davis et al., 2014; Holt & Gaines, 1992; Hyde & Peltier, 1993; Jackson et al., 2000; McGuire & Davis, 2013; J. Soberón, 2007; Williams et al., 2013). Paleodistribution estimates from Davis et al. (2014) and Waltari et al. (2007) predicted a similar southern bias in northern Boreal mammals and, when compared with the predictions made here, indicate an even more pronounced southward shift in both groups maintaining the same north and south parapatric relationship observed in modern distributions of high- and mid-latitude species. The general agreement of southern biased predictions suggests that individual modeling errors are not the root cause of hindcast ENM and fossil discordance. Moreover, fossil occurrences suggest that boreal (northern coniferous forest) and Great Plains species co-occurred in the central Great Plains during LGM timeframes. While niche conservatism could be a potential issue skewing models, provided the rapid rate of turnover experienced by small mammals (Hope et al., 2017; Peterson, 2011), historic cooccurrence of regionally distinct species through time strongly

suggests no-analog faunal communities and associated conditions persisted through the past. Countering strict niche conservatism, the primary driver of distribution among these mammals is likely habitat association in combination with climate across temperate latitudes as opposed to strict physiological tolerances to temperature and precipitation (Dreier et al., 2015; Kerr & Packer, 1997). Additionally, novel environmental conditions and no-analog communities during the past are still not accounted for based on models projected from current conditions (Williams & Jackson, 2007). Particularly across the Great Plains, where GCMs have proven to be poor predictors of vegetative communities during historic and future timeframes, the primary drivers of dominant prairie ecosystems remain unresolved (Cotton et al., 2016; Epstein et al., 1996; Epstein et al., 1997; Nordt et al., 2008; Ratajczak et al., 2014; Seager et al., 2018; Still et al., 2019).

Conclusions

A unifying biogeographic pattern has emerged across all ten study species, irrespective of faunal element, in their shared long-term histories through the southern Great Plains, forming a persistent suture zone that has influenced evolutionary dynamics within and between lineages, among species, and across regional communities. The Great Plains has long been recognized as a contact zone or suture zone for biota associated with both forest and prairie ecosystems (Bock et al., 1977; Remington, 1968; Rising, 1983; Root et al., 1981). The results here for small mammals suggest that woodland communities and grassland communities, generally considered as discrete entities, form a long-term and continuous association in the southern Great Plains. This region oscillates north to south with repeated episodes of environmental change but constitutes a single complex assemblage and region of biotic “spillover”. Species with more southern distributions

spill through this region northward and differentiate. Species from eastern North America spill through this region and differentiate to the south. Species with more central distributions spill back and forth from north to south. Phylogeographic structure, niche models, and fossil occurrences for glacial phase climate point towards southwest, south, and eastern-central refugia with long-term interactions maintained across the central and southern Great Plains (Seersholm et al., 2020; Waltari et al., 2007). The process driving these refugia mirrors those observed in northern boreal species (Hope et al., 2019), resulting in repeated patterns of east and west differentiation driven by soft allopatry. It is acknowledged that the evidence offered here for each individual species is only based on a single locus that is likely subject to phylogenetic discordance, stochastic sorting, and variable rates of evolution among taxa (Riddle & Jezkova, 2019; Toews & Brelsford, 2012) and ENMs, which as exemplified here, are inevitably subject to a degree of error (Davis et al., 2014; Soberón, 2007; Warren, 2012). However, the consistent pattern of geographically concordant phylogeographic breaks (Allen, 1990; Aubry et al., 2009; Barton & Wisely, 2012; Bock et al., 1977, 1977; Carling et al., 2011; Harding & Dragoo, 2012; McDonough et al., 2022; Puckett et al., 2015; Reding et al., 2012; Remington, 1968; Rising, 1983; Root et al., 1981, 1981; Swenson, 2006; Swenson & Howard, 2005; Wooding & Ward, 1997) strongly indicates a unifying biogeographic process across the southern Great Plains. Providing robust implications for the southern Great Plains region as a hotspot for emerging eco-evolutionary interactions in response to climate change (Albery et al., 2020; Avise, 2009; Gerhold et al., 2015; Han et al., 2015; Hope et al., 2017; Swenson, 2013; Swenson & Howard, 2005). Limitations still faced in providing fine-scale predictions of the numerous biogeographic dynamics predicted by future climate change include poor geographic coverage of molecular-quality samples, limitations on multi-locus or phylogenomic coverage of diversity, and a lack of

qualification and analysis of the general ecological traits impacting flora and fauna responses to climate change. Next steps should include increased sampling of species associated with the southern Great Plains to both monitor for emerging eco-evolutionary interactions in responses to future environmental change and further investigate the evolutionary and ecological dynamics driving western and eastern assemblage interactions. Implications towards conservation suggest community management must consider not only the composition of species across areas of suturing assemblages, but also the intraspecific identity of discrete evolutionary units. The assemblage "spillover" described here suggests that species consist of intra-specific lineages that have a long history of interaction with lineages belonging to species of different regional assemblages, but all species also exhibit lineages that are more characteristically allopatric from lineage of other assemblages. Further investigation towards the ecological and evolutionary impact of shared interactions between regionally distinct species is needed to understand how this shared history will influence the outcome of altered ecological interactions and assemblage turnover to future environmental change.

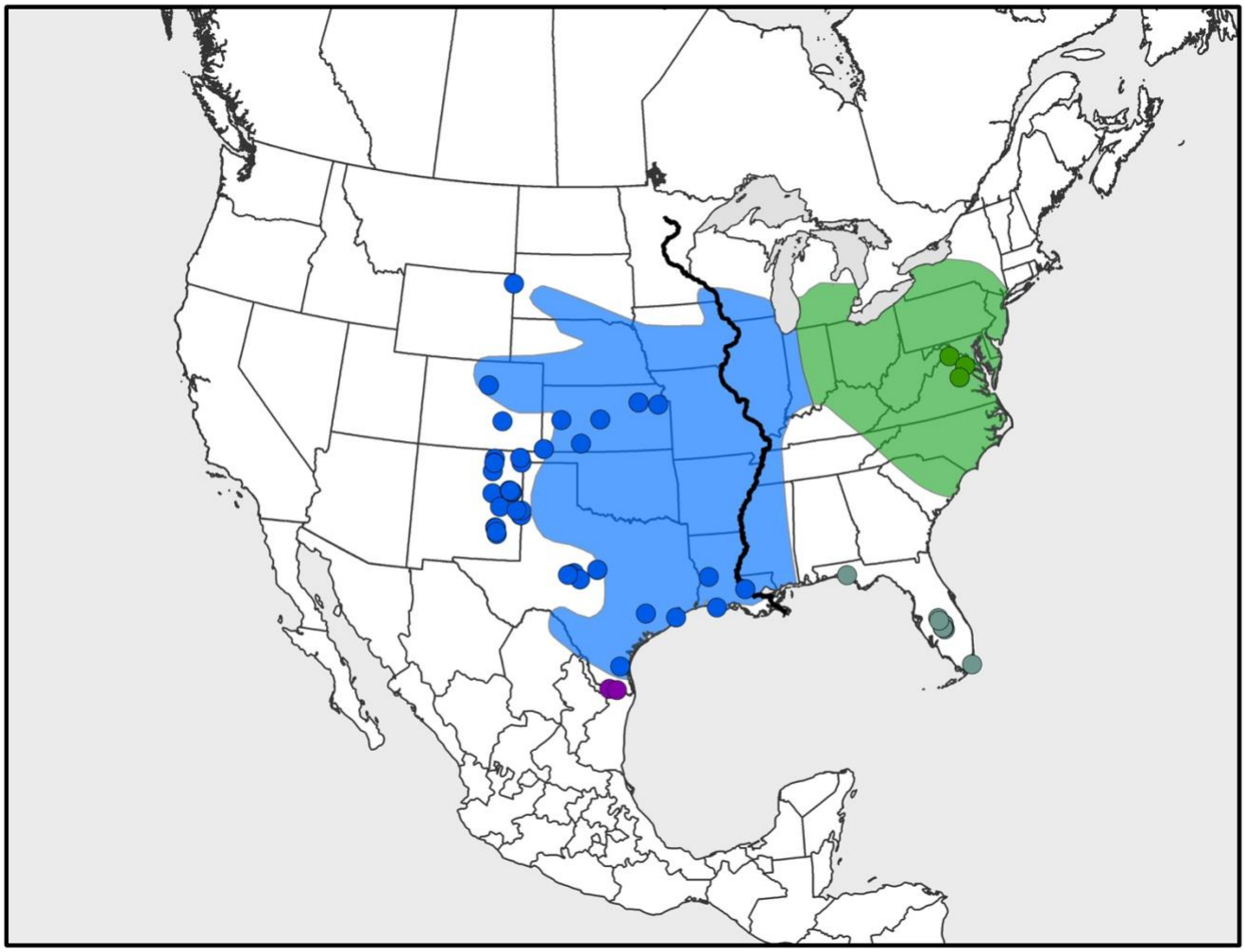

Figure 1A.

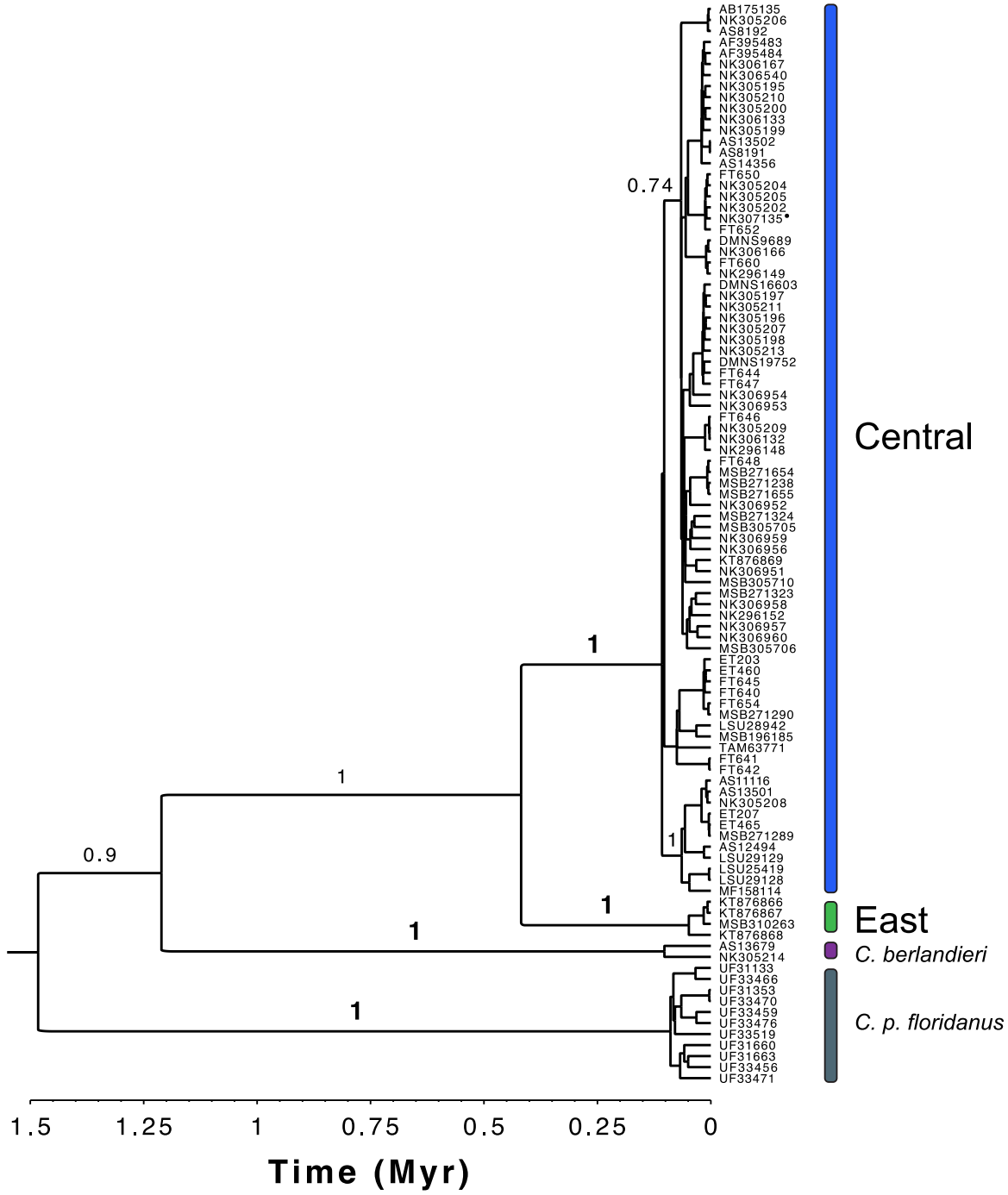
AB175135
NK305206
AS8192
AF395483
AF395484
NK306167
NK306540
NK305195
NK305210
NK305200
NK306133
NK305199
AS13502
AS8191
AS14356
FT650
NK305204
NK305205
NK305202
NK307135
FT652
DMNS9689
NK306166
FT660
NK296149
DMNS16603
NK305197
NK305211
NK305196
NK305207
NK305198
NK305213
DMNS19752
FT644
FT647
NK306954
NK306953
FT646
NK305209
NK306132
NK296148
FT648
MSB271654
MSB271238
MSB271655
NK306952
MSB271324
MSB305705
NK306959
NK306956
KT876869
NK306951
MSB305710
MSB271323
NK306958
NK296152
NK306957
NK306960
MSB305706
ET203
ET460
FT645
FT640
FT654
MSB271290
LSU28942
MSB196185
TAM63771
FT641
FT642
AS11116
AS13501
NK305208
ET207
ET465
MSB271289
AS12494
LSU29129
LSU25419
LSU29128
MF158114
KT876866
KT876867
MSB310263
KT876868
AS13679
NK305214
UF31133
UF33466
UF31353
UF33470
UF33459
UF33476
UF33519
UF31660
UF31663
UF33456
UF33471
0.74
1
1
0.9
1
1
1
1
Central
East
C. berlandieri
C. p. floridanus
1.5
1.25
1
0.75
0.5
0.25
0
Time (Myr)

Figure 1B.

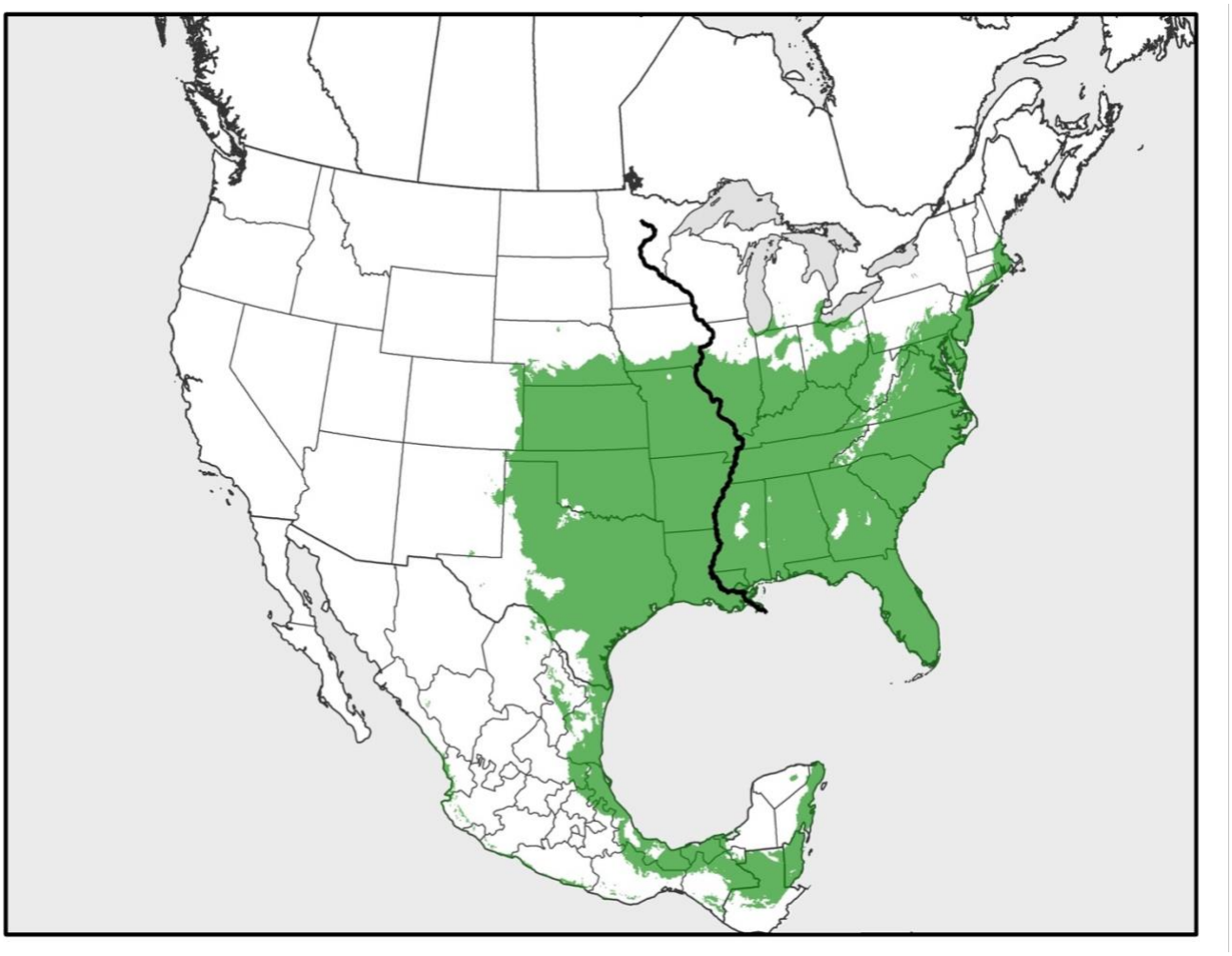

Figure 1C.

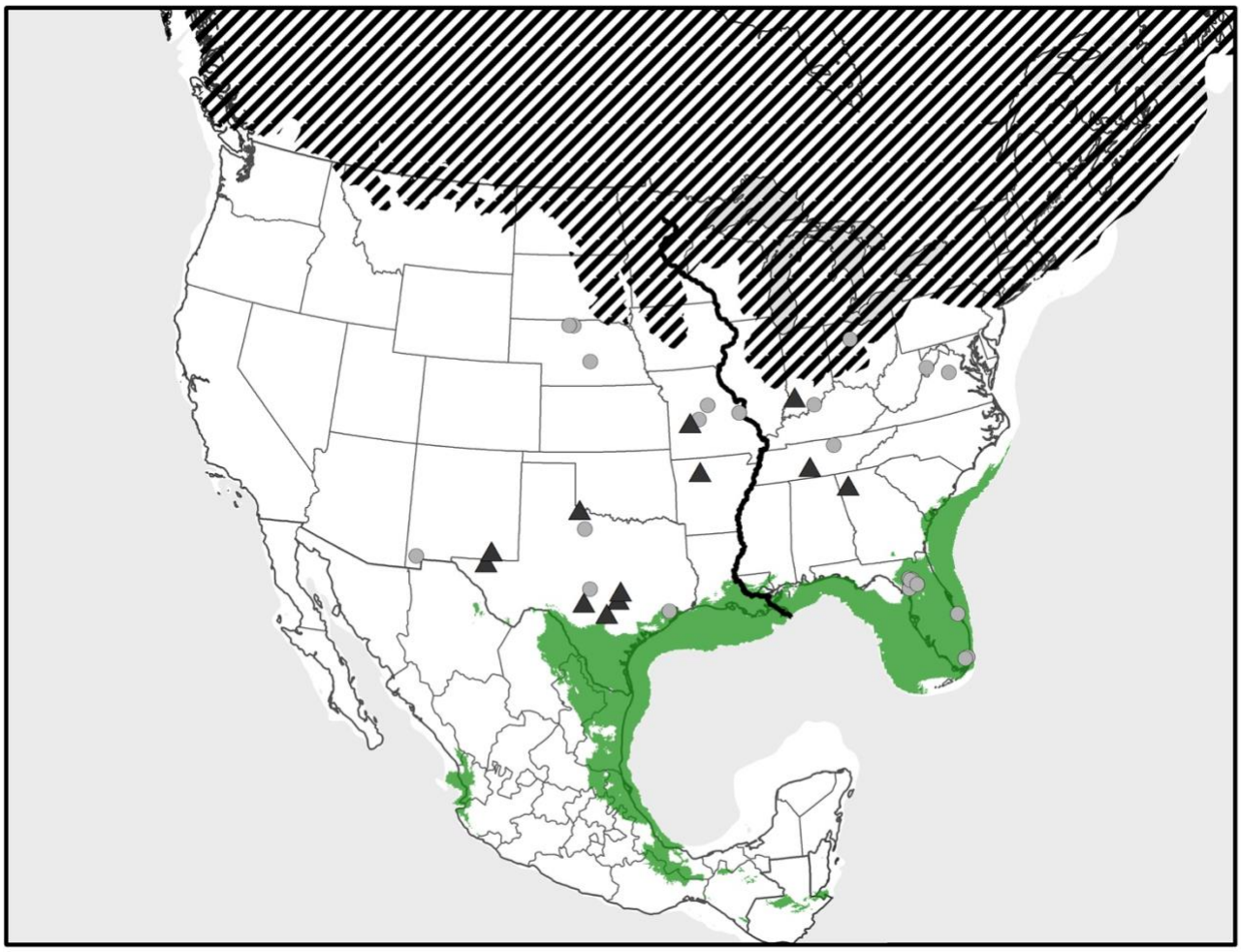

Figure 1D.

Figure 1. (A) Sampling and phylogeographic structure for *Cryptotis parvus*. Colored polygons represent the estimated distribution of distinct lineages modified from IUCN Red List rangewide distribution maps, and transitions between lineages correspond to equidistant boundaries between occurrence points. Colors of polygons and points correspond to designated lineages. Points represented by two colors are localities where two lineages were detected; **(B)** Bayesian cytochrome b genealogy for *Cryptotis parvus*. Colors correspond to supported geographically discrete lineages. Tip labels correspond to GenBank identifiers (Supplementary Information Table1), and branch labels represent posterior probability support for lineages. The Y-axis represents a timeline in millions of years before present; **(C)** ENM for current conditions. Predicted areas of suitability are shaded in green; **(D)** ENM for LGM conditions. Points signify FAUNMAP fossil occurrences during the Late Wisconsin (11.8 - 29 kya), and hash lines indicate extent of glacial ice sheets. Black triangles represent fossil records dated to temporal confidence interval completely contained within the Late Wisconsin timeframe (both maximum and minimum ages within 11.8 - 29 kya). Grey circles represent fossil occurrences dated to a temporal confidence interval that intersects but is not contained within the Late Wisconsin timeframe (maximum and minimum ages may be outside 11.8 - 19 kya).

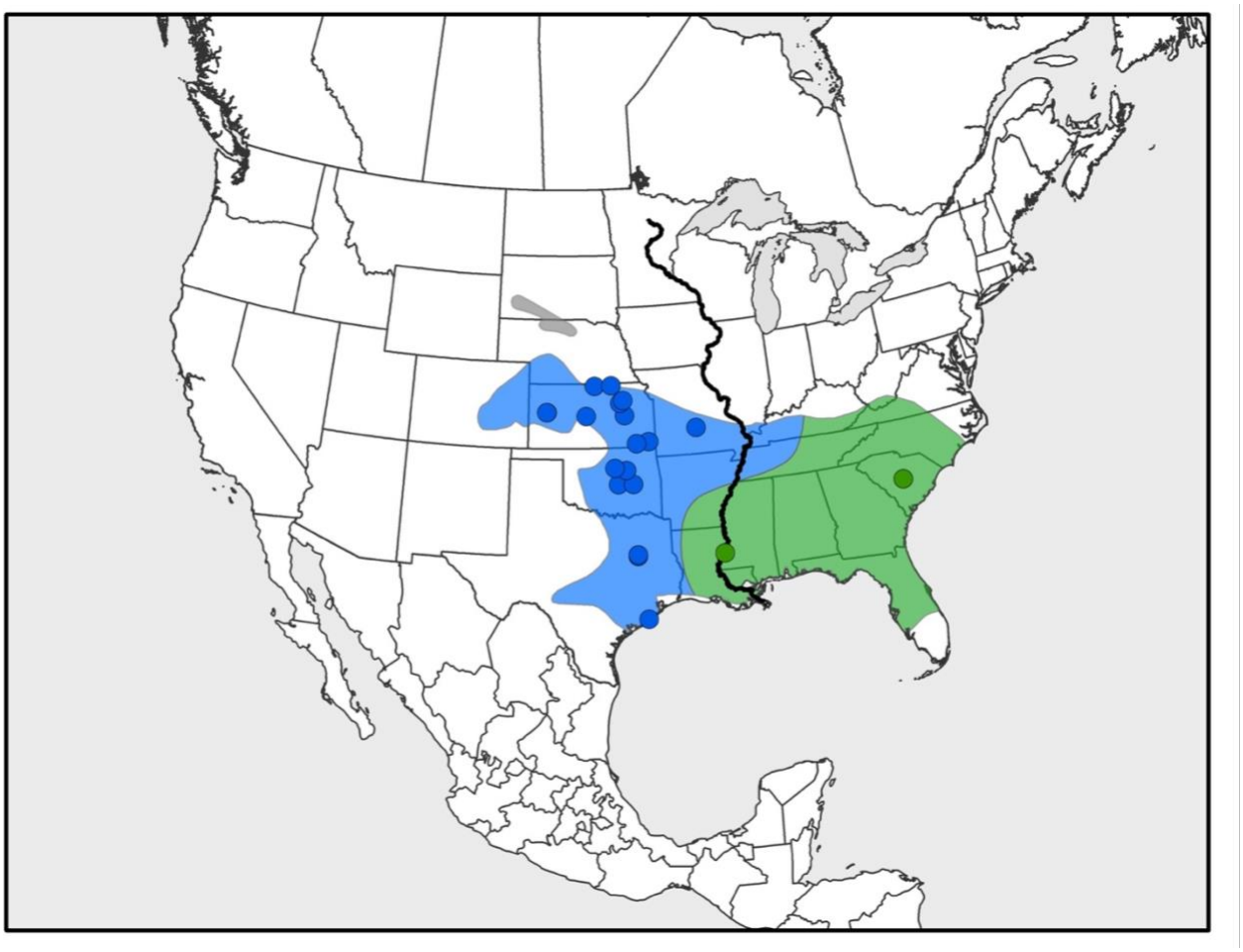

Figure 2A.

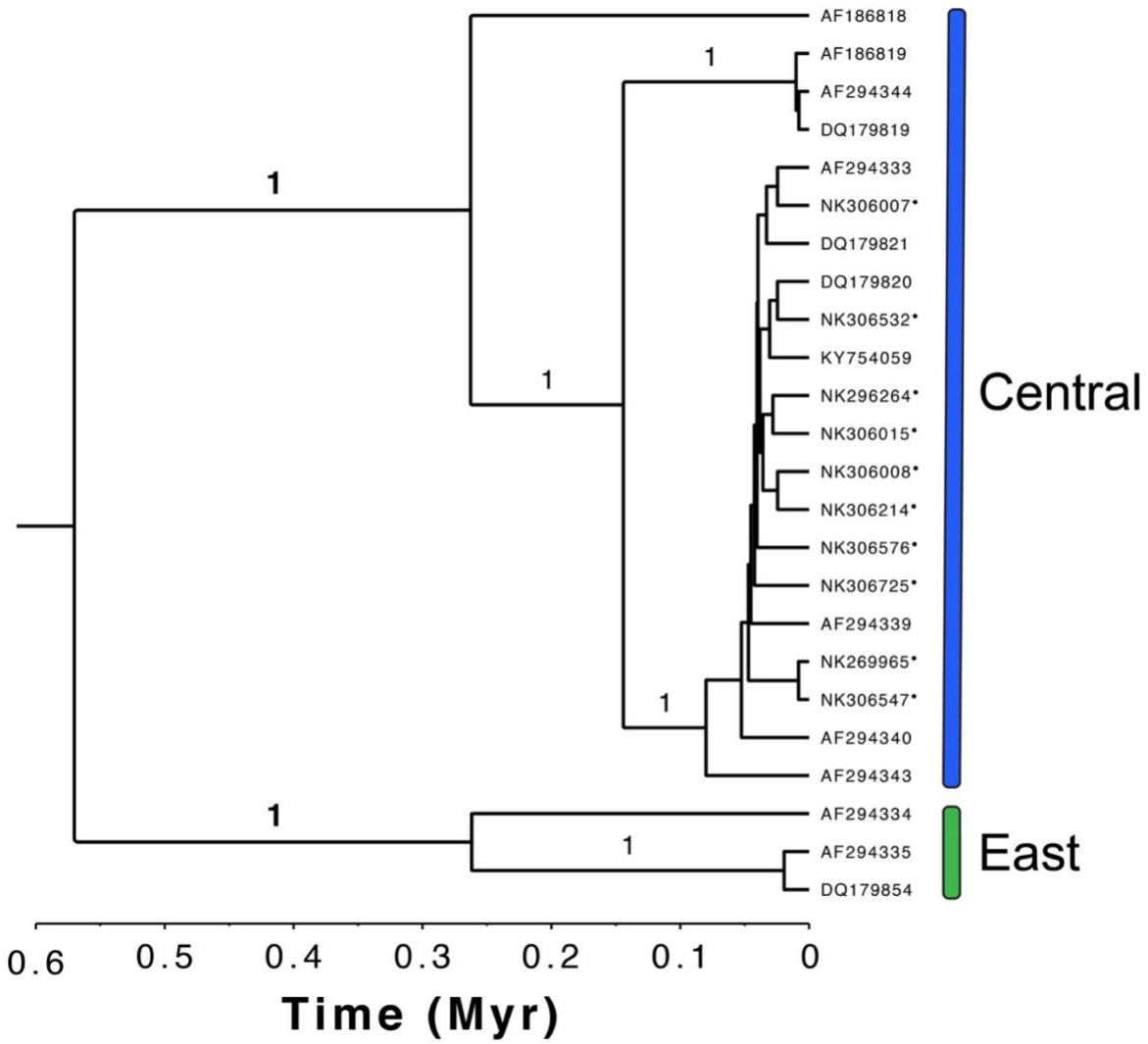
AF186818
AF186819
AF294344
DQ179819
AF294333
NK306007•
DQ179821
DQ179820
NK306532•
KY754059
NK296264•
NK306015•
NK306008•
NK306214•
NK306576•
NK306725•
AF294339
NK269965•
NK306547•
AF294340
AF294343
AF294334
AF294335
DQ179854
1
1
1
1
1
1
Central
East
0.6
0.5
0.4
0.3
0.2
0.1
0
Time (Myr)

Figure 2B.

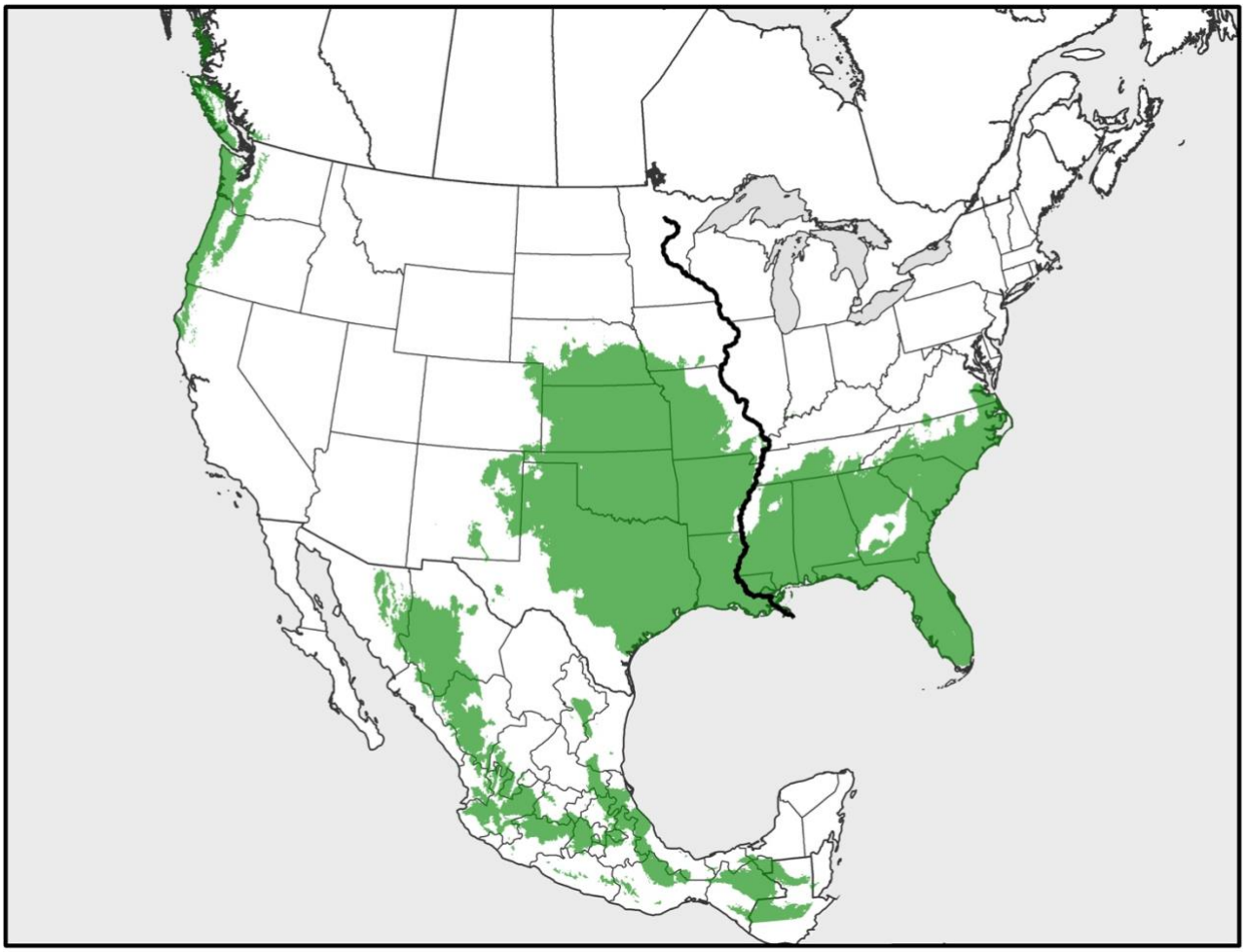

Figure 2C.

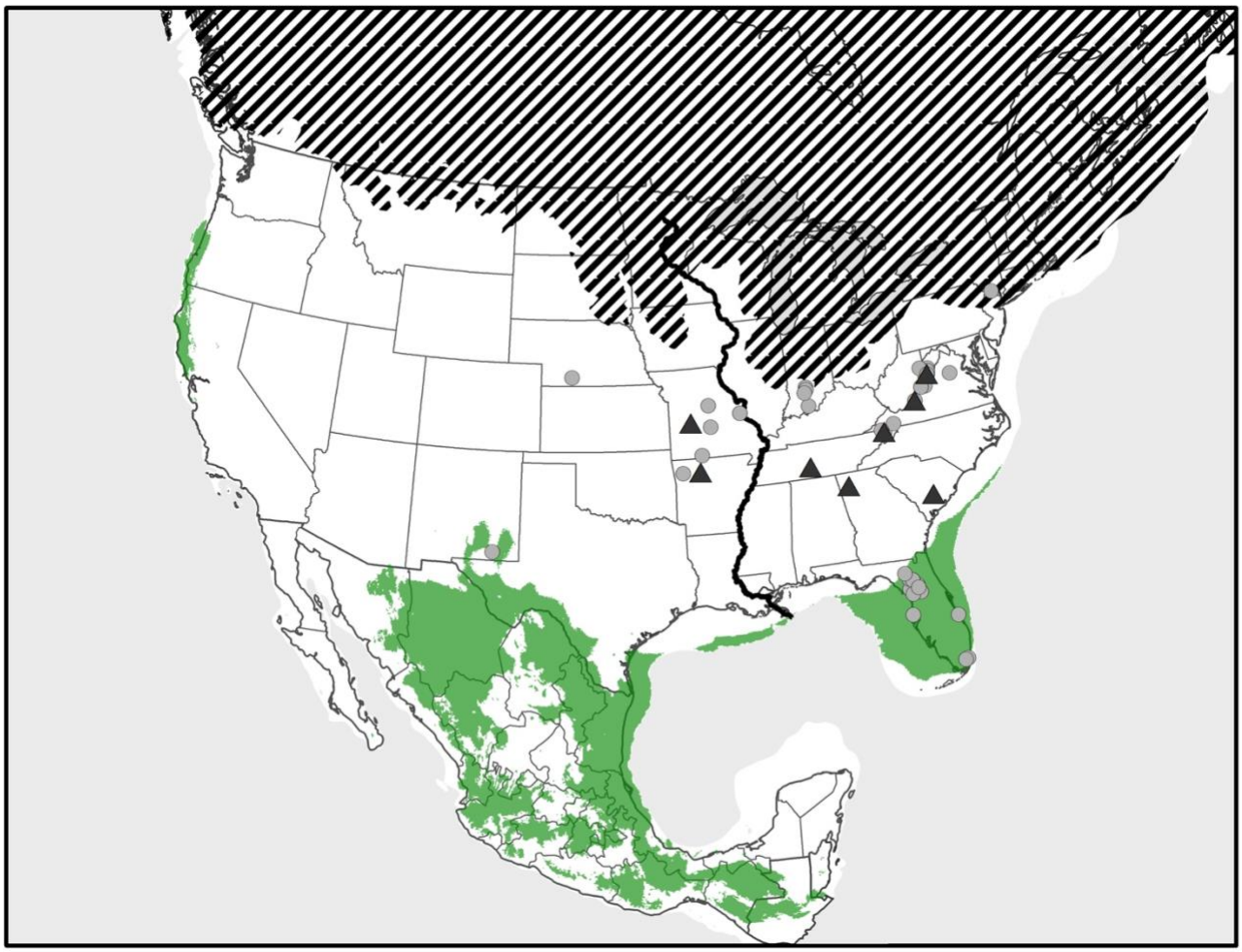

Figure 2D.

Figure 2. (A) Sampling and phylogeographic structure for *Neotoma floridana*. Colored polygons represent the estimated distribution of distinct lineages modified from IUCN Red List rangewide distribution maps, and transitions between lineages correspond to equidistant boundaries between occurrence points. Colors of polygons and points correspond to designated lineages. Points represented by two colors are localities where two lineages were detected; **(B)** Bayesian cytochrome b genealogy for *Neotoma floridana*. Colors correspond to geographically and genetically discrete lineages. Tip labels correspond to GenBank identifiers (Supplementary Information Table1), and branch labels represent posterior probability support for lineages. The Y-axis represents a timeline in millions of years before present; **(C)** ENM for current conditions. Predicted areas of suitability are shaded in green; **(D)** ENM for LGM conditions. Points signify FAUNMAP fossil occurrences during the Late Wisconsin (11.8 - 29 kya), and hash lines indicate extent of glacial ice sheets. Black triangles represent fossil occurrences dated to temporal confidence interval completely contained within the Late Wisconsin timeframe (both maximum and minimum ages between 11.8 - 29 kya). Grey circles represent fossil occurrences dated to a temporal confidence interval that intersects but is not contained within the Late Wisconsin timeframe (maximum and minimum ages may be outside 11.8 - 29 kya).

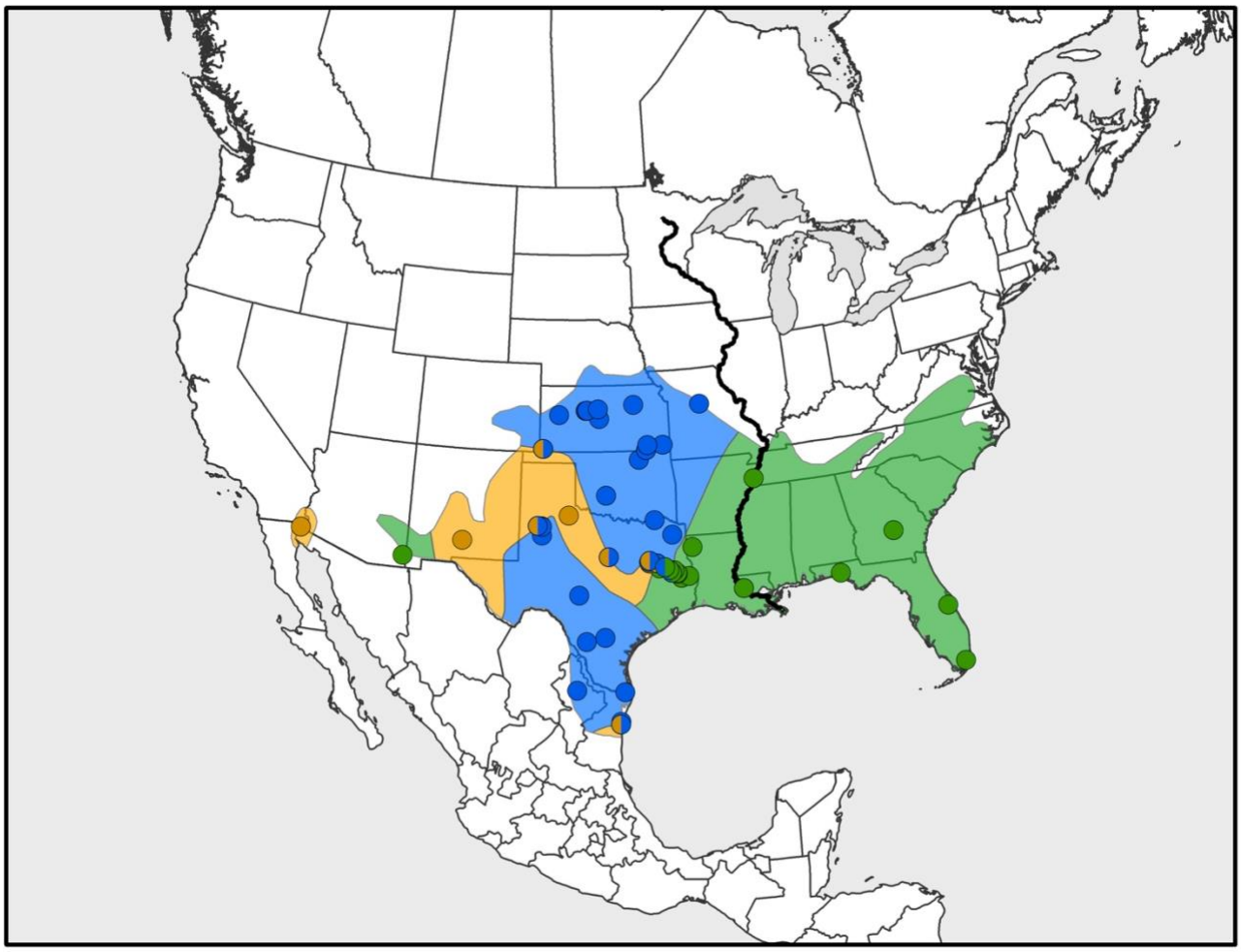

Figure 3A.

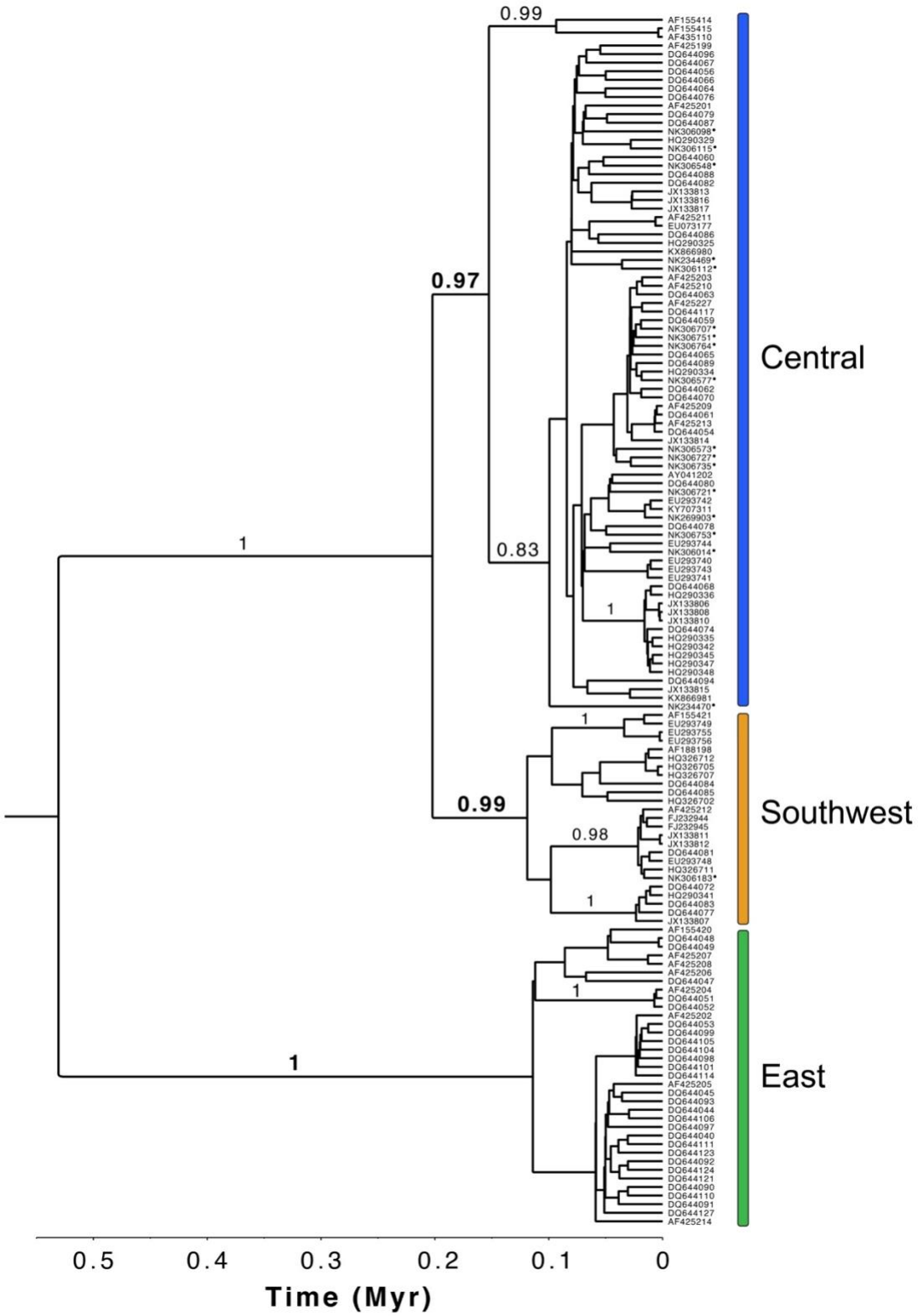
0.99
0.97
0.83
1
0.99
0.98
1
1
1
1
Central
Southwest
East
0.5
0.4
0.3
0.2
0.1
0
Time (Myr)

Figure 3B.

Figure 3C.

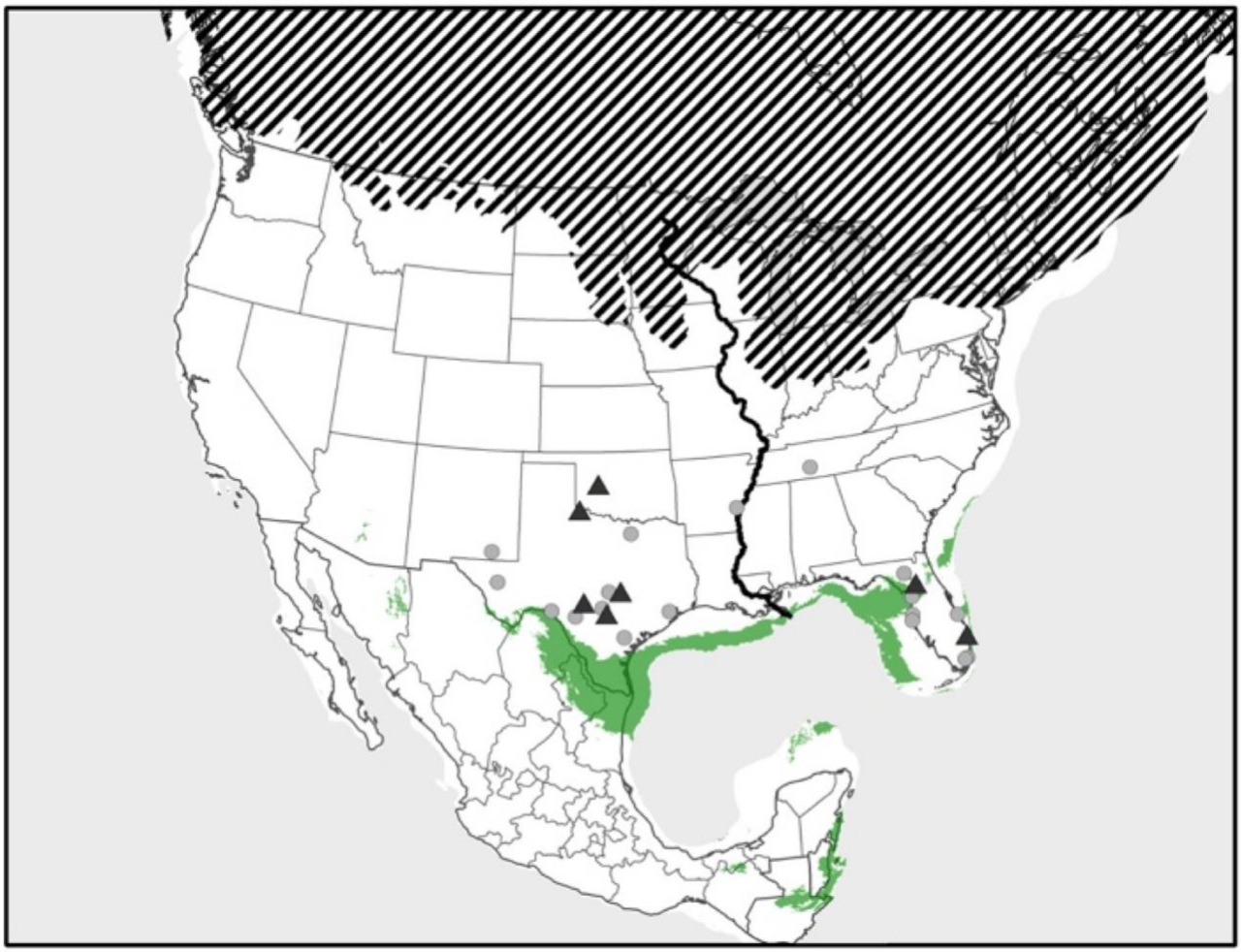

Figure 3D.
Figure 3. (A) Sampling and phylogeographic structure for *Sigmodon hispidus*. Colored polygons represent the estimated distribution of distinct lineages modified from IUCN Red List rangewide distribution maps, and transitions between lineages correspond to equidistant boundaries between occurrence points. Colors of polygons and points correspond to designated lineages. Points represented by two colors are localities where two lineages were detected; **(B)** Bayesian cytochrome b genealogy for *Sigmodon hispidus*. Colors correspond to supported geographically discrete lineages. Tip labels correspond to GenBank identifiers (Supplementary Information Table1), and branch labels represent posterior probability support for lineages. The Y-axis represents a timeline in millions of years before present; **(C)** ENM for current conditions. Predicted areas of suitability are shaded in green; **(D)** ENM for LGM conditions. Points signify FAUNMAP fossil occurrences during the Late Wisconsin (11.8 - 29 kya), and hash lines indicate extent of glacial sheets. Black triangles represent fossil occurrences dated to temporal confidence interval completely contained within the Late Wisconsin timeframe (both maximum and minimum ages within 11.8 - 29 kya). Grey circles represent fossil occurrences dated to a temporal confidence interval that intersects but is not contained within the Late Wisconsin timeframe (maximum and minimum ages may be outside 11.8 - 19 kya).

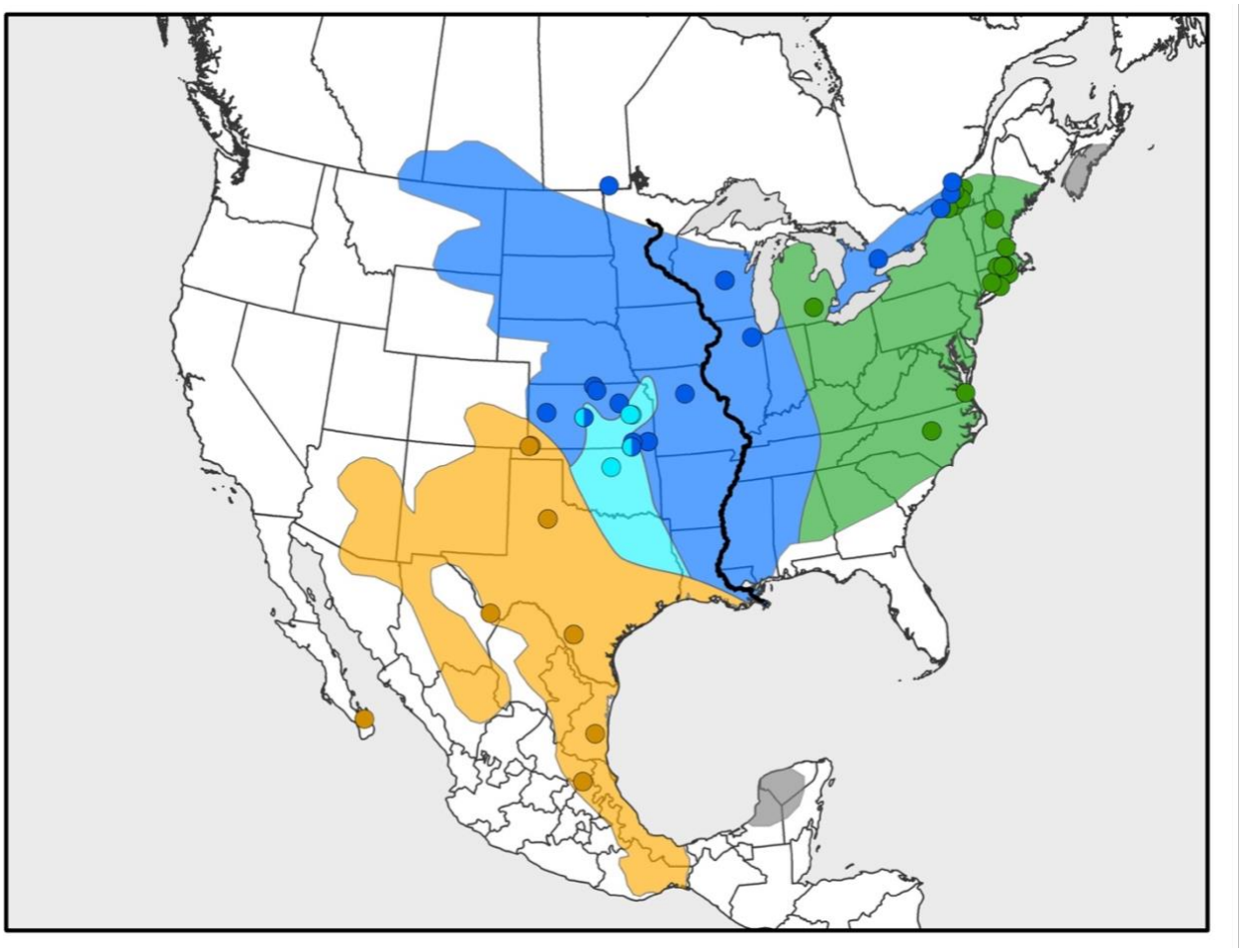

Figure 4A.

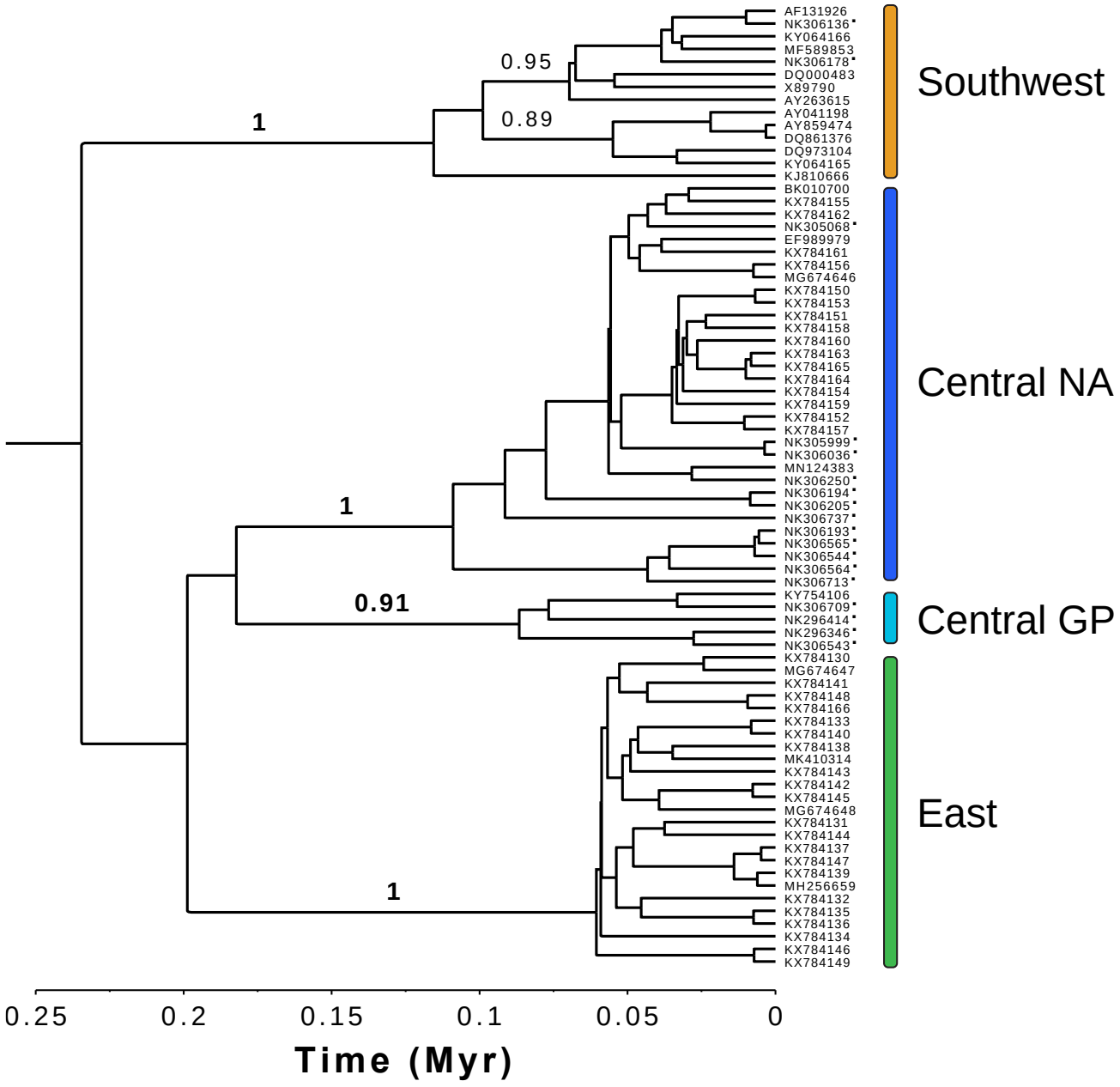
AF131926
NK306136
KY064166
MF589853
NK306178
DQ000483
X89790
AY263615
AY041198
AY859474
DQ861376
DQ973104
KY064165
KJ810666
BK010700
KX784155
KX784162
NK305068
EF989979
KX784161
KX784156
MG674646
KX784150
KX784153
KX784151
KX784158
KX784160
KX784163
KX784165
KX784164
KX784154
KX784159
KX784152
KX784157
NK305999
NK306036
MN124383
NK306250
NK306194
NK306205
NK306737
NK306193
NK306565
NK306544
NK306564
NK306713
KY754106
NK306709
NK296414
NK296346
NK306543
KX784130
MG674647
KX784141
KX784148
KX784166
KX784133
KX784140
KX784138
MK410314
KX784143
KX784142
KX784145
MG674648
KX784131
KX784144
KX784137
KX784147
KX784139
MH256659
KX784132
KX784135
KX784136
KX784134
KX784146
KX784149
0.95
0.89
1
1
0.91
1
Southwest
Central NA
Central GP
East
0.25
0.2
0.15
0.1
0.05
0
Time (Myr)

Figure 4B.

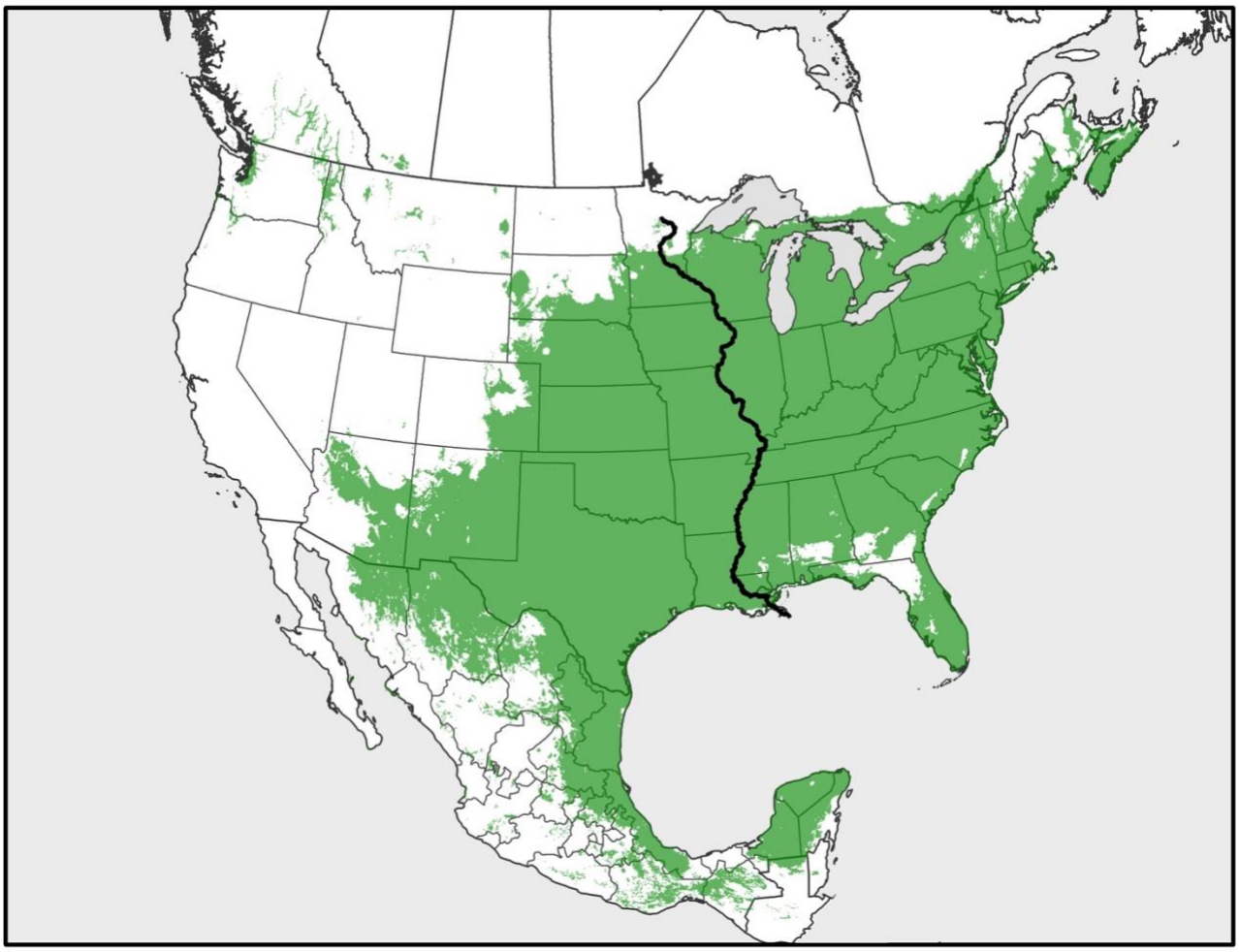

Figure 4C.

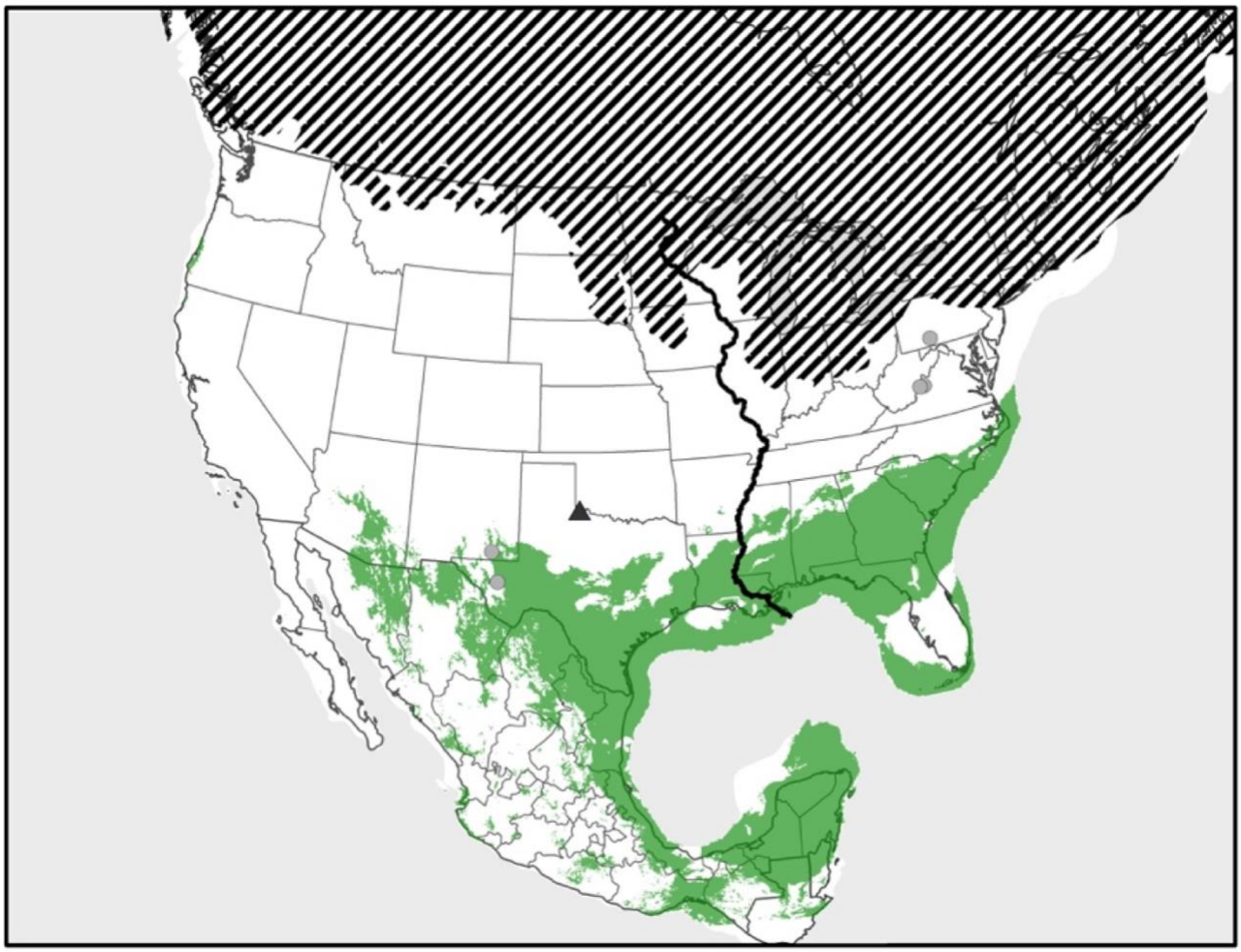

Figure 4D.

Figure 4. (A) Sampling and phylogeographic structure for *Peromyscus leucopus*. Colored polygons represent the estimated distribution of distinct lineages modified from IUCN Red List rangewide distribution maps, and transitions between lineages correspond to equidistant boundaries between occurrence points. Colors of polygons and points correspond to designated lineages. Points represented by two colors are localities where two lineages were detected; **(B)** Bayesian cytochrome b genealogy for *Peromyscus leucopus*. Colors correspond to supported geographically discrete lineages. Tip labels correspond to GenBank identifiers (Supplementary Information Table1), and branch labels represent posterior probability support for lineages. The Y-axis represents a timeline in millions of years before present; **(C)** ENM for current conditions. Predicted areas of suitability are shaded in green; **(D)** ENM for LGM conditions. Points signify FAUNMAP fossil occurrences during the Late Wisconsin (11.8 - 29 kya), and hash lines indicate extent of glacial sheets. Black triangles represent fossil occurrences dated to temporal confidence interval completely contained within the Late Wisconsin timeframe (both maximum and minimum ages within 11.8 - 29 kya). Grey circles represent fossil occurrences dated to a temporal confidence interval that intersects but is not contained within the Late Wisconsin timeframe (maximum and minimum ages may be outside 11.8 - 19 kya).

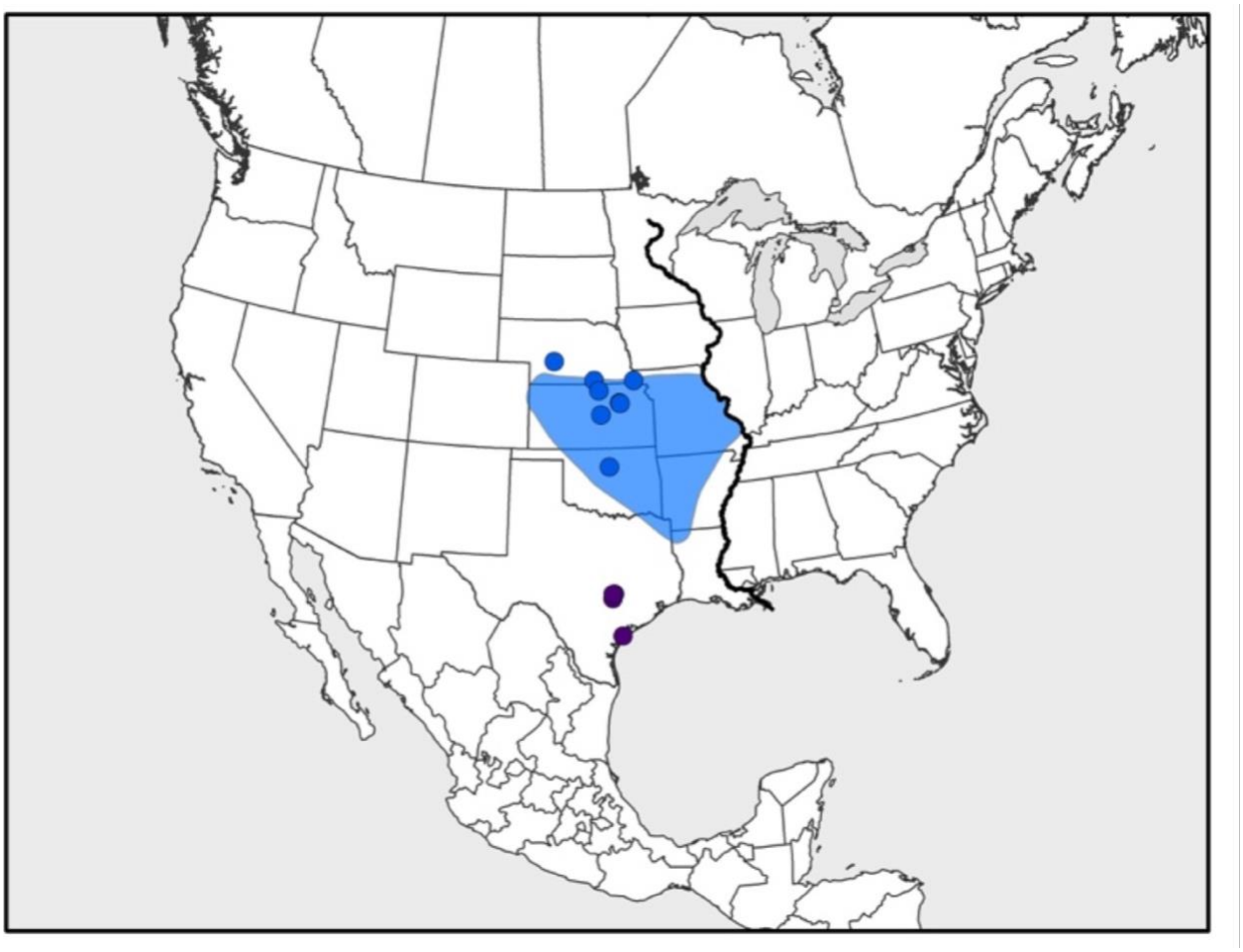

Figure 5A.

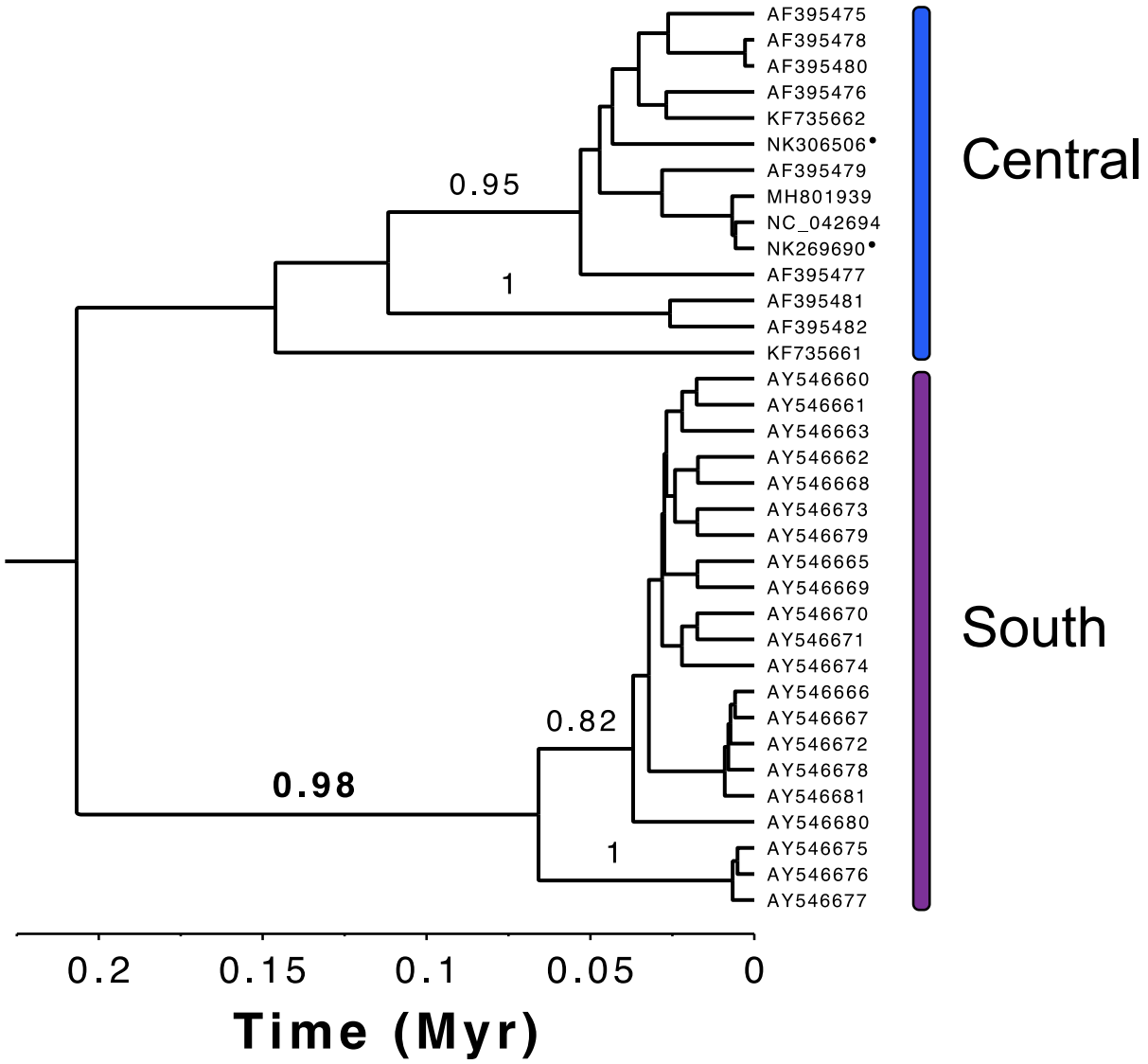
AF395475
AF395478
AF395480
AF395476
KF735662
NK306506
AF395479
MH801939
NC_042694
NK269690
AF395477
AF395481
AF395482
KF735661
AY546660
AY546661
AY546663
AY546662
AY546668
AY546673
AY546679
AY546665
AY546669
AY546670
AY546671
AY546674
AY546666
AY546667
AY546672
AY546678
AY546681
AY546680
AY546675
AY546676
AY546677
0.95
1
0.82
0.98
1
Central
South
0.2
0.15
0.1
0.05
0
Time (Myr)

Figure 5B.

Figure 5C.

Figure 5D.

Figure 5. (A) Sampling and phylogeographic structure for *Blarina hylophaga*. Colored polygons represent the estimated distribution of distinct lineages modified from IUCN Red List rangewide distribution maps, and transitions between lineages correspond to equidistant boundaries between occurrence points. Colors of polygons and points correspond to designated lineages; **(B)** Bayesian cytochrome b genealogy for *Blarina hylophaga*. Colors correspond to supported geographically discrete lineages. Tip labels correspond to GenBank identifiers (Supplementary Information Table1), and branch labels represent posterior probability support for lineages. The Y-axis represents a timeline in millions of years before present; **(C)** ENM for current conditions. Predicted areas of suitability are shaded in green; **(D)** ENM for LGM conditions. Points signify FAUNMAP fossil occurrences during Late Wisconsin (11.8 - 29 kya), and hash lines indicate extent of glacial sheets. Black triangles represent fossil occurrences dated to temporal confidence interval completely contained within the Late Wisconsin timeframe (both maximum and minimum ages within 11.8 - 29 kya). Grey circles represent fossil occurrences dated to a temporal confidence interval that intersects but is not contained within the Late Wisconsin timeframe (maximum and minimum ages may be outside 11.8 - 19 kya).

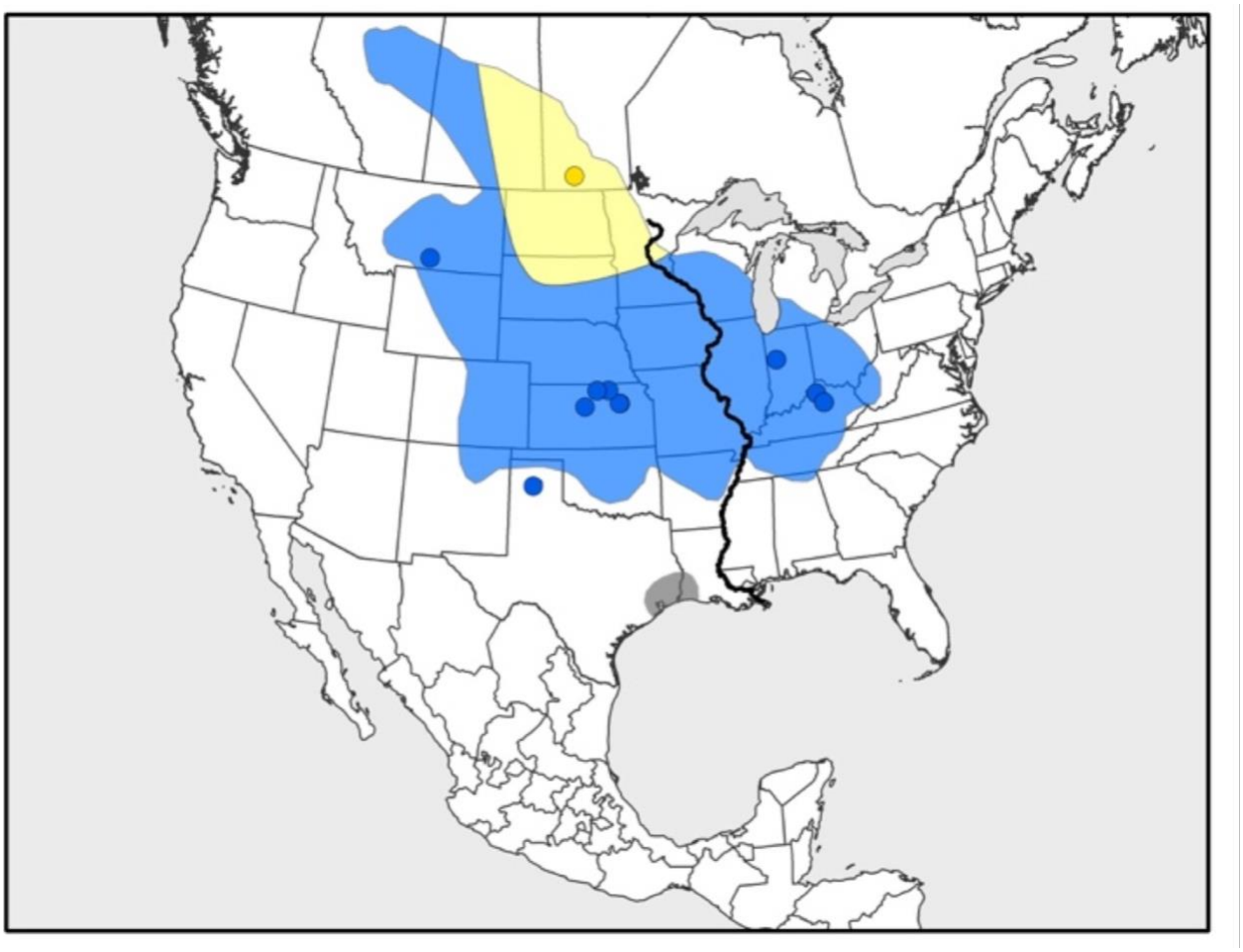

Figure 6A.

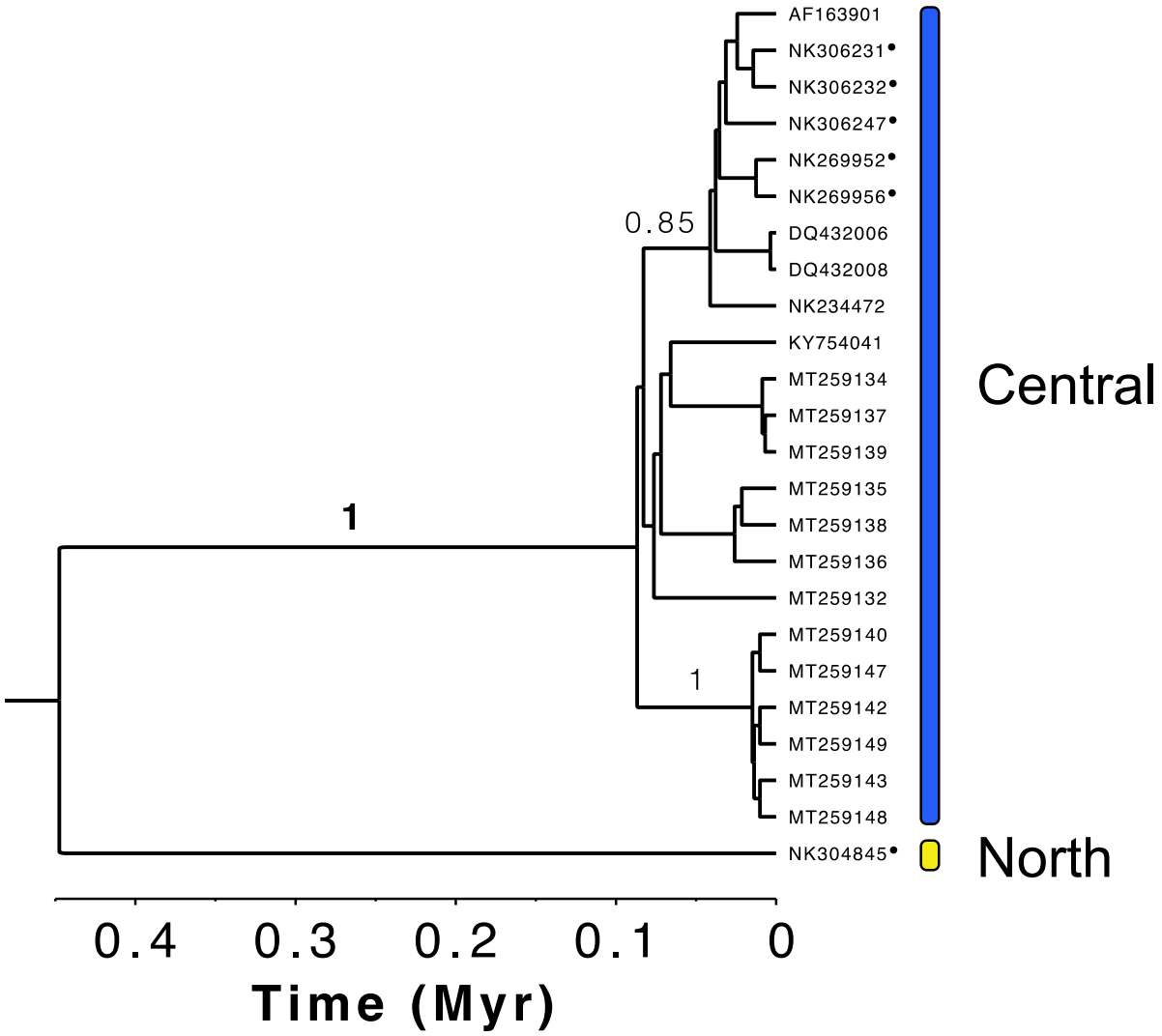
AF163901
NK306231
NK306232
NK306247
NK269952
NK269956
DQ432006
DQ432008
NK234472
KY754041
MT259134
MT259137
MT259139
MT259135
MT259138
MT259136
MT259132
MT259140
MT259147
MT259142
MT259149
MT259143
MT259148
NK304845
0.85
1
1
Central
North
0.4
0.3
0.2
0.1
0
Time (Myr)

Figure 6B.

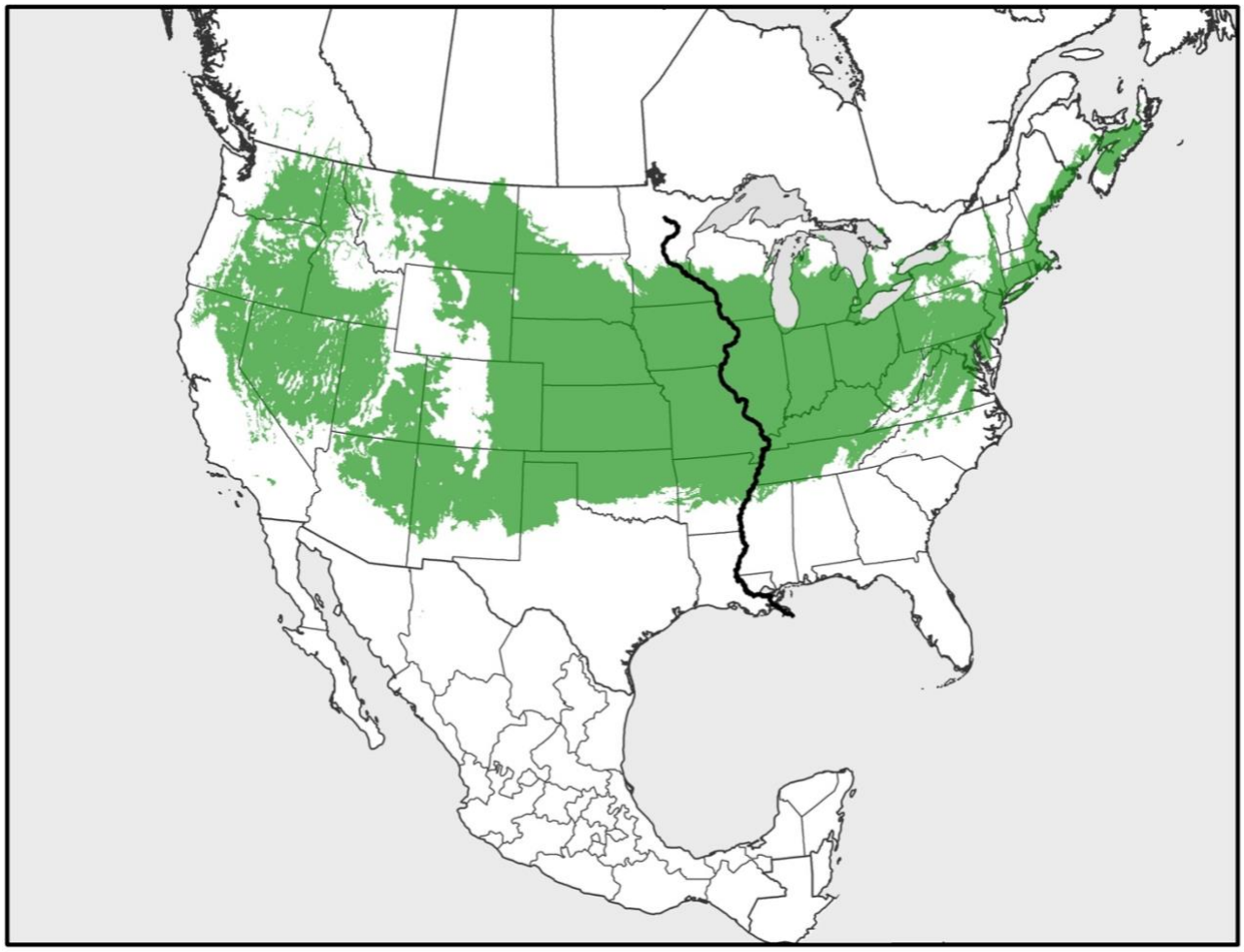

Figure 6C.

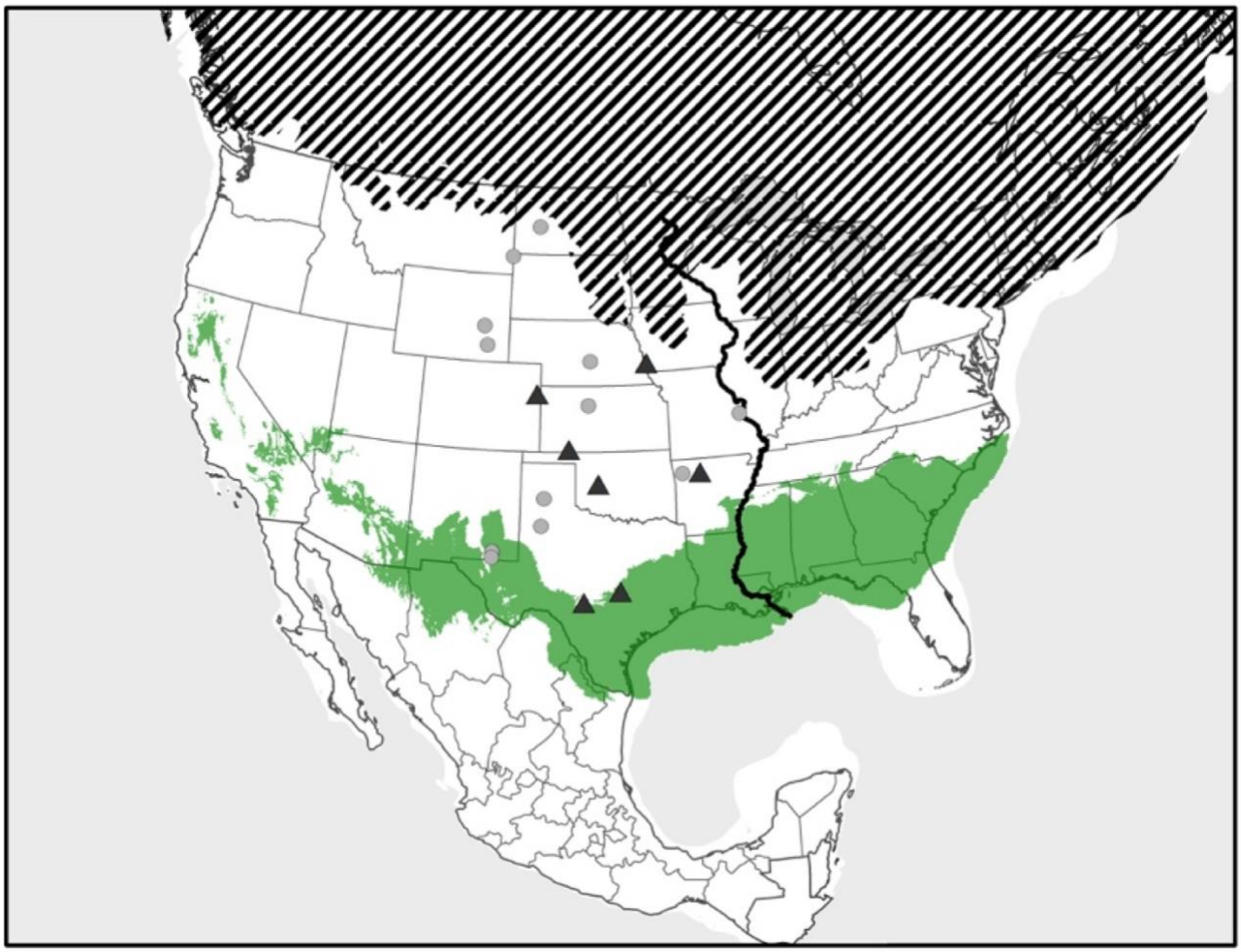

Figure 6D.

Figure 6. (A) Sampling and phylogeographic structure for *Microtus ochrogaster*. Colored polygons represent the estimated distribution of distinct lineages modified from IUCN Red List rangewide distribution maps, and transitions between lineages correspond to equidistant boundaries between occurrence points. Colors of polygons and points correspond to designated lineages, and the gray polygon represents a disjunct population absent of genetic records; **(B)** Bayesian cytochrome b genealogy for *Microtus ochrogaster*. Colors correspond to supported geographically discrete lineages. Tip labels correspond to GenBank identifiers (Supplementary Information Table1), and branch labels represent posterior probability support for lineages. The Y-axis represents a timeline in millions of years before present; **(C)** ENM for current conditions. Predicted areas of suitability are shaded in green; **(D)** ENM for LGM conditions. Points signify FAUNMAP fossil occurrences during the Late Wisconsin (11.8 - 29 kya), and hash lines indicate extent of glacial sheets. Black triangles represent fossil occurrences dated to temporal confidence interval completely contained within the Late Wisconsin timeframe (both maximum and minimum ages within 11.8 - 29 kya). Gray circles represent fossil occurrences dated to a temporal confidence interval that intersects but is not contained within the Late Wisconsin timeframe (maximum and minimum ages may be outside 11.8 - 19 kya).

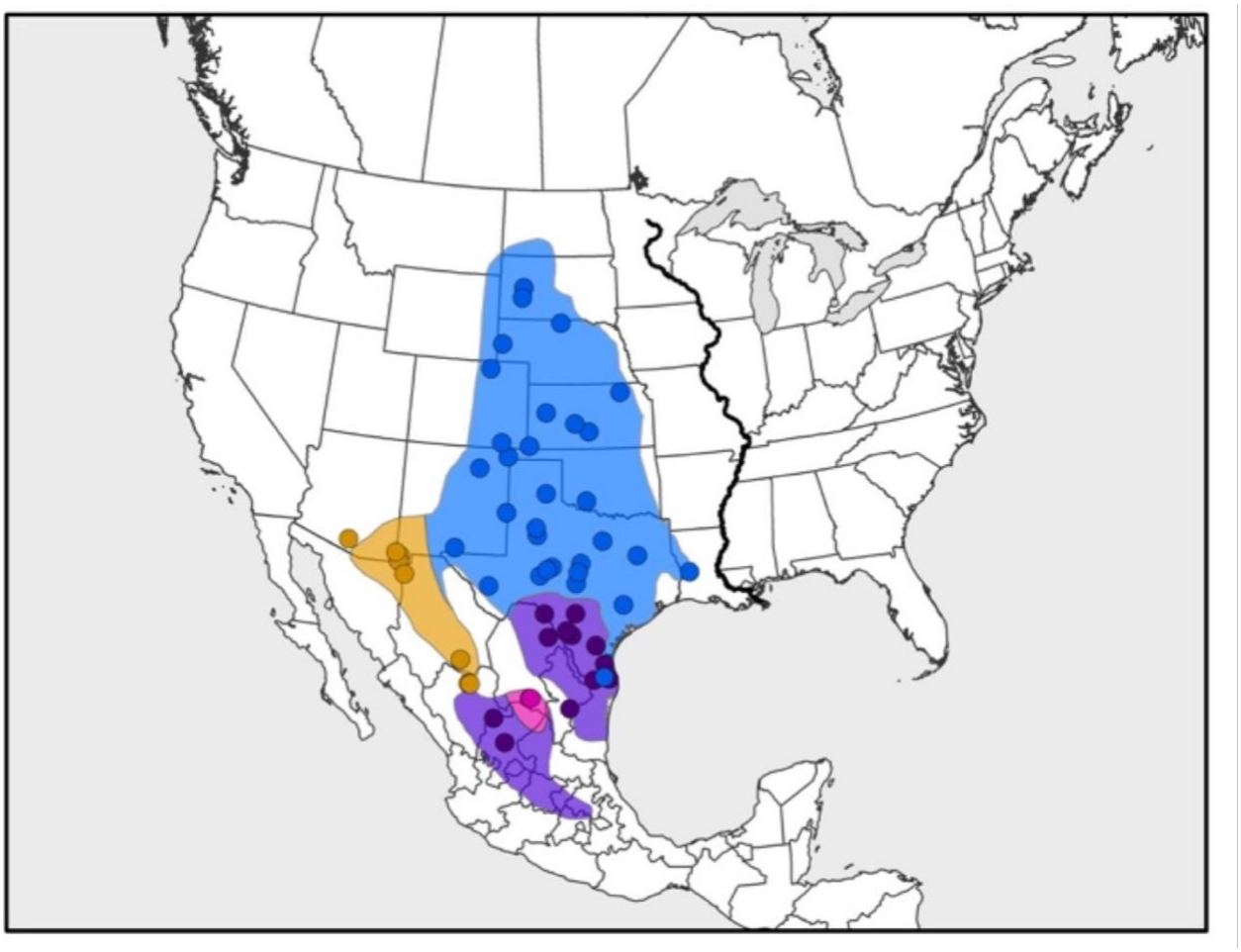

Figure 7A.

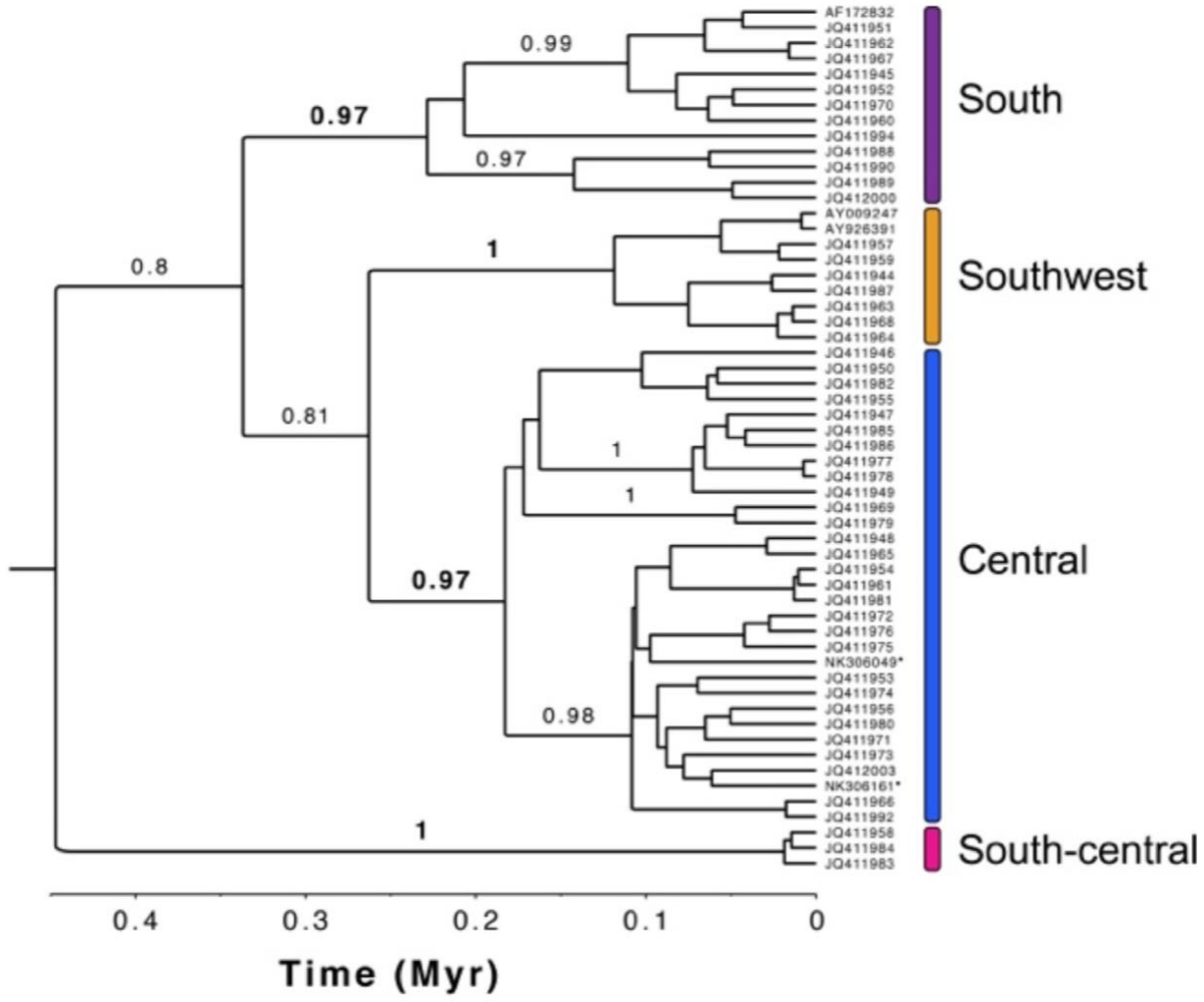
AF172832
JQ411951
JQ411962
JQ411967
JQ411945
JQ411952
JQ411970
JQ411960
JQ411994
JQ411988
JQ411990
JQ411989
JQ412000
AY009247
AY926391
JQ411957
JQ411959
JQ411944
JQ411987
JQ411963
JQ411968
JQ411964
JQ411946
JQ411950
JQ411982
JQ411955
JQ411947
JQ411985
JQ411986
JQ411977
JQ411978
JQ411949
JQ411969
JQ411979
JQ411948
JQ411965
JQ411954
JQ411961
JQ411981
JQ411972
JQ411976
JQ411975
NK306049*
JQ411953
JQ411974
JQ411956
JQ411980
JQ411971
JQ411973
JQ412003
NK306161*
JQ411966
JQ411992
JQ411958
JQ411984
JQ411983
0.99
0.97
0.97
0.8
1
0.81
1
1
0.97
0.98
1
South
Southwest
Central
South-central
0.4
0.3
0.2
0.1
0
Time (Myr)

Figure 7B.

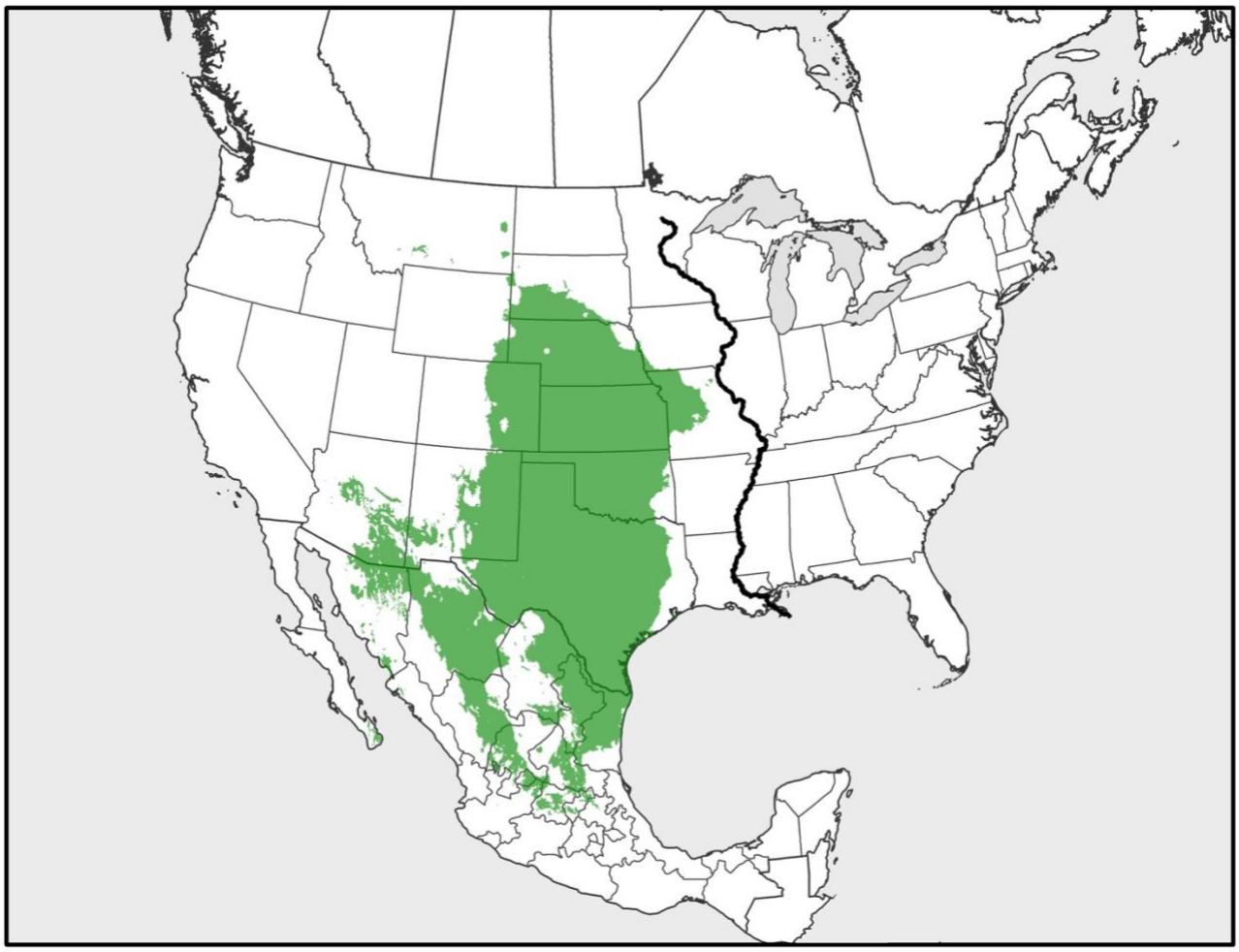

Figure 7C.

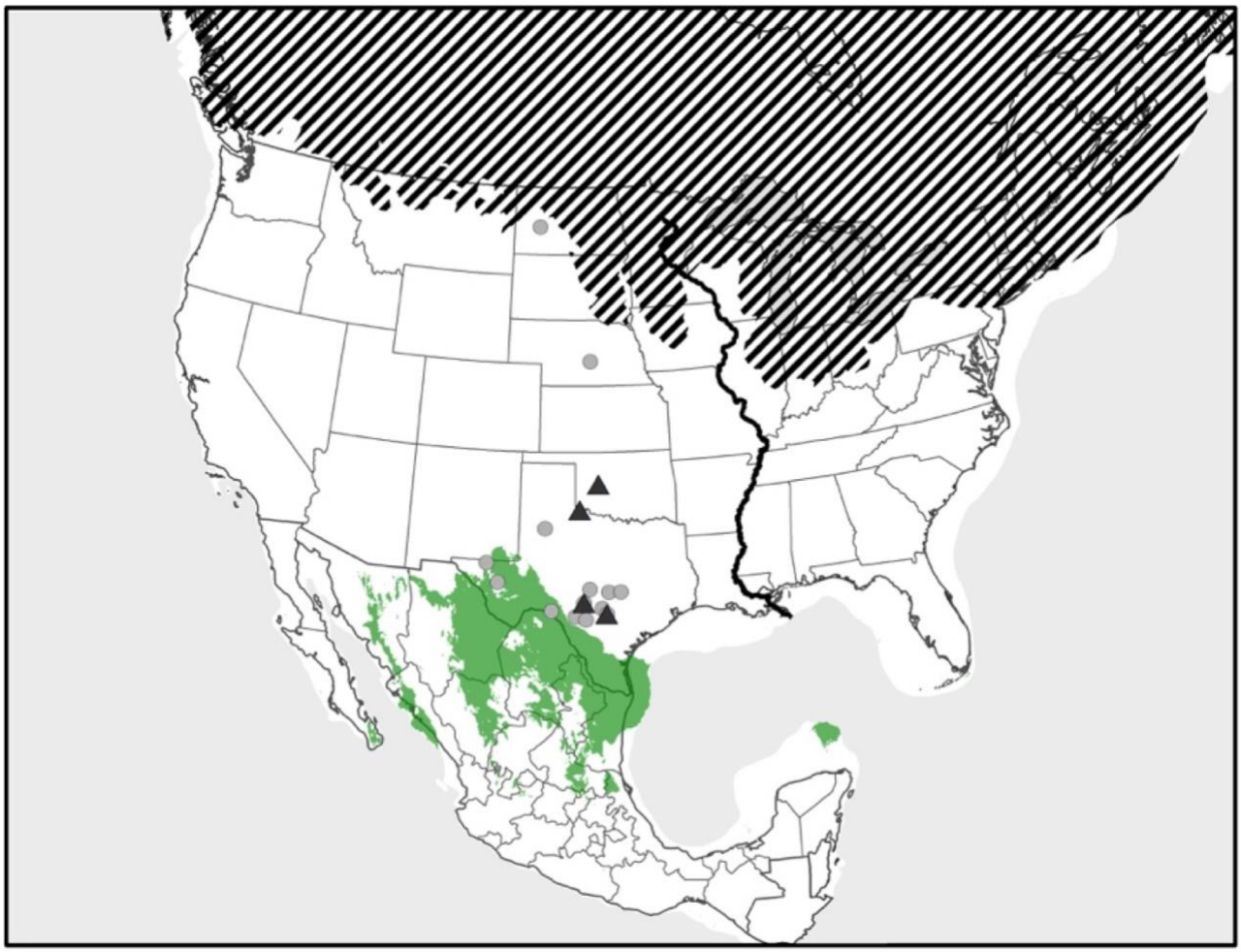

Figure 7D.

Figure 7. (A) Bayesian cytochrome b genealogy for *Chatodipus hispidus*. Colors correspond to supported geographically discrete lineages. Tip labels correspond to GenBank identifiers (Supplementary Information Table1), and branch labels represent posterior probability support for lineages. The Y-axis represents a timeline in millions of years before present; **(B)** Sampling and phylogeographic structure for *Chatodipus hispidus*. Colored polygons represent the estimated distribution of distinct lineages modified from IUCN Red List rangewide distribution maps, and transitions between lineages correspond to equidistant boundaries between occurrence points. Colors of polygons and points correspond to designated lineages; **(C)** ENM for current conditions. Predicted areas of suitability are shaded in green; **(D)** ENM for LGM conditions. Points signify FAUNMAP fossil occurrences during the Late Wisconsin (11.8 - 29 kya), and hash lines indicate extent of glacial sheets. Black triangles represent fossil occurrences dated to temporal confidence interval completely contained within the Late Wisconsin timeframe (both maximum and minimum ages within 11.8 - 29 kya). Grey circles represent fossil occurrences dated to a temporal confidence interval that intersects but is not contained within the Late Wisconsin timeframe (maximum and minimum ages may be outside 11.8 - 19 kya).

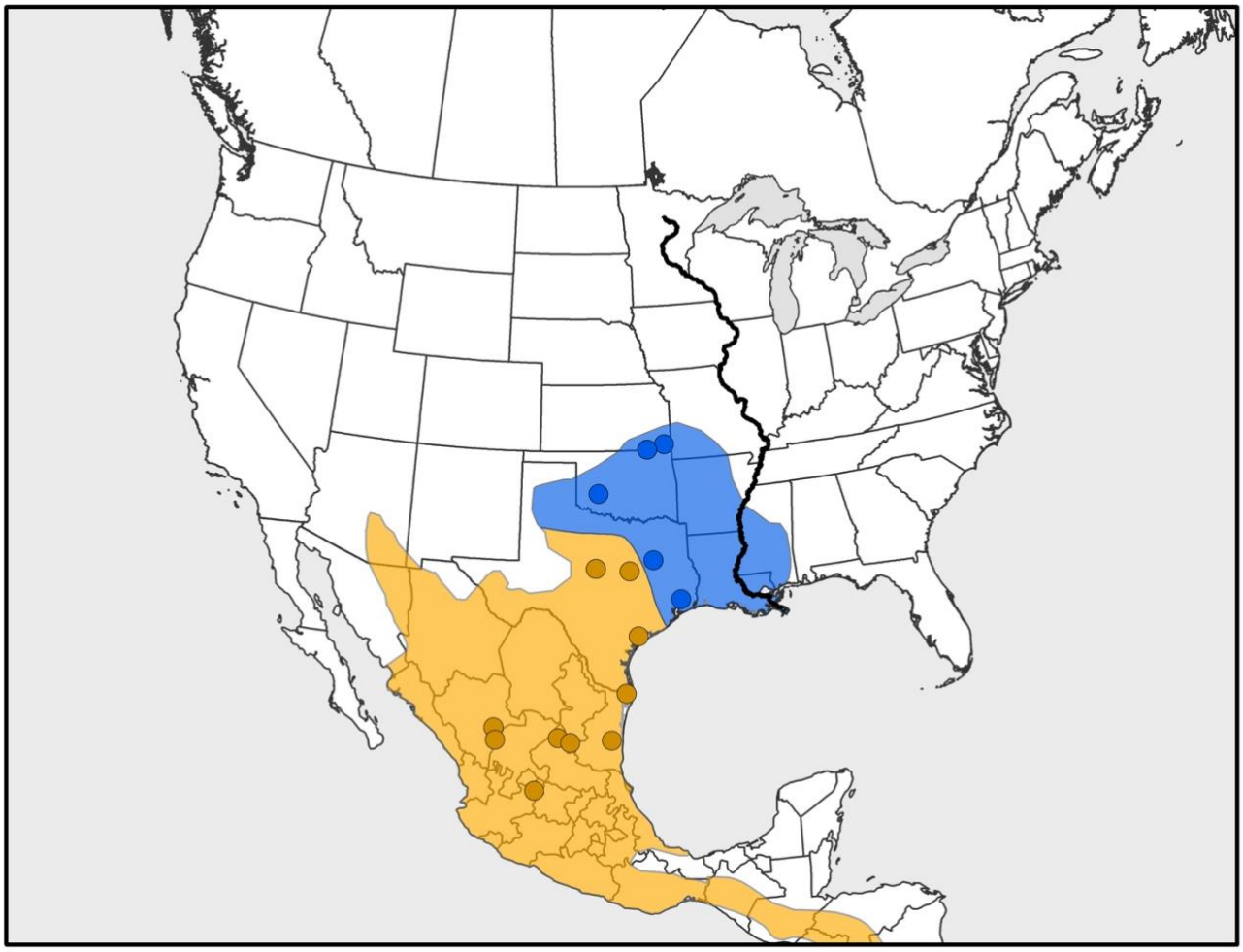

Figure 8A.

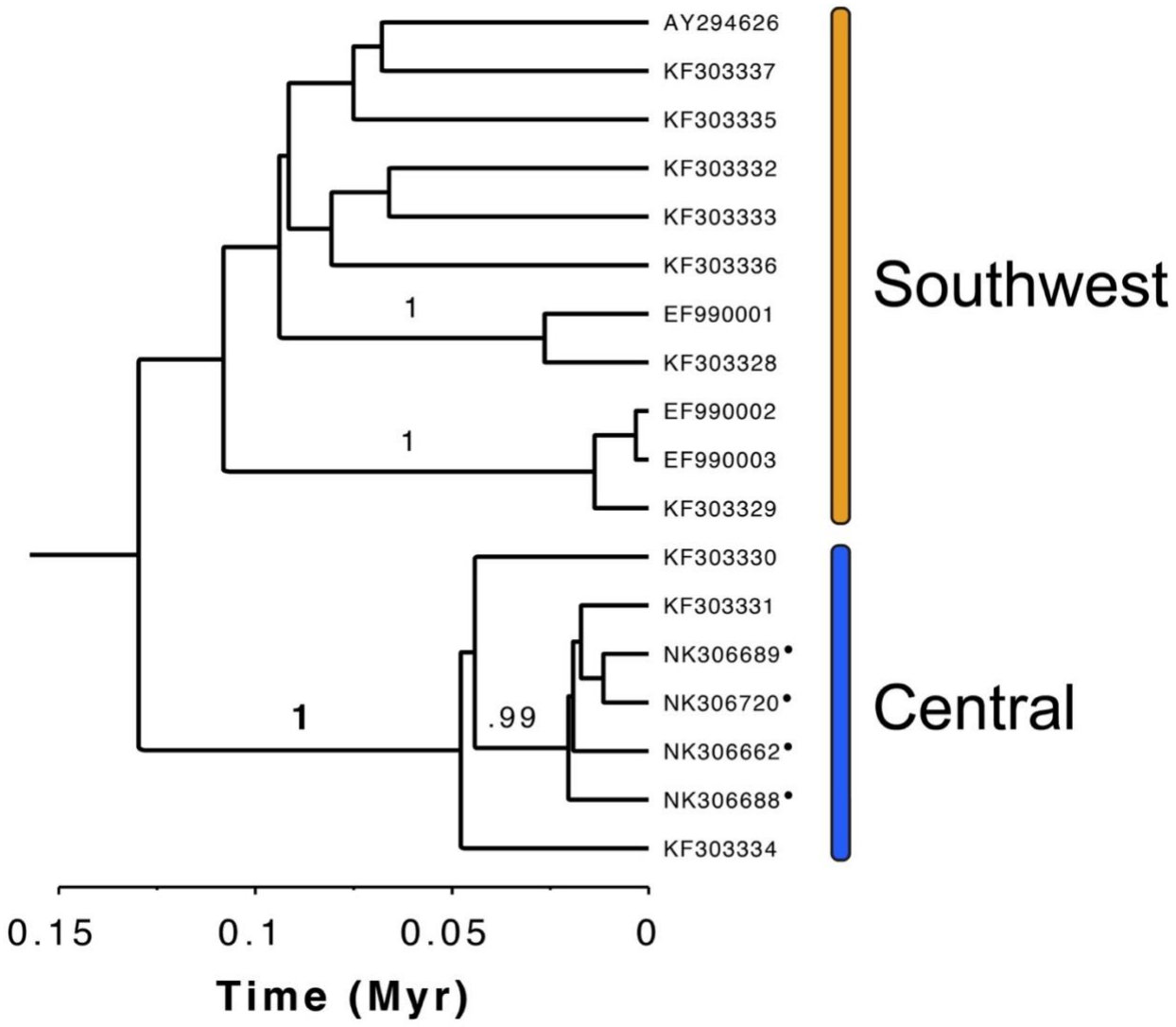
AY294626
KF303337
KF303335
KF303332
KF303333
KF303336
1
EF990001
KF303328
EF990002
1
EF990003
KF303329
Southwest
KF303330
KF303331
NK306689
NK306720
1
.99
NK306662
NK306688
KF303334
Central
0.15
0.1
0.05
0
Time (Myr)

Figure 8B.

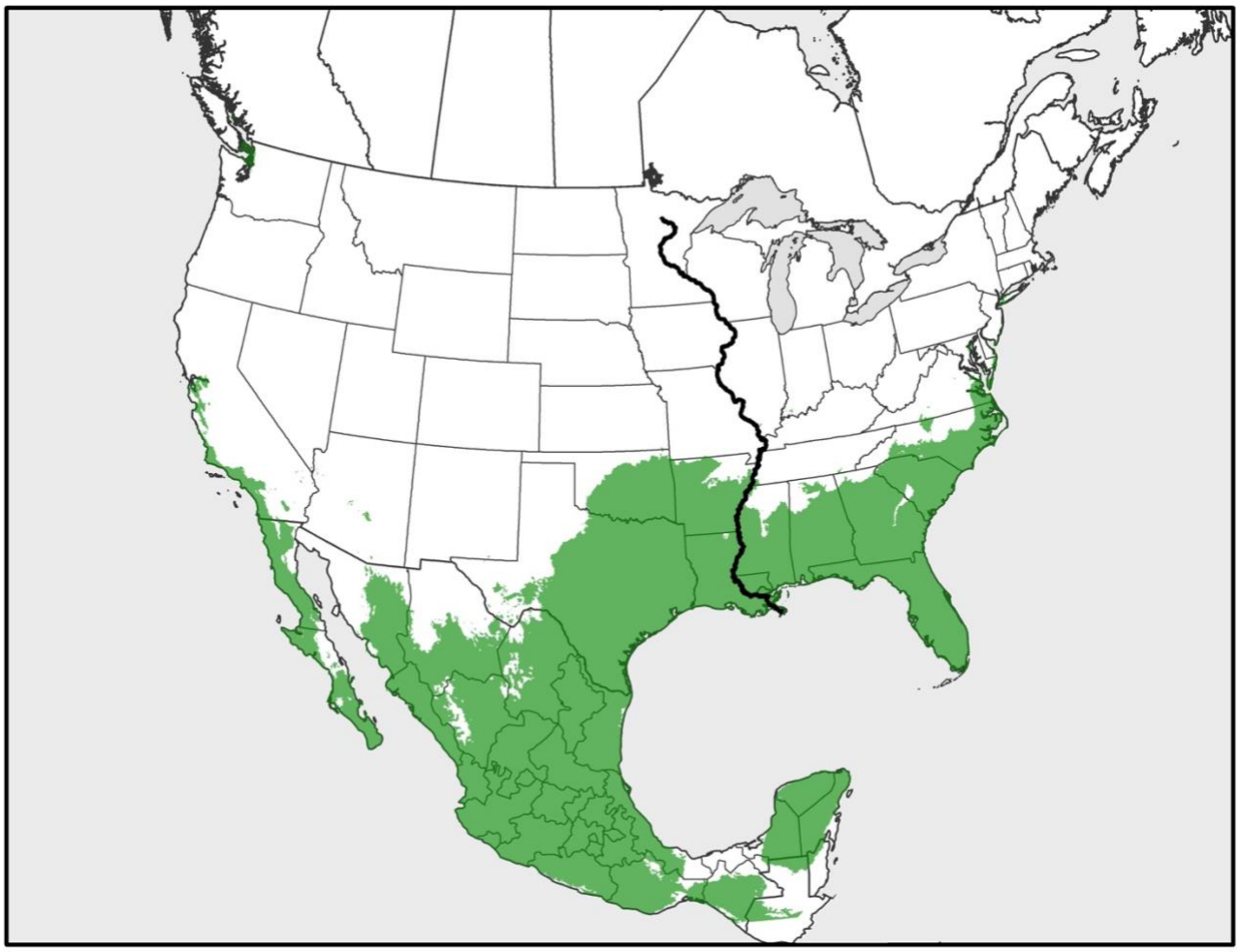

Figure 8C.

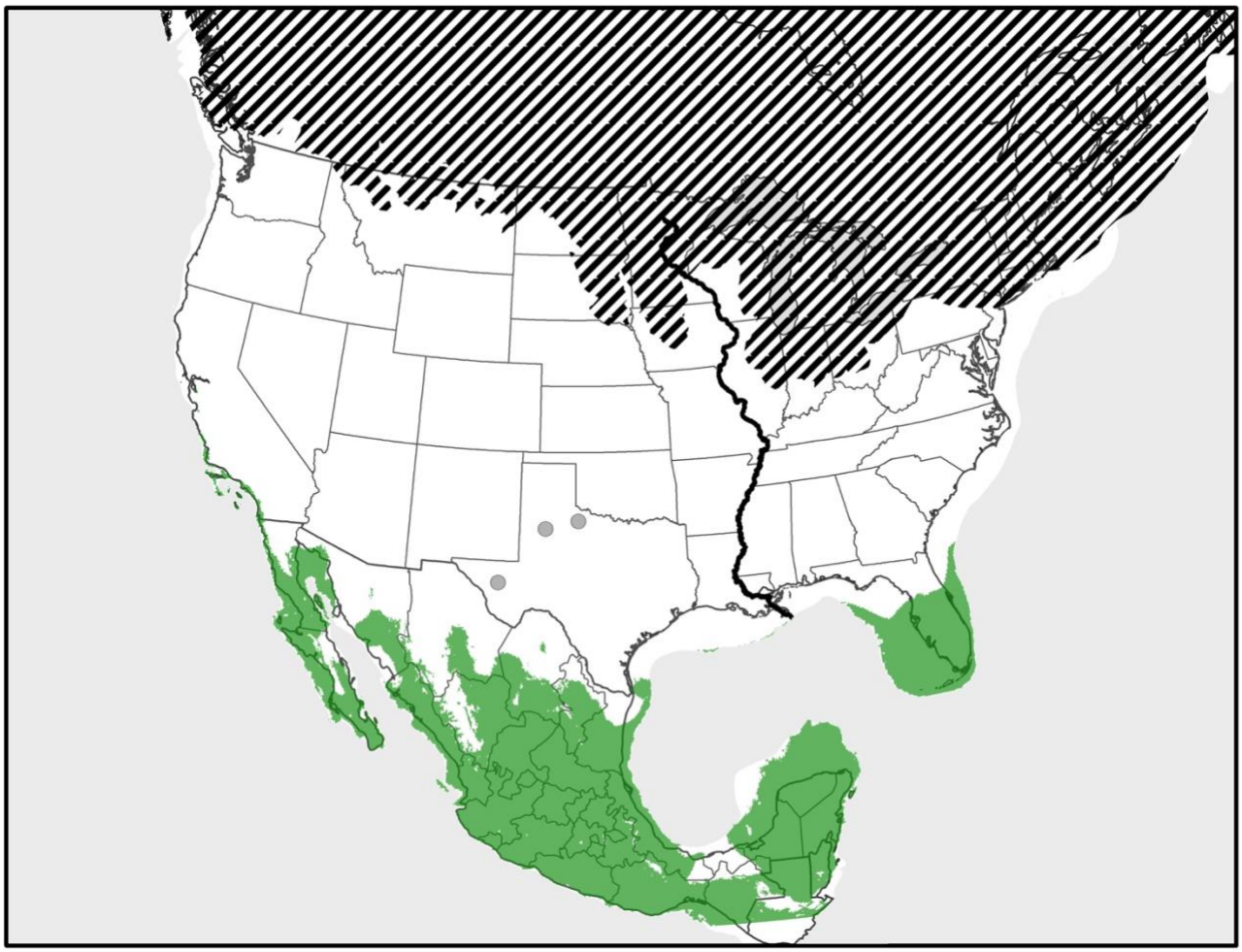

Figure 8D.
Figure 8. (A) Sampling and phylogeographic structure for *Reithrodontomys fulvescens*. Colored polygons represent the estimated distribution of distinct lineages modified from IUCN Red List rangewide distribution maps, and transitions between lineages correspond to equidistant boundaries between occurrence points. Colors of polygons and points correspond to designated lineages; **(B)** Bayesian cytochrome b genealogy for *Reithrodontomys fulvescens*. Colors correspond to supported geographically discrete lineages. Tip labels correspond to GenBank identifiers (Supplementary Information Table1), and branch labels represent posterior probability support for lineages. The Y-axis represents a timeline in millions of years before present; **(C)** ENM for current conditions. Predicted areas of suitability are shaded in green; **(D)** ENM for LGM conditions. Points signify FAUNMAP fossil occurrences during the Late Wisconsin (11.8 - 29 kya), and hash lines indicate extent of glacial sheets. Black triangles represent fossil occurrences dated to temporal confidence interval completely contained within the Late Wisconsin timeframe (both maximum and minimum ages within 11.8 - 29 kya). Grey circles represent fossil occurrences dated to a temporal confidence interval that intersects but is not contained within the Late Wisconsin timeframe (maximum and minimum ages may be outside 11.8 - 19 kya).

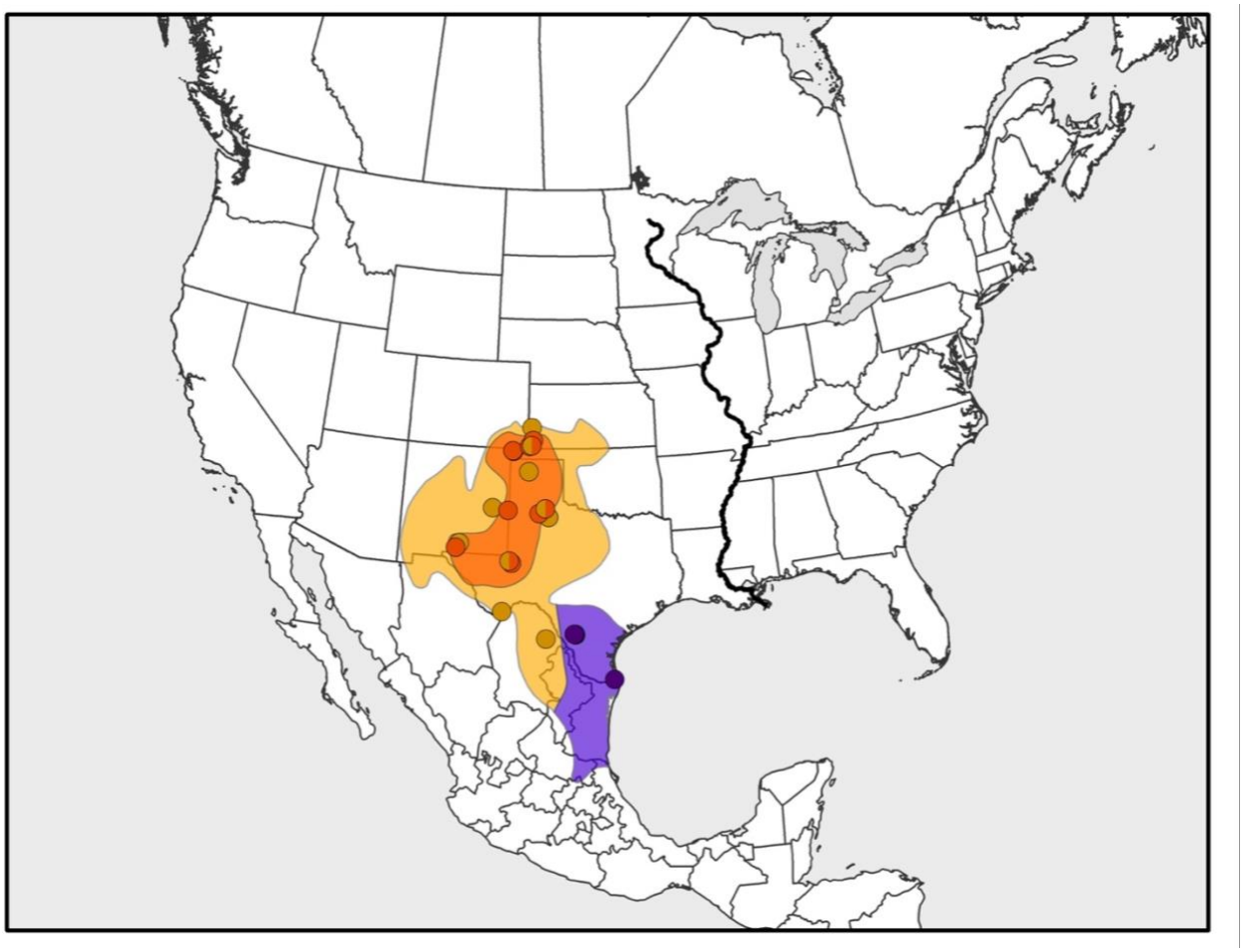

Figure 9A.

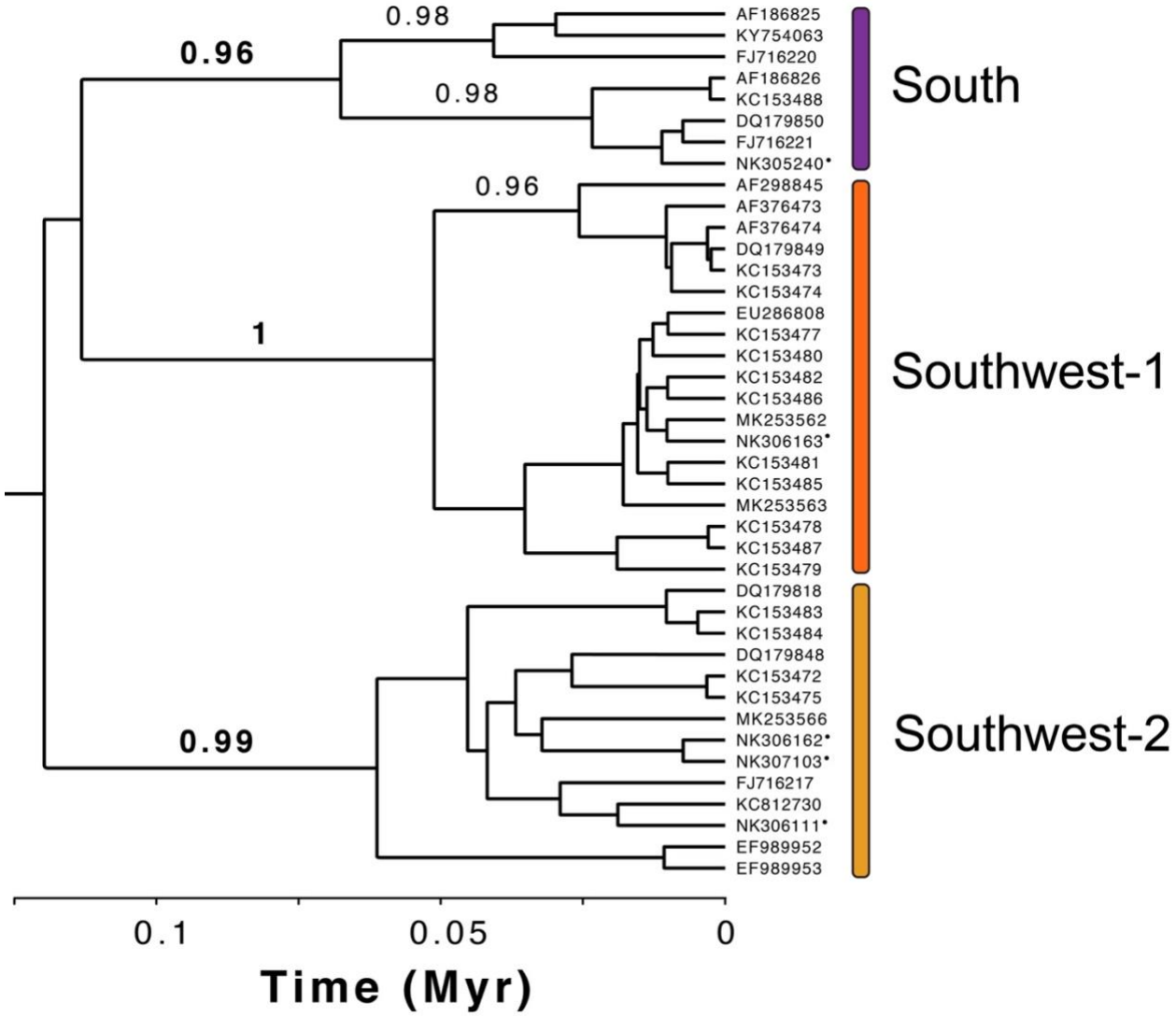
0.98
0.96
0.98
0.96
1
0.99
AF186825
KY754063
FJ716220
AF186826
KC153488
DQ179850
FJ716221
NK305240
AF298845
AF376473
AF376474
DQ179849
KC153473
KC153474
EU286808
KC153477
KC153480
KC153482
KC153486
MK253562
NK306163
KC153481
KC153485
MK253563
KC153478
KC153487
KC153479
DQ179818
KC153483
KC153484
DQ179848
KC153472
KC153475
MK253566
NK306162
NK307103
FJ716217
KC812730
NK306111
EF989952
EF989953
South
Southwest-1
Southwest-2
0.1
0.05
0
Time (Myr)

Figure 9B.

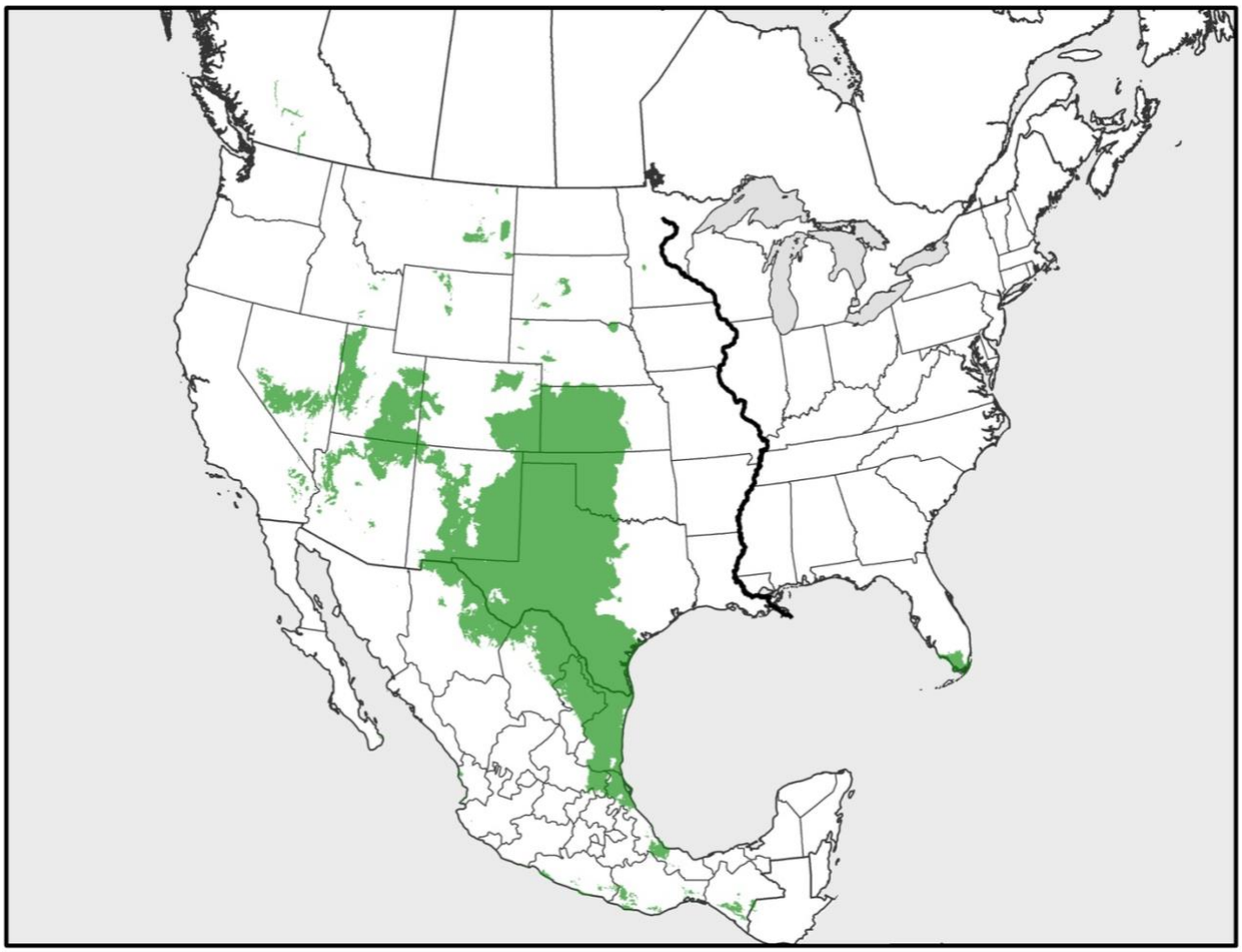

Figure 9C.

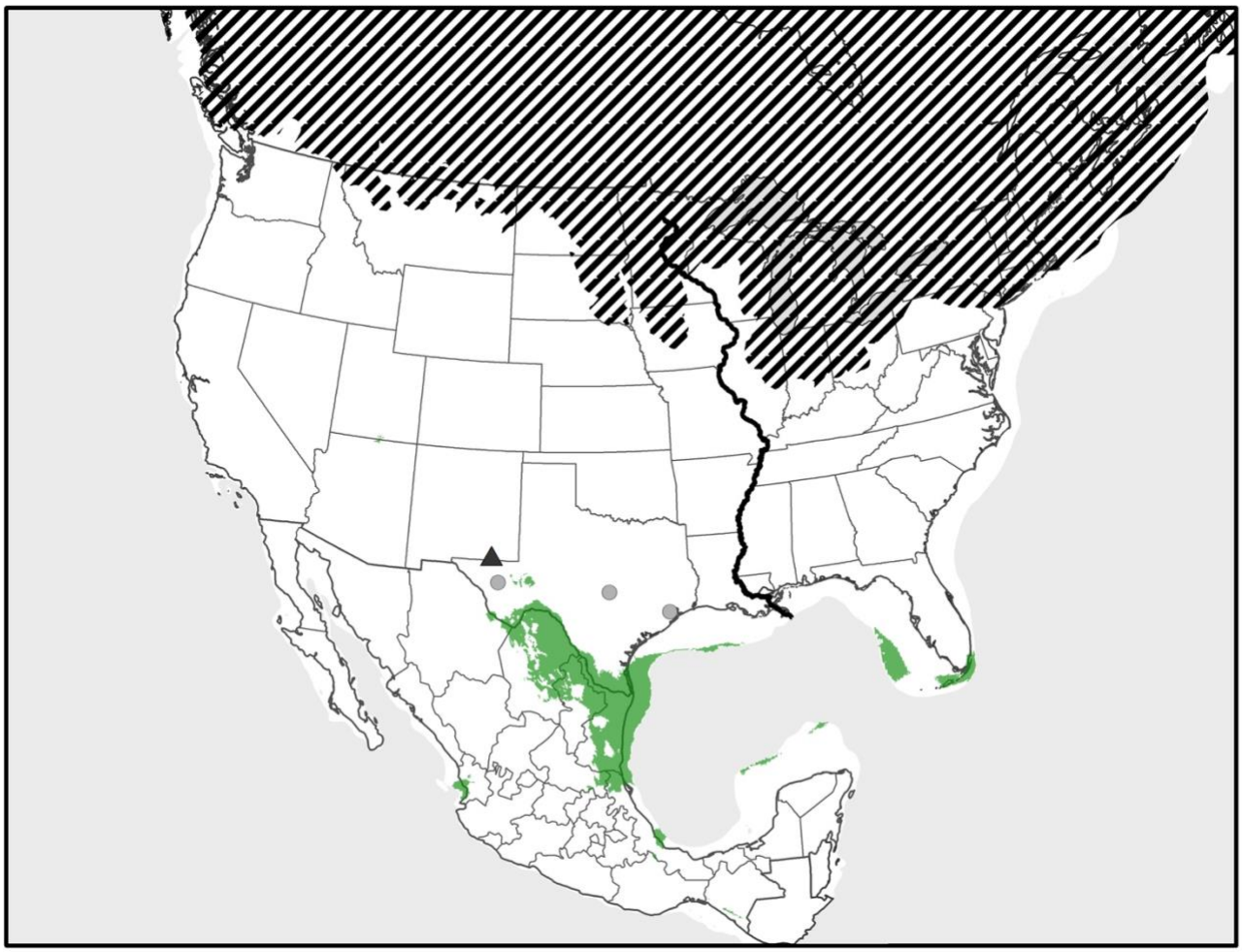

Figure 9D.

Figure 9. **(A)** Sampling and phylogeographic structure for *Neotoma micropus*. Colored polygons represent the estimated distribution of geographically distinct lineages modified from IUCN Red List rangewide distribution maps, and transitions between lineages correspond to equidistant boundaries between occurrence points. Colors of polygons and points correspond to designated lineages. Points represented by two colors are localities where two lineages were detected; **(B)** Bayesian cytochrome b genealogy for *Neotoma micropus*. Colors correspond to supported geographically discrete lineages. Tip labels correspond to GenBank identifiers (Supplementary Information Table1), and branch labels represent posterior probability support for lineages. The Y-axis represents a timeline in millions of years before present; **(C)** ENM for current conditions. Predicted areas of suitability are shaded in green; **(D)** ENM for LGM conditions. Points signify FAUNMAP fossil occurrences during the Late Wisconsin (11.8 - 29 kya), and hash lines indicate extent of glacial sheets. Black triangles represent fossil occurrences dated to temporal confidence interval completely contained within the Late Wisconsin timeframe (both maximum and minimum ages within 11.8 - 29 kya). Grey circles represent fossil occurrences dated to a temporal confidence interval that intersects but is not contained within the Late Wisconsin timeframe (maximum and minimum ages may be outside 11.8 - 19 kya).

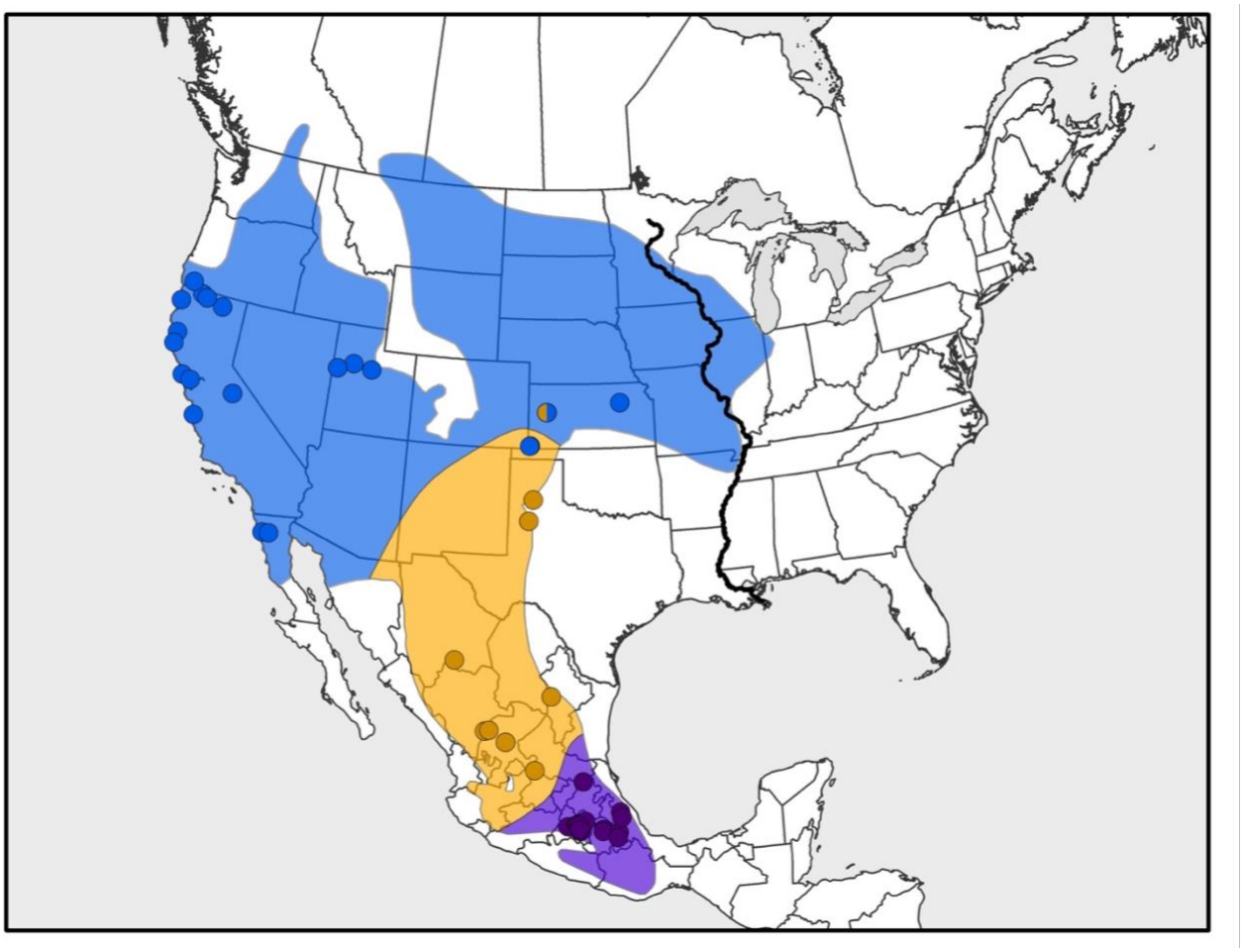

Figure 10A.

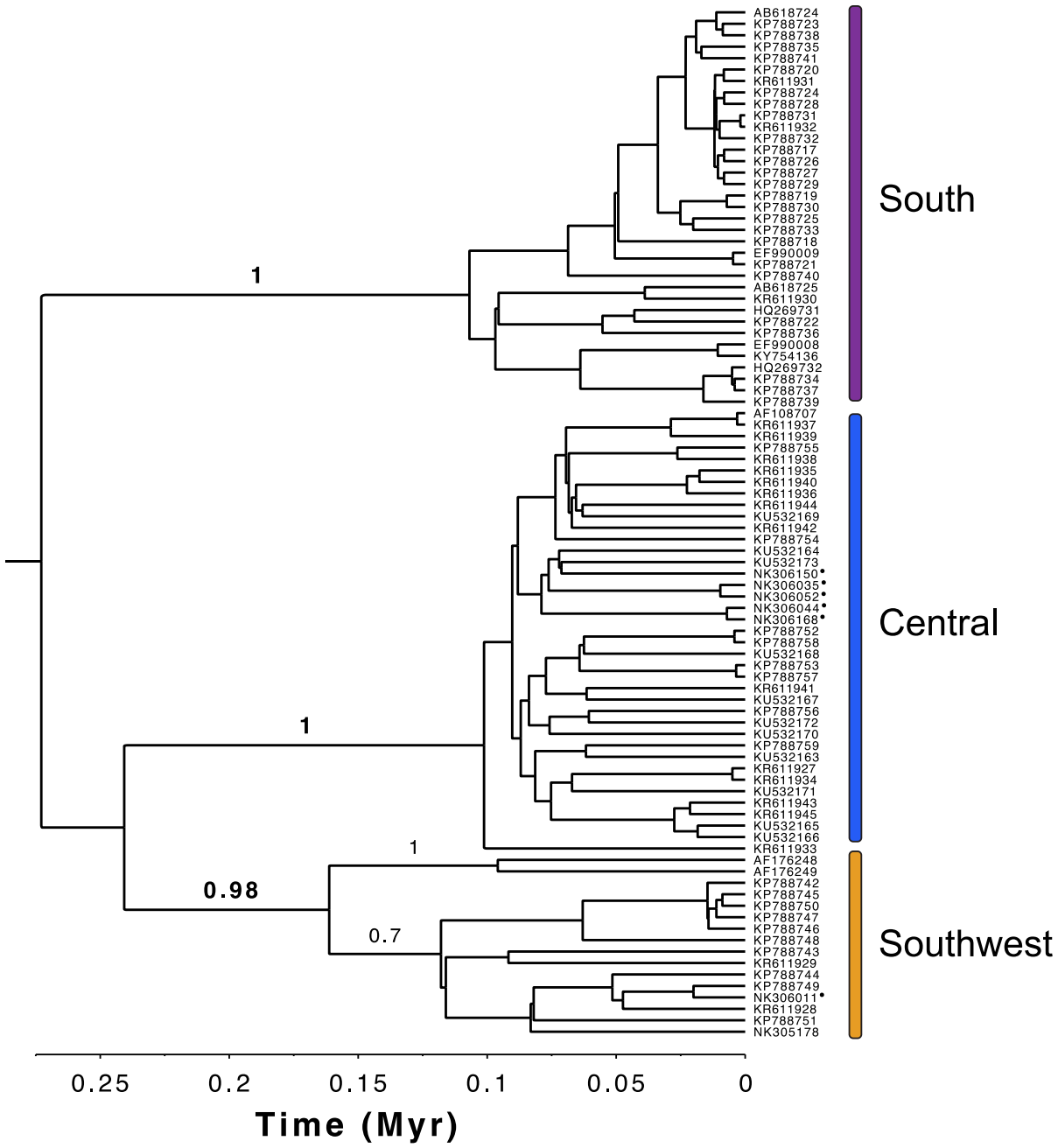
AB618724
KP788723
KP788738
KP788735
KP788741
KP788720
KR611931
KP788724
KP788728
KP788731
KR611932
KP788732
KP788717
KP788726
KP788727
KP788729
KP788719
KP788730
KP788725
KP788733
KP788718
EF990009
KP788721
KP788740
AB618725
KR611930
HQ269731
KP788722
KP788736
EF990008
KY754136
HQ269732
KP788734
KP788737
KP788739
AF108707
KR611937
KR611939
KP788755
KR611938
KR611935
KR611940
KR611936
KR611944
KU532169
KR611942
KP788754
KU532164
KU532173
NK306150
NK306035
NK306052
NK306044
NK306168
KP788752
KP788758
KU532168
KP788753
KP788757
KR611941
KU532167
KP788756
KU532172
KU532170
KP788759
KU532163
KR611927
KR611934
KU532171
KR611943
KR611945
KU532165
KU532166
KR611933
AF176248
AF176249
KP788742
KP788745
KP788750
KP788747
KP788746
KP788748
KP788743
KR611929
KP788744
KP788749
NK306011
KR611928
KP788751
NK305178
1
1
0.98
1
0.7
South
Central
Southwest
0.25
0.2
0.15
0.1
0.05
0
Time (Myr)

Figure 10B.

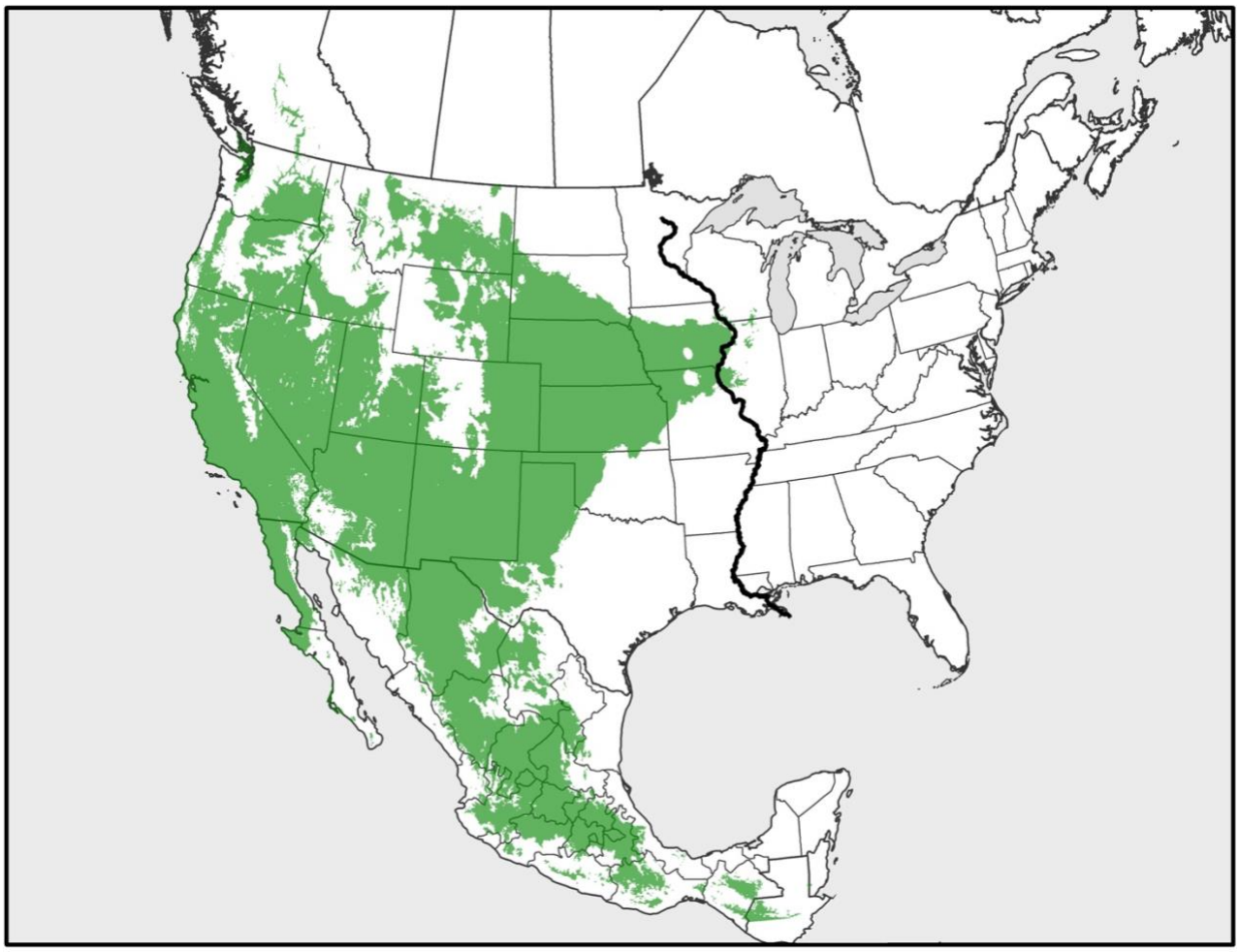

Figure 10C.

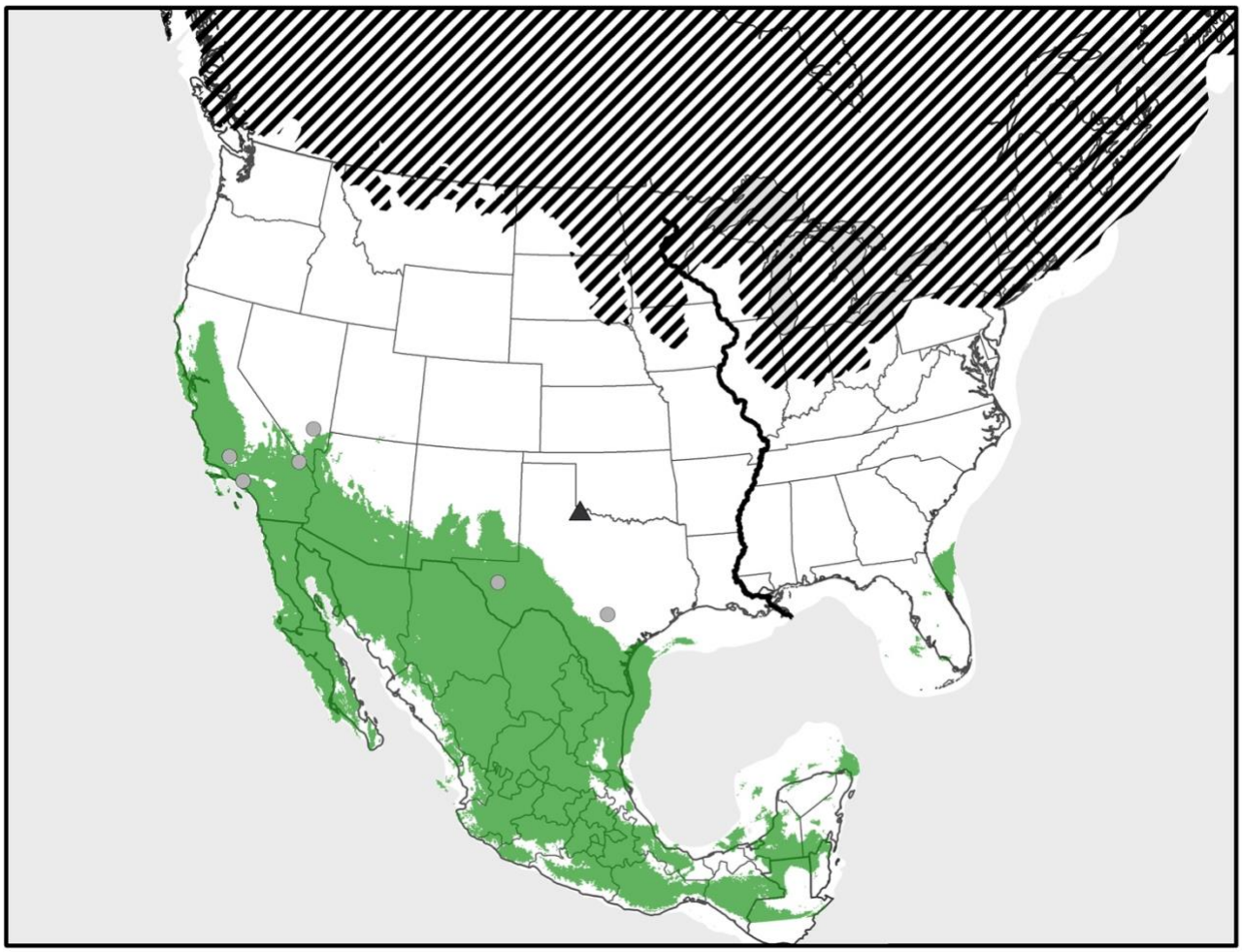

Figure 10D.

Figure 10. (A) Bayesian cytochrome b genealogy for *Reithrodontomys megalotis*. Colors correspond to supported geographically discrete lineages. Tip labels correspond to GenBank identifiers (Supplementary Information Table1), and branch labels represent posterior probability support for lineages. The Y-axis represents a timeline in millions of years before present; **(B)** Sampling and phylogeographic structure for *Reithrodontomys megalotis*. Colored polygons represent the estimated distribution of genetically distinct lineages modified from IUCN Red List rangewide distribution maps, and transitions between lineages correspond to equidistant boundaries between occurrence points. Colors of polygons and points correspond to designated lineages. Points represented by two colors are localities where two lineages were detected; **(C)** ENM for current conditions. Predicted areas of suitability are shaded in green; **(D)** ENM for LGM conditions. Points signify FAUNMAP fossil occurrences during the Late Wisconsin (11.8 - 29 kya), and hash lines indicate extent of glacial sheets. Black triangles represent fossil occurrences dated to temporal confidence interval completely contained within the Late Wisconsin timeframe (both maximum and minimum ages within 11.8 - 29 kya). Grey circles represent fossil occurrences dated to a temporal confidence interval that intersects but is not contained within the Late Wisconsin timeframe (maximum and minimum ages may be outside 11.8 - 19 kya).

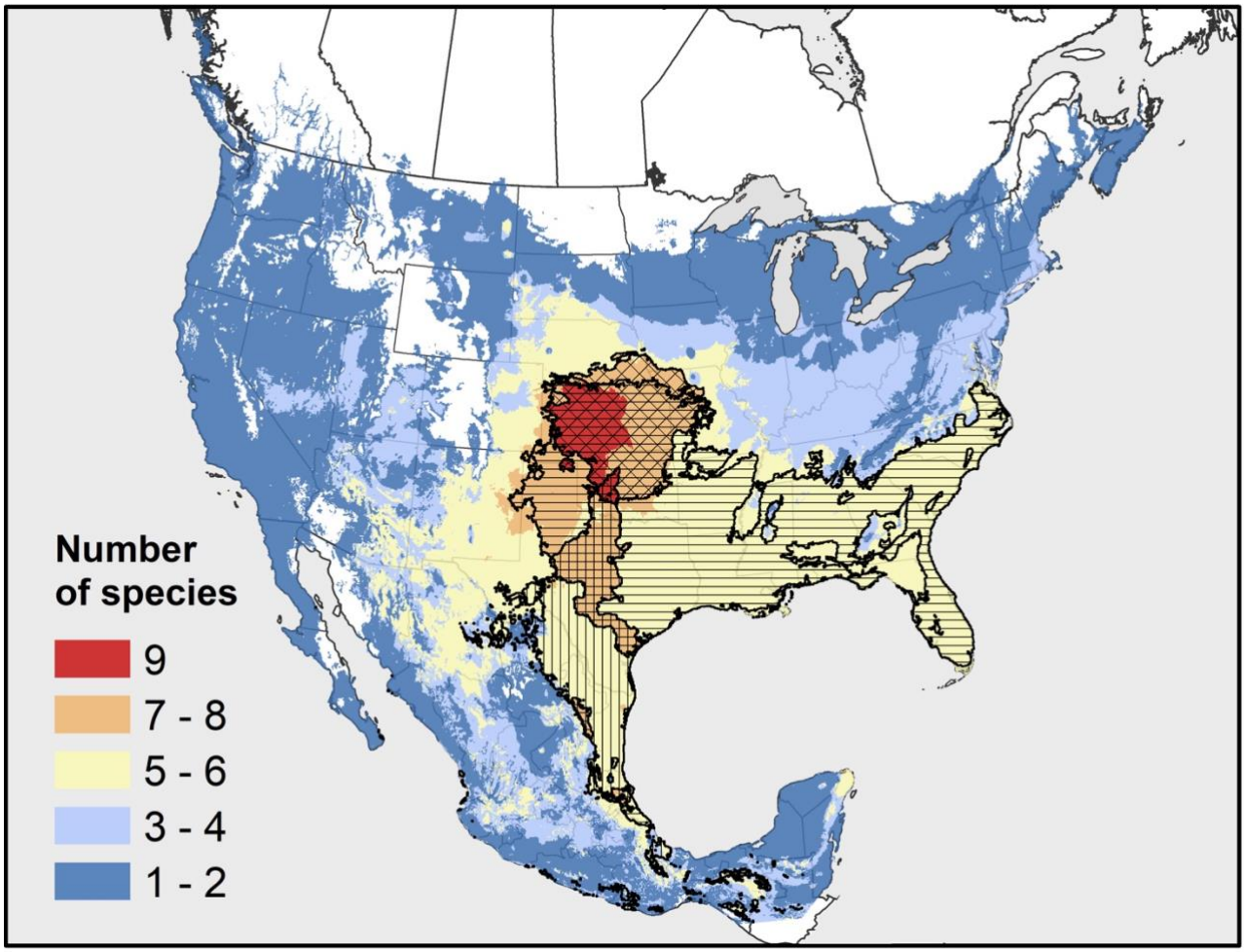

Figure 11.
Combined ENMs for current areas of suitability of all ten species. Colors represent the number of overlapping distributions. Horizontal lines represent areas where all four Eastern species overlap (*C. parvus, N. floridana, S. hispidus,* and *P. leucopus*). Crosshatch lines represent areas where all three Campestrian species overlap (*B. hylophaga, M. ochrogaster,* and *C. hispidus*). Vertical lines represent areas where all three Chihuahuan species overlap (*R. fulvescens, N. micropus,* and *R. megalotis*).

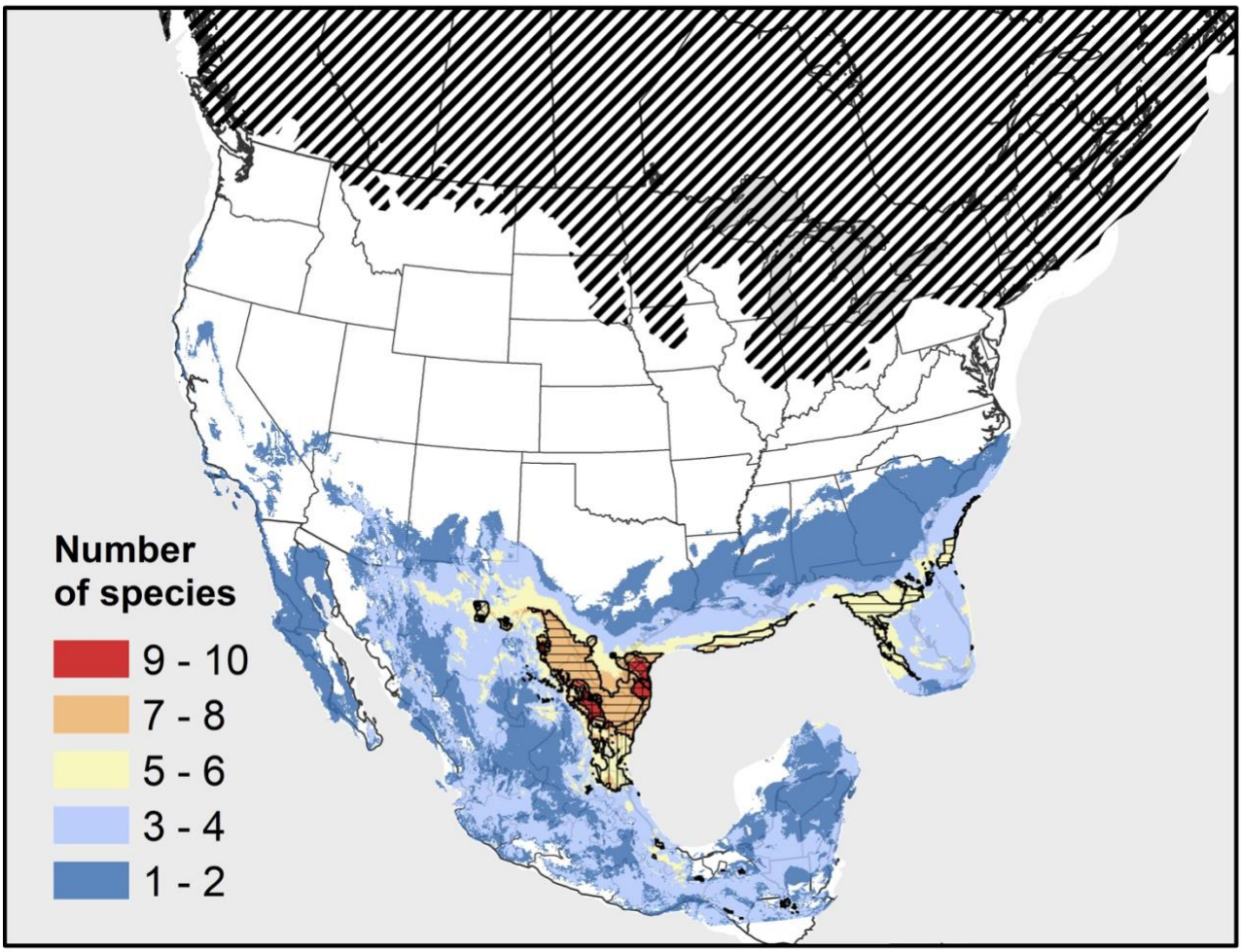

Figure 12.
Combined LGM predictions of all ten species. Colors represent the number of overlapping distributions. Horizontal lines represent areas where all four Eastern species overlap (*C. parvus*, *N. floridana*, *S. hispidus*, and *P. leucopus*). Crosshatch lines represent areas where all three Campestrian species overlap (*B. hylophaga*, *M. ochrogaster*, and *C. hispidus*). Vertical lines represent areas where all three Chihuahuan species overlap (*R. fulvescens*, *N. micropus*, and *R. megalotis*).

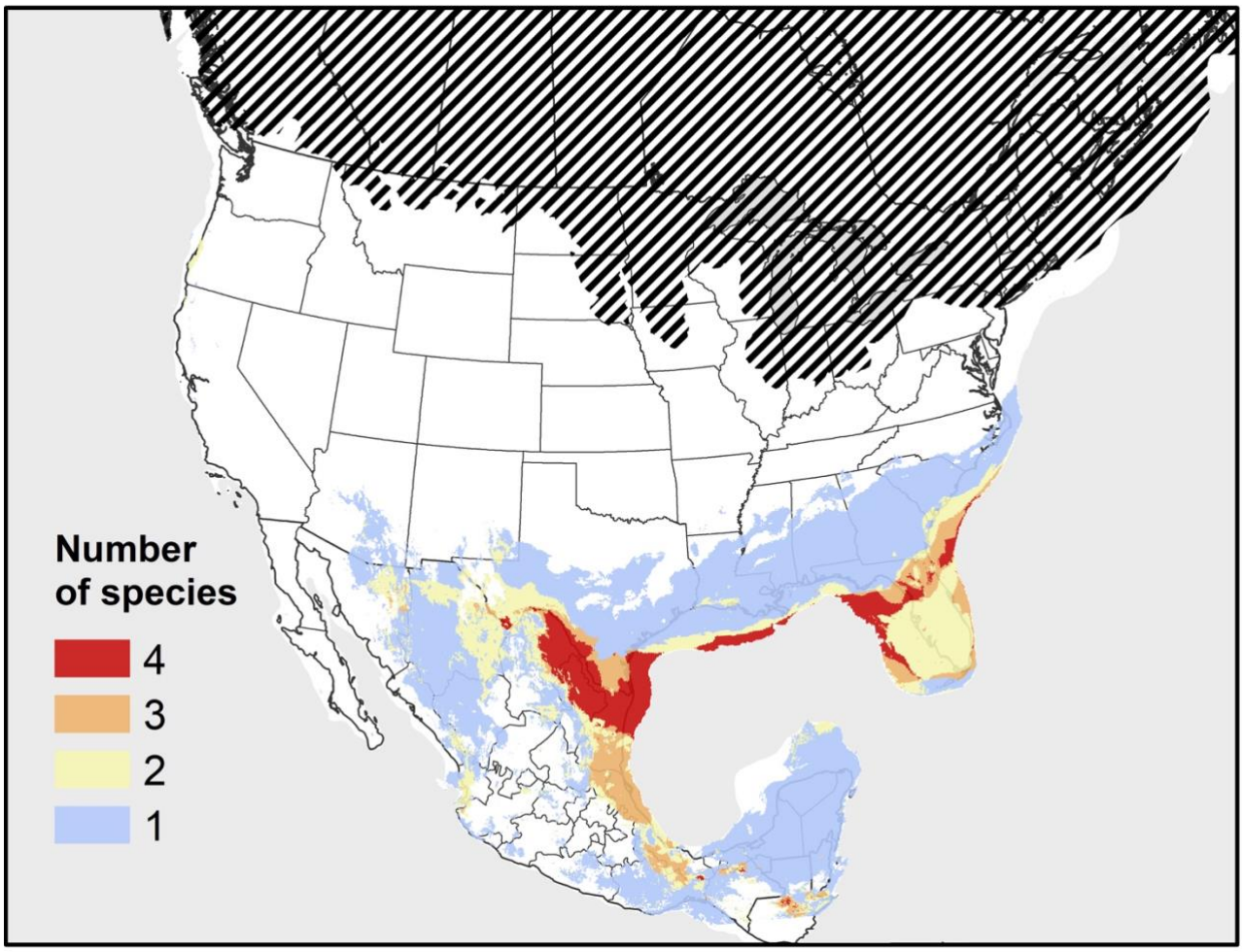

Figure 13.
Combined LGM predictions of Eastern species (*C. parvus, N. floridana, S. hispidus, P. leucopus*). Colored polygons correspond to the number of agreeing species models over an area. Hash lines represent extent of glacial sheets and the black line represents the Mississippi River outflow.

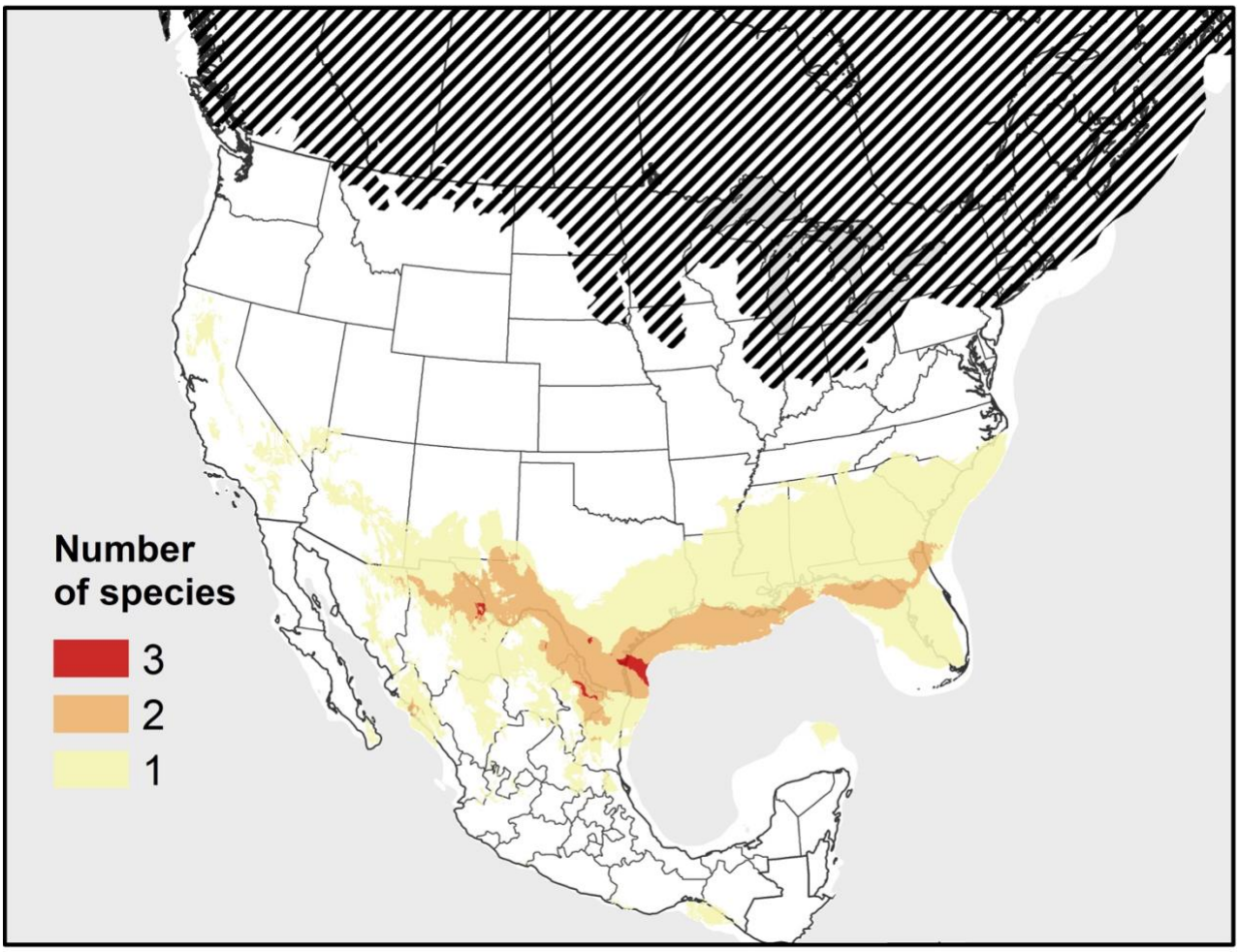

Figure 14.
Combined LGM predictions of Campestrian species (*B. hylophaga*, *M. ochrogaster*, *C. hispidus*). Colored polygons correspond to the number of agreeing species models over an area. Hash lines represent extent of glacial sheets and the black line represents the Mississippi River outflow.

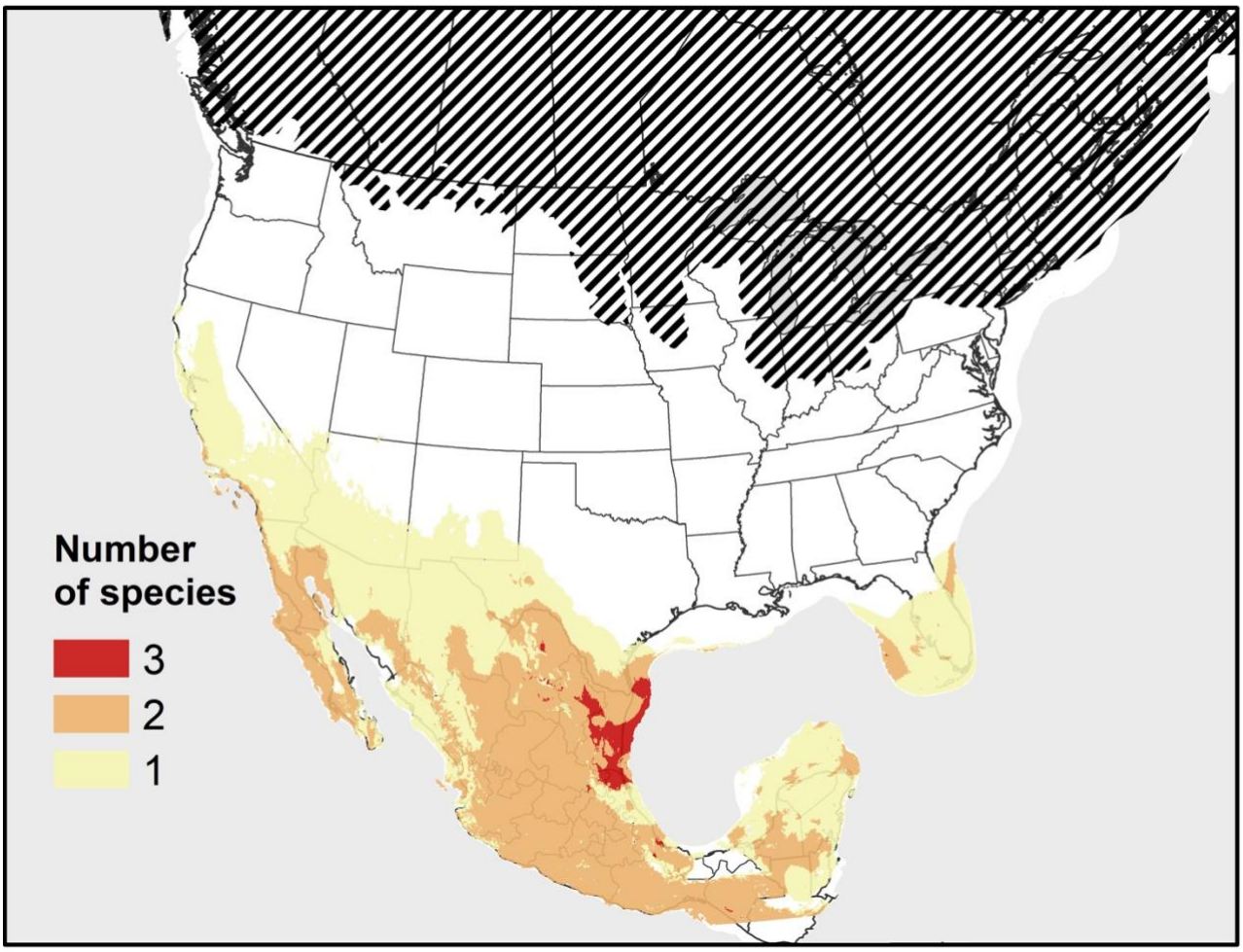

Figure 15.
Combined LGM predictions of Chihuahuan species (*R. fulvescens, N. micropus, R. megalotis*). Colored polygons correspond to the number of agreeing species models over an area. Hash lines represent extent of glacial sheets and the black line represents the Mississippi River outflow.

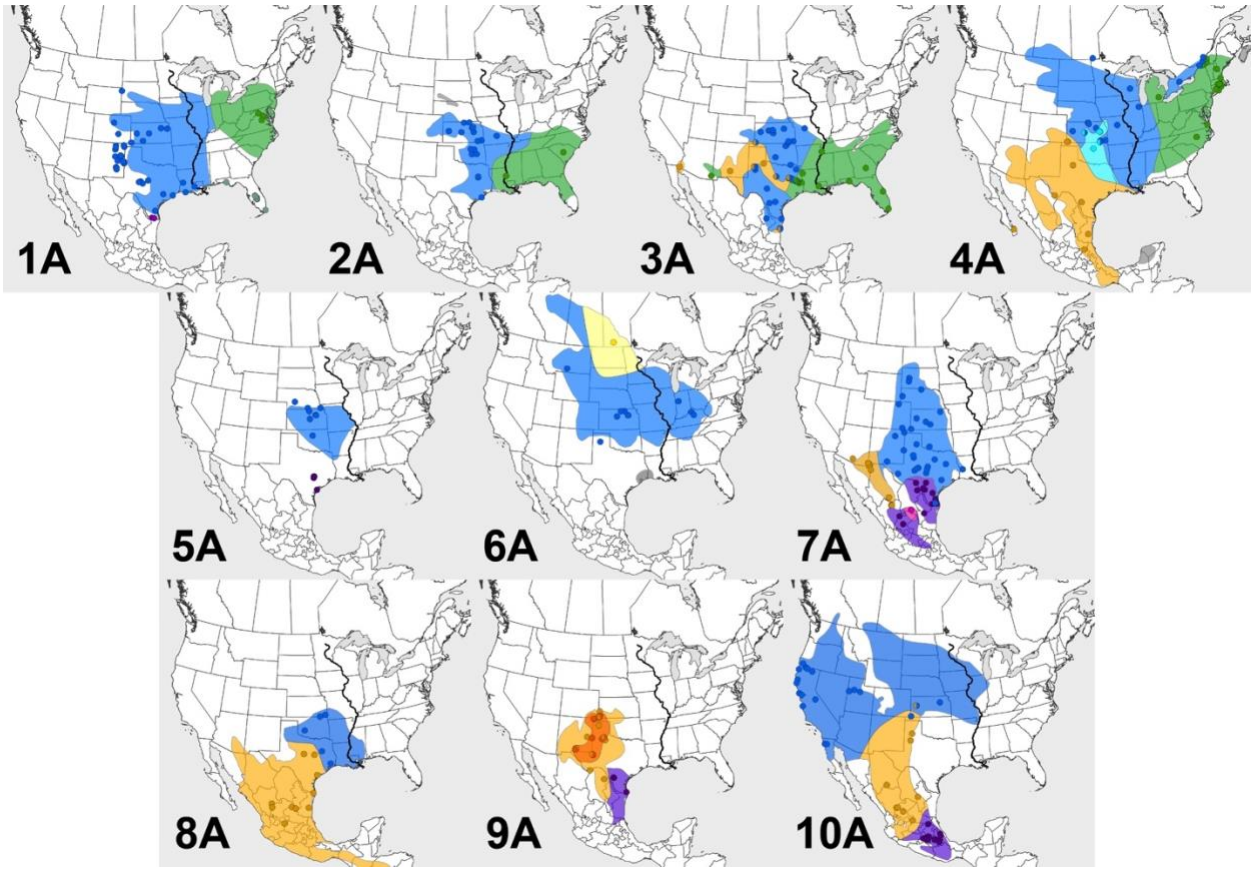

Figure 16.
Compound of species' phylogeographic distributions starting with Eastern species (1A: *C. parvus;* 2A: *N. floridana;* 3A: *S. hispidus;* 4A: *P. leucopus*), Campestrian species (5A: *B. hylophaga;* 6A: *M. ochrogaster;* 7A: *C. hispidus*), and Chihuahuan species (8A: *R. fulvescens;* 9A: *N. micropus;* 10A: *R. megalotis*).

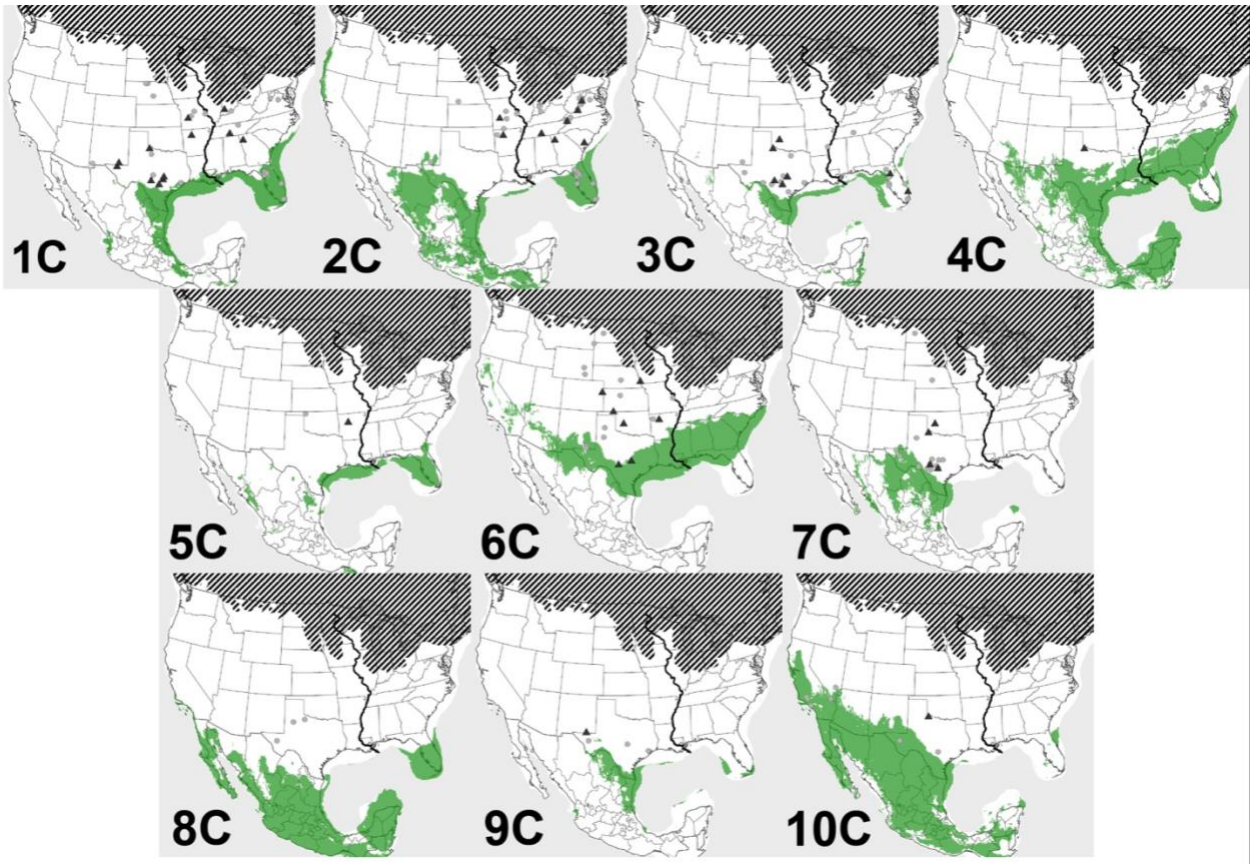

Figure 17.
Compound of species' hindcast ENMs starting with Eastern species (1C: *C. parvus;* 2C: *N. floridana;* 3C: *S. hispidus;* 4C: *P. leucopus*), Campestrian species (5C: *B. hylophaga;* 6C: *M. ochrogaster;* 7C: *C. hispidus*), and Chihuahuan species (8C: *R. fulvescens;* 9C: *N. micropus;* 10C: *R. megalotis*).

Table 1.
List of 10 species examined and ENM metrics, including number of occurrence points, point buffer-radius used for study area (km), selected model (regularization parameter and feature class), and model selection criteria

Species	Number of Occurrences	Study Area (M)	Model (RM_FC)	Partial ROC (*p*-value)	Delta AICc	AICc	Omission rate (*E* = 10%)
Blarina hylophaga	185	200	4_lhp	0	0	3924.341	0.081
Chaetodipus hispidus	548	200	3_lqhpt	0	0	13124.100	0.241
Cryptotis parvus	625	200	2_lqhpt	0	0	15462.760	0.221
Microtus ochrogaster	497	150	3_lqhpt	0	0	12019.460	0.331
Neotoma floridana	350	200	4.5_lqhpt	0	0	8230.201	0.272
Neotoma micropus	499	150	2_lqp	0	0	11186.010	0.198
Peromyscus leucopus	2626	250	1_lqhpt	0	0	67755.390	0.286
Reithrodontomys fulvescens	878	200	1_lqp	0	0	20874.860	0.137
Reithrodontomys megalotis	1539	200	1_lqhpt	0	0	38733.670	0.228
Sigmodon hispidus	1491	200	1_lqhpt	0	0	35837.570	0.160

References

6X GelRed® Prestain Loading Buffer with Tracking Dye. (n.d.). *Biotium*. Retrieved May 23, 2022, from https://biotium.com/product/6x-gelred-prestain-loading-buffer-with-tracking-dye/

Aiello-Lammens, M. E., Boria, R. A., Radosavljevic, A., & Vilela, B. (2015). spThin: An R package for spatial thinning of species occurrence records for use in ecological niche models. *Ecography*, *38(5)*, 541–545.

Albery, G. F., Eskew, E. A., Ross, N., & Olival, K. J. (2020). Predicting the global mammalian viral sharing network using phylogeography. *Nature Communications*, *11*(1), 2260. https://doi.org/10.1038/s41467-020-16153-4

Allen, R. K. (1990). The Distribution of Southwest North American Mayfly Genera (Ephemeroptera) in the Mexican Transition Zone. In I. C. Campbell (Ed.), *Mayflies and Stoneflies: Life Histories and Biology* (pp. 169–180). Springer Netherlands. https://doi.org/10.1007/978-94-009-2397-3_21

Andersen, J. J., & Light, J. E. (2012). Phylogeography and subspecies revision of the hispid pocket mouse, *Chaetodipus hispidus* (Rodentia: Heteromyidae). *Journal of Mammalogy*, *93*(4), 1195–1215. https://doi.org/10.1644/11-MAMM-A-341.3

Arai, S., Song, J.-W., Sumibcay, L., Bennett, S. N., Nerurkar, V. R., Parmenter, C., Cook, J. A., Yates, T. L., & Yanagihara, R. (2007). Hantavirus in Northern Short-tailed Shrew, United States. *Emerging Infectious Diseases*, *13*(9), 1420–1423. https://doi.org/10.3201/eid1309.070484

Arbogast, B. S., & Kenagy, G. J. (2001). Comparative phylogeography as an integrative approach to historical biogeography. *Journal of Biogeography*, *28*(7), 819–825. https://doi.org/10.1046/j.1365-2699.2001.00594.x

Armstrong, D. M. (1972). *Distribution of mammals in Colorado*. University of Kansas Printing Service. https://scholar.google.com/scholar_lookup?title=Distribution+of+mammals+in+Colorado&author=Armstrong%2C+David+Michael&publication_year=1972

Aubry, K. B., Statham, M. J., Sacks, B. N., Perrine, J. D., & Wisely, S. M. (2009). Phylogeography of the North American red fox: Vicariance in Pleistocene forest refugia. *Molecular Ecology*, *18*(12), 2668–2686. https://doi.org/10.1111/j.1365-294X.2009.04222.x

Avise, J. C. (1998). The history and purview of phylogeography: A personal reflection. *Molecular Ecology*, *7*(4), 371–379. https://doi.org/10.1046/j.1365-294x.1998.00391.x

Avise, J. C. (2000). *Phylogeography: The History and Formation of Species*. Harvard University Press.

Avise, J. C. (2009). Phylogeography: Retrospect and prospect. *Journal of Biogeography*, *36*(1), 3–15. https://doi.org/10.1111/j.1365-2699.2008.02032.x

Avise, J. C., Arnold, J., Ball, R. M., Bermingham, E., Lamb, T., Neigel, J. E., Reeb, C. A., & Saunders, N. C. (1987). INTRASPECIFIC PHYLOGEOGRAPHY: The Mitochondrial DNA Bridge Between Population Genetics and Systematics. *Annual Review of Ecology and Systematics*, *18*(1), 489–522. https://doi.org/10.1146/annurev.es.18.110187.002421

Banks, W., Derrico, F., Peterson, A., Kageyama, M., & Colombeau, G. (2008). Reconstructing ecological niches and geographic distributions of caribou (Rangifer tarandus) and red

deer (Cervus elaphus) during the Last Glacial Maximum. *Quaternary Science Reviews*, *27*(27–28), 2568–2575. https://doi.org/10.1016/j.quascirev.2008.09.013

Barrow, L. N., Soto-Centeno, J. A., Warwick, A. R., Lemmon, A. R., & Moriarty Lemmon, E. (2017). Evaluating hypotheses of expansion from refugia through comparative phylogeography of south-eastern Coastal Plain amphibians. *Journal of Biogeography*, *44*(12), 2692–2705. https://doi.org/10.1111/jbi.13069

Barton, H. D., & Wisely, S. M. (2012). Phylogeography of striped skunks (Mephitis mephitis) in North America: Pleistocene dispersal and contemporary population structure. *Journal of Mammalogy*, *93*(1), 38–51. https://doi.org/10.1644/10-MAMM-A-270.1

Berg, M. P., Kiers, E. T., Driessen, G., Van Der HEIJDEN, M., Kooi, B. W., Kuenen, F., Liefting, M., Verhoef, H. A., & Ellers, J. (2010). Adapt or disperse: Understanding species persistence in a changing world. *Global Change Biology*, *16*(2), 587–598. https://doi.org/10.1111/j.1365-2486.2009.02014.x

Bigg, G. R., Cunningham, C. W., Ottersen, G., Pogson, G. H., Wadley, M. R., & Williamson, P. (2008). Ice-age survival of Atlantic cod: Agreement between palaeoecology models and genetics. *Proceedings of the Royal Society B: Biological Sciences*, *275*(1631), 163–173. https://doi.org/10.1098/rspb.2007.1153

Blonder, B., Nogués-Bravo, D., Borregaard, M. K., Donoghue II, J. C., Jørgensen, P. M., Kraft, N. J. B., Lessard, J.-P., Morueta-Holme, N., Sandel, B., Svenning, J.-C., Violle, C., Rahbek, C., & Enquist, B. J. (2015). Linking environmental filtering and disequilibrium to biogeography with a community climate framework. *Ecology*, *96*(4), 972–985. https://doi.org/10.1890/14-0589.1

Blum, M. D., Guccione, M. J., & Wysocki, D. A. (2000). Late Pleistocene evolution of the lower Mississippi River valley, southern Missouri to Arkansas. *Geological Society of America Bulletin*, 15.

Bock, C. E., Bock, J. H., & Lepthien, L. W. (1977). Abundance Patterns of Some Bird Species Wintering on the Great Plains of the U.S.A. *Journal of Biogeography*, *4*(1), 101. https://doi.org/10.2307/3038132

Bouckaert, R. R., & Drummond, A. J. (2017). bModelTest: Bayesian phylogenetic site model averaging and model comparison. *BMC Evolutionary Biology*, *17*(1), 42. https://doi.org/10.1186/s12862-017-0890-6

Bouckaert, R., Vaughan, T. G., Barido-Sottani, J., Duchêne, S., Fourment, M., Gavryushkina, A., Heled, J., Jones, G., Kühnert, D., De Maio, N., Matschiner, M., Mendes, F. K., Müller, N. F., Ogilvie, H. A., du Plessis, L., Popinga, A., Rambaut, A., Rasmussen, D., Siveroni, I., … Drummond, A. J. (2019). BEAST 2.5: An advanced software platform for Bayesian evolutionary analysis. *PLOS Computational Biology*, *15*(4), e1006650. https://doi.org/10.1371/journal.pcbi.1006650

Bradley, R. D., Henson, D. D., & Durish, N. D. (2008). RE-EVALUATION OF THE GEOGRAPHIC DISTRIBUTION AND PHYLOGEOGRAPHY OF THE SIGMODON HISPIDUS COMPLEX BASED ON MITOCHONDRIAL DNA SEQUENCES. *The Southwestern Naturalist*, *53*(3), 301–310. https://doi.org/10.1894/MRD-03.1

Bradley, R. D., Lack, J. B., Pfau, R. S., Peppers, L. L., Henson, D. D., Stallings, A. O., Hoang, C. N., & Van Den Bussche, R. A. (2012). Genetic and Conservation Status of a Relictual Population of the Hispid Cotton Rat (*Sigmodon hispidus eremicus*). *The Southwestern Naturalist*, *57*(3), 231–239. https://doi.org/10.1894/0038-4909-57.3.231

Brant, S. V., & Ortí, G. (2003). Phylogeography of the Northern short-tailed shrew, *Blarina brevicauda* (Insectivora: Soricidae): past fragmentation and postglacial recolonization. *Molecular Ecology*, *12*(6), 1435–1449. https://doi.org/10.1046/j.1365-294X.2003.01789.x

Brant, S. V., & Ortí, G. (2002). Molecular Phylogeny of Short-Tailed Shrews, Blarina (Insectivora: Soricidae). *Molecular Phylogenetics and Evolution*, *22*(2), 163–173. https://doi.org/10.1006/mpev.2001.1057

Braun, J., & Mares, M. (1989). *Neotoma micropus* (Vols. 1–9).

Breshears, D. D., Cobb, N. S., Rich, P. M., Price, K. P., Allen, C. D., Balice, R. G., Romme, W. H., Kastens, J. H., Floyd, M. L., Belnap, J., Anderson, J. J., Myers, O. B., & Meyer, C. W. (2005). Regional vegetation die-off in response to global-change-type drought. *Proceedings of the National Academy of Sciences*, *102*(42), 15144–15148. https://doi.org/10.1073/pnas.0505734102

Brooker, R. W., Maestre, F. T., Callaway, R. M., Lortie, C. L., Cavieres, L. A., Kunstler, G., Liancourt, P., Tielbörger, K., Travis, J. M. J., Anthelme, F., Armas, C., Coll, L., Corcket, E., Delzon, S., Forey, E., Kikvidze, Z., Olofsson, J., Pugnaire, F., Quiroz, C. L., … Michalet, R. (2008). Facilitation in plant communities: The past, the present, and the future. *Journal of Ecology*, *0*(0). https://doi.org/10.1111/j.1365-2745.2007.01295.x

Brooks, D. R., & Hoberg, E. P. (2007). How will global climate change affect parasite–host assemblages? *Trends in Parasitology*, *23*(12), 571–574. https://doi.org/10.1016/j.pt.2007.08.016

Bruno, J. F., Stachowicz, J. J., & Bertness, M. D. (2003). Inclusion of facilitation into ecological theory. *Trends in Ecology & Evolution*, *18*(3), 119–125. https://doi.org/10.1016/S0169-5347(02)00045-9

Caire, W., Tyler, J. D., Glass, B. P., & Mares, M. A. (1989). *MAMMALS OF OKLAHOMA*. Univ. Oklahoma Press. https://k-state.primo.exlibrisgroup.com

Cameron, G. (1999). *The Smithsonian Book of North American Mammals*. Washington: Smithsonian Institution Press.

Carling, M. D., Serene, L. G., & Lovette, I. J. (2011). Using Historical Dna to Characterize Hybridization Between Baltimore Orioles (Icterus galbula) and Bullock's Orioles (I. bullockii). *The Auk*, *128*(1), 61–68. https://doi.org/10.1525/auk.2010.10164

Carstens, B. C., & Richards, C. L. (2007). Integrating Coalescent and Ecological Niche Modeling in Comparative Phylogeography. *Evolution*, *61*(6), 1439–1454. https://doi.org/10.1111/j.1558-5646.2007.00117.x

Chamberlain, S., Barve, V., Mcglinn, D., Oldoni, D., Desmet, P., Geffert, L., & Ram, K. (2021). *rgbif: Interface to the Global Biodiversity Information Facility* (3.6.0) [Computer software]. https://CRAN.R-project.org/package=rgbif

Cheddadi, R., Vendramin, G. G., Litt, T., Francois, L., Kageyama, M., Lorentz, S., Laurent, J.-M., de Beaulieu, J.-L., Sadori, L., Jost, A., & Lunt, D. (2006). Imprints of glacial refugia in the modern genetic diversity of Pinus sylvestris. *Global Ecology and Biogeography*, *15*(3), 271–282. https://doi.org/10.1111/j.1466-822X.2006.00226.x

Choate, J., Jones, J., & Jones, C. (1994). *Handbook Of Mammals of the South-Central States*. Baton Rouge and London: Louisiana State University Press.

Clark, B. K., & Kaufman, D. W. (1990). Short-term responses of small mammals to experimental fire in tallgrass prairie. *Canadian Journal of Zoology*, *68*(11), 2450–2454. https://doi.org/10.1139/z90-340

Cobos, M. E., Peterson, A. T., Barve, N., & Osorio-Olvera, L. (2019). kuenm: An R package for detailed development of ecological niche models using Maxent. *PeerJ*, *7*, e6281. https://doi.org/10.7717/peerj.6281

Collins, S. L., Nippert, J. B., Blair, J. M., Briggs, J. M., Blackmore, P., & Ratajczak, Z. (2021). Fire frequency, state change and hysteresis in tallgrass prairie. *Ecology Letters*, *24*(4), 636–647. https://doi.org/10.1111/ele.13676

Cook, E. R., Seager, R., Cane, M. A., & Stahle, D. W. (2007). North American drought: Reconstructions, causes, and consequences. *Earth-Science Reviews*, *81*(1–2), 93–134. https://doi.org/10.1016/j.earscirev.2006.12.002

Coppedge, B. R., Engle, D. M., Fuhlendorf, S. D., & Masters, R. E. (2001). *Landscape cover type and pattern dynamics in fragmented southern Great Plains grasslands, USA*. 14.

Cotton, J. M., Cerling, T. E., Hoppe, K. A., Mosier, T. M., & Still, C. J. (2016a). Climate, CO_2, and the history of North American grasses since the Last Glacial Maximum. *Science Advances*, *2*(3), e1501346. https://doi.org/10.1126/sciadv.1501346

Cotton, J. M., Cerling, T. E., Hoppe, K. A., Mosier, T. M., & Still, C. J. (2016b). Climate, CO2, and the history of North American grasses since the Last Glacial Maximum. *Science Advances*, *2*(3), e1501346. https://doi.org/10.1126/sciadv.1501346

Dansgaard, W., Johnsen, S. J., Clausen, H. B., Dahl-Jensen, D., Gundestrup, N. S., Hammer, C. U., Hvidberg, C. S., Steffensen, J. P., Sveinbjörnsdottir, A. E., Jouzel, J., & Bond, G.

(1993). Evidence for general instability of past climate from a 250-kyr ice-core record. *Nature*, *364*(6434), 218–220. https://doi.org/10.1038/364218a0

Davis, E. B., McGuire, J. L., & Orcutt, J. D. (2014). Ecological niche models of mammalian glacial refugia show consistent bias. *Ecography*, n/a-n/a. https://doi.org/10.1111/ecog.01294

Davis, J., Pavlova, A., Thompson, R., & Sunnucks, P. (2013). Evolutionary refugia and ecological refuges: Key concepts for conserving Australian arid zone freshwater biodiversity under climate change. *Global Change Biology*, *19*(7), 1970–1984. https://doi.org/10.1111/gcb.12203

Davis, M. B., & Shaw, R. G. (2001). Range Shifts and Adaptive Responses to Quaternary Climate Change. *Science*, *292*(5517), 673–679. https://doi.org/10.1126/science.292.5517.673

Davis, W. B., & Schmidly, D. J. (1994). *The mammals of Texas*. University of Texas Press.

Dawson, M. N. (2014). Natural experiments and meta-analyses in comparative phylogeography. *Journal of Biogeography*, *41*(1), 52–65. https://doi.org/10.1111/jbi.12190

Dietrich, N., Pruden, S., Ksiazek, T. G., Morzunov, S. P., & Camp, J. W. (n.d.). *A SMALL-SCALE SURVEY OF HANTAVIRUS IN MAMMALS FROM INDIANA | Journal of Wildlife Diseases*. Retrieved May 9, 2022, from https://meridian.allenpress.com/jwd/article/33/4/818/122534/A-SMALL-SCALE-SURVEY-OF-HANTAVIRUS-IN-MAMMALS-FROM

Dixon, K. L. (1989). Contact Zones of Avian Congeners on the Southern Great Plains. *The Condor*, *91*(1), 15–22. https://doi.org/10.2307/1368143

Dornelas, M., Gotelli, N. J., McGill, B., Shimadzu, H., Moyes, F., Sievers, C., & Magurran, A. E. (2014). Assemblage Time Series Reveal Biodiversity Change but Not Systematic Loss. *Science*, *344*(6181), 296–299. https://doi.org/10.1126/science.1248484

Dragoo, J. W., Lackey, J. A., Moore, K. E., Lessa, E. P., Cook, J. A., & Yates, T. L. (2006). Phylogeography of the deer mouse (Peromyscus maniculatus) provides a predictive framework for research on hantaviruses. *Journal of General Virology*, *87*(7), 1997–2003. https://doi.org/10.1099/vir.0.81576-0

Dreier, C. A., Geluso, K., Frisch, J. D., Adams, B. N., Lingenfelter, A. R., Freeman, P. W., Lemen, C. A., White, J. A., Andersen, B. R., Otto, H. W., & Schmidt, C. J. (2015). *Mammalian Records from Southwestern Kansas and Northwestern Oklahoma, including the First Record of Crawford's Desert Shrew (Notiosorex crawfordi) from Kansas*. 14.

Dupanloup, I., Schneider, S., & Excoffier, L. (2002). A simulated annealing approach to define the genetic structure of populations: DEFINING THE GENETIC STRUCTURE OF POPULATIONS. *Molecular Ecology*, *11*(12), 2571–2581. https://doi.org/10.1046/j.1365-294X.2002.01650.x

Dupont, L. M., Donner, B., Schneider, R., & Wefer, G. (2001). Mid-Pleistocene environmental change in tropical Africa began as early as 1.05 Ma. *Geology*, *29*(3), 195–198. https://doi.org/10.1130/0091-7613(2001)029<0195:MPECIT>2.0.CO;2

Edgar, R. C. (2004). MUSCLE: Multiple sequence alignment with high accuracy and high throughput. *Nucleic Acids Research*, *32*(5), 1792–1797. https://doi.org/10.1093/nar/gkh340

Edwards, C. W., & Bradley, R. D. (2001). Molecular Phylogenetics of the Neotoma Floridana Species Group. *Journal of Mammalogy*, *82*(3), 791–798. https://doi.org/10.1644/1545-1542(2001)082<0791:MPOTNF>2.0.CO;2

Emlen, S., Rising, J., & Thompson, W. (1975). A behavioral and morphological study of sympatry in the Indigo and Lazuli Buntings of the Great Plains. *Wilson Bulletin*, *87*.

Epstein, H. e., Lauenroth, W. k., Burke, I. c., & Coffin, D. p. (1996). Ecological responses of dominant grasses along two climatic gradients in the Great Plains of the United States. *Journal of Vegetation Science*, *7*(6), 777–788. https://doi.org/10.2307/3236456

Epstein, H. E., Lauenroth, W. K., Burke, I. C., & Coffin, D. P. (1997). Productivity Patterns of C3 and C4 Functional Types in the U.s. Great Plains. *Ecology*, *78*(3), 722–731. https://doi.org/10.1890/0012-9658(1997)078[0722:PPOCAC]2.0.CO;2

Escobar, L. E., Qiao, H., Cabello, J., & Peterson, A. T. (2018). Ecological niche modeling re-examined: A case study with the Darwin's fox. *Ecology and Evolution*, *8*(10), 4757–4770. https://doi.org/10.1002/ece3.4014

Evaluating predictive models of species' distributions: Criteria for selecting optimal models—ScienceDirect. (n.d.). Retrieved May 9, 2022, from https://www.sciencedirect.com/science/article/pii/S0304380002003496

Evans, J. S. (2021). *SpatialEco* (1.3) [Computer software].

Feng, X., Park, D. S., Liang, Y., Pandey, R., & Papeş, M. (2019). Collinearity in ecological niche modeling: Confusions and challenges. *Ecology and Evolution*, *9*(18), 10365–10376. https://doi.org/10.1002/ece3.5555

Fick, S. E., & Hijmans, R. J. (2017). WorldClim 2: New 1km spatial resolution climate surfaces for global land areas. *International Journal of Climatology*, *37*(12), 4302–4315.

Forman, S. L., Oglesby, R., & Webb, R. S. (2001). Temporal and spatial patterns of Holocene dune activity on the Great Plains of North America: Megadroughts and climate links. *Global and Planetary Change*, *29*(1), 1–29. https://doi.org/10.1016/S0921-8181(00)00092-8

Fox, D. L., & Koch, P. L. (2003). Tertiary history of C4 biomass in the Great Plains, USA. *Geology*, *31*(9), 809. https://doi.org/10.1130/G19580.1

Freestone, A. L. (2006). Facilitation Drives Local Abundance and Regional Distribution of a Rare Plant in a Harsh Environment. *Ecology*, *87*(11), 2728–2735. https://doi.org/10.1890/0012-9658(2006)87[2728:FDLAAR]2.0.CO;2

Frisch, J. D., Geluso, K., & Springer, J. T. (2015). *Distributional expansion of the hispid cotton rat (Sigmodon hispidus) into Dawson County, Nebraska*.

Galbreath, K. E., Hoberg, E. P., Cook, J. A., Armién, B., Bell, K. C., Campbell, M. L., Dunnum, J. L., Dursahinhan, A. T., Eckerlin, R. P., Gardner, S. L., Greiman, S. E., Henttonen, H., Jiménez, F. A., Koehler, A. V. A., Nyamsuren, B., Tkach, V. V., Torres-Pérez, F., Tsvetkova, A., & Hope, A. G. (2019). Building an integrated infrastructure for exploring biodiversity: Field collections and archives of mammals and parasites. *Journal of Mammalogy*, *100*(2), 382–393. https://doi.org/10.1093/jmammal/gyz048

Galfano, T. (2021). A conservation and taxonomic assessment of the least shrew (Cryptotis parvus) complex through rangewide phylogeographic analyses and population genomics. *Kansas State University*, 111.

García, K., Melero, Y., Palazón, S., Gosálbez, J., & Castresana, J. (2017). Spatial mixing of mitochondrial lineages and greater genetic diversity in some invasive populations of the

American mink (Neovison vison) compared to native populations. *Biological Invasions*, *19*(9), 2663–2673. https://doi.org/10.1007/s10530-017-1475-4

Gasmi, S., Ogden, N., Lindsay, L., Burns, S., Fleming, S., Badcock, J., Hanan, S., Gaulin, C., Leblanc, M., Russell, C., Nelder, M., Hobbs, L., Graham-Derham, S., Lachance, L., Scott, A., Galanis, E., & Koffi, J. (2017). Surveillance for Lyme disease in Canada: 2009–2015. *Canada Communicable Disease Report*, *43*(10), 194–199. https://doi.org/10.14745/ccdr.v43i10a01

George, S. (1999). Elliot's short-tailed shrew, Blarina hylophaga. In *The Smithsonian Book of North American Mammals* (pp. 51–52). Smithsonian Institution Press.

Gerhold, P., Cahill, J. F., Winter, M., Bartish, I. V., & Prinzing, A. (2015). Phylogenetic patterns are not proxies of community assembly mechanisms (they are far better). *Functional Ecology*, *29*(5), 600–614. https://doi.org/10.1111/1365-2435.12425

Gleason, H. A. (1939). The Individualistic Concept of the Plant Association. *The American Midland Naturalist*, *21*(1), 92–110. https://doi.org/10.2307/2420377

Goodall, D. W. (1963). The Continuum and the Individualistic Association. *Vegetatio*, *11*(5/6), 297–316.

Grumbine, R. E. (1994). What Is Ecosystem Management? *Conservation Biology*, *8*(1), 27–38.

Guralnick, R., & Pearman, P. B. (2010). Using species occurrence databases to determine niche dynamics of montane and lowland species since the Last Glacial Maximum. *Data Mining for Global Trends in Mountain Biodiversity*, 125–134.

Hall, E. R. (1955). *Handbook of Mammals of Kansas* (Vol. 7). University of Kansas Museum of Natural History.

Hall, E. R. (Eugene R. (1981). *The mammals of North America* (2nd ed). Wiley.

Hamilton, W. (1944). The Biology of the Little Short-Tailed Shrew, Cryptotis parva. *Journal of Mammalogy*, *25*(1), 1–7.

Han, B. A., Schmidt, J. P., Bowden, S. E., & Drake, J. M. (2015). Rodent reservoirs of future zoonotic diseases. *Proceedings of the National Academy of Sciences*, *112*(22), 7039–7044. https://doi.org/10.1073/pnas.1501598112

Harding, L. E., & Dragoo, J. W. (2012). Out of the tropics: A phylogeographic history of the long-tailed weasel, *Mustela frenata*. *Journal of Mammalogy*, *93*(4), 1178–1194. https://doi.org/10.1644/11-MAMM-A-280.1

Hargrove, W. W., & Hoffman, F. M. (2004). Potential of Multivariate Quantitative Methods for Delineation and Visualization of Ecoregions. *Environmental Management*, *34*(S1), S39–S60. https://doi.org/10.1007/s00267-003-1084-0

Hengeveld, R. (1992). *Dynamic Biogeography*. Cambridge University Press.

Hewitt, G. (1996). Some genetic consequences of ice ages, and their role in divergence and speciation. *Biological Journal of the Linnean Society*, *58*(3), 247–276. https://doi.org/10.1006/bijl.1996.0035

Hewitt, G. (2000). The genetic legacy of the Quaternary ice ages. *Nature*, *405*(6789), 907–913. https://doi.org/10.1038/35016000

Hewitt, G. M. (2001). Speciation, hybrid zones and phylogeography—Or seeing genes in space and time. *Molecular Ecology*, *10*(3), 537–549. https://doi.org/10.1046/j.1365-294x.2001.01202.x

Hewitt, G. M. (2011). Quaternary phylogeography: The roots of hybrid zones. *Genetica*, *139*(5), 617–638. https://doi.org/10.1007/s10709-011-9547-3

Hoerling, M., Eischeid, J., Kumar, A., Leung, R., Mariotti, A., Mo, K., Schubert, S., & Seager, R. (2014). Causes and predictability of the 2012 Great Plains drought: The 2012 summertime drought over Central Great Plains--the most severe seasonal drought in 117 years--resulted mostly from natural variations in weather. *Bulletin of the American Meteorological Society*, *95*(2), 269–283. https://doi.org/10.1175/BAMS-D-13-00055.1

Hoffmann, A. A., & Sgrò, C. M. (2011). Climate change and evolutionary adaptation. *Nature*, *470*(7335), 479–485. https://doi.org/10.1038/nature09670

Holt, R. D., & Gaines, M. S. (1992). Analysis of adaptation in heterogeneous landscapes: Implications for the evolution of fundamental niches. *Evolutionary Ecology*, *6*(5), 433–447. https://doi.org/10.1007/BF02270702

Hope, A. (2019). CSM08 Small mammal host-parasite sampling data for 16 linear trapping transects located in 8 LTER burn treatment watersheds at Konza Prairie. *Environmental Data Initiative*.

Hope, A. G., & Parmenter, R. R. (2007). *Food Habits of Rodents Inhabiting Arid and Semi-arid Ecosystems of Central New Mexico*. 76.

Hope, A. G., Stephens, R. B., Mueller, S. D., Tkach, V. V., & Demboski, J. R. (2019). Speciation of North American pygmy shrews (Eulipotyphla: Soricidae) supports spatial but not temporal congruence of diversification among boreal species. *Biological Journal of the Linnean Society*, blz139. https://doi.org/10.1093/biolinnean/blz139

Hope, A. G., Waltari, E., Dokuchaev, N. E., Abramov, S., Dupal, T., Tsvetkova, A., Henttonen, H., MacDonald, S. O., & Cook, J. A. (2010). High-latitude diversification within Eurasian least shrews and Alaska tiny shrews (Soricidae). *Journal of Mammalogy, 91*(5), 1041–1057. https://doi.org/10.1644/09-MAMM-A-402.1

Hope, A. G., Waltari, E., Morse, N. R., Flamme, M. J., Cook, J. A., & Talbot, S. L. (2017). Small mammals as indicators of climate, biodiversity, and ecosystem change. *Alaska Park Science*, *16*(1), 72–78.

Huang, Q., Baum, L., & Fu, W.-L. (2010). Simple and Practical Staining of DNA with GelRed in Agarose Gel Electrophoresis. *Clinical Laboratory*, *56*, 149–152.

Hughes, A. C., Orr, M. C., Yang, Q., & Qiao, H. (2021). Effectively and accurately mapping global biodiversity patterns for different regions and taxa. *Global Ecology and Biogeography*, *30*(7), 1375–1388. https://doi.org/10.1111/geb.13304

Hyde, W. T., & Peltier, W. R. (1993). Effect of altered boundary conditions on GCM studies of the climate of the Last Glacial Maximum. *Geophysical Research Letters*, *20*(10), 939–942. https://doi.org/10.1029/92GL02626

Irwin, D. M., Kocher, T. D., & Wilson, A. C. (1991). Evolution of the cytochromeb gene of mammals. *Journal of Molecular Evolution*, *32*(2), 128–144. https://doi.org/10.1007/BF02515385

IUCN. (2021). *The IUCN Red List of Threatened Species*. IUCN Red List of Threatened Species. https://www.iucnredlist.org/en

Jackson, S. T., Webb, R. S., Anderson, K. H., Overpeck, J. T., Webb III, T., Williams, J. W., & Hansen, B. C. S. (2000). Vegetation and environment in Eastern North America during the Last Glacial Maximum. *Quaternary Science Reviews*, *19*(6), 489–508. https://doi.org/10.1016/S0277-3791(99)00093-1

Jacobson, A. P., Riggio, J., M. Tait, A., & E. M. Baillie, J. (2019). Global areas of low human impact ('Low Impact Areas') and fragmentation of the natural world. *Scientific Reports*, *9*(1), 14179. https://doi.org/10.1038/s41598-019-50558-6

Johnson, M. T. J., & Stinchcombe, J. R. (2007). An emerging synthesis between community ecology and evolutionary biology. *Trends in Ecology & Evolution*, *22*(5), 250–257. https://doi.org/10.1016/j.tree.2007.01.014

Kareiva, P. M., Kingsolver, J. G., & Huey, R. B. (1993). *Biotic interactions and global change*. https://www.osti.gov/etdeweb/biblio/6250460

Kass, J. M., Muscarella, R., Galante, P. J., Bohl, C. L., Pinilla-Buitrago, G. E., Boria, R. A., Soley-Guardia, M., & Anderson, R. P. (2021). ENMeval 2.0: Redesigned for customizable and reproducible modeling of species' niches and distributions. *Methods in Ecology and Evolution.*

Kaufman, G. A., Matlack, R. S., Kaufman, D. W., & Higgins, J. J. (2012). Multiple factors limit use of local sites by Elliot's short-tailed shrews (*Blarina hylophaga*) in tallgrass prairie. *Canadian Journal of Zoology*, *90*(2), 210–221. https://doi.org/10.1139/z11-128

Kays, R., Lasky, M., Allen, M. L., Dowler, R. C., Hawkins, M. T. R., Hope, A. G., Kohli, B. A., Mathis, V. L., McLean, B., Olson, L. E., Thompson, C. W., Thornton, D., Widness, J., & Cove, M. V. (2022). Which mammals can be identified from camera traps and crowdsourced photographs? *Journal of Mammalogy*, gyac021. https://doi.org/10.1093/jmammal/gyac021

Kearse, M., Moir, R., Wilson, A., Stones-Havas, S., Cheung, M., Sturrock, S., Buxton, S., Cooper, A., Markowitz, S., Duran, C., Thierer, T., Ashton, B., Meintjes, P., & Drummond, A. (2012). Geneious Basic: An integrated and extendable desktop software platform for the organization and analysis of sequence data. *Bioinformatics*, *28*(12), 1647–1649. https://doi.org/10.1093/bioinformatics/bts199

Kerr, J. T., & Packer, L. (1997). Habitat heterogeneity as a determinant of mammal species richness in high-energy regions. *Nature*, *385*(6613), 252–254. https://doi.org/10.1038/385252a0

Klemm, T., Briske, D. D., & Reeves, M. C. (2020). Potential natural vegetation and NPP responses to future climates in the U.S. Great Plains. *Ecosphere*, *11*(10), e03264. https://doi.org/10.1002/ecs2.3264

Knowles, L. L., Carstens, B. C., & Keat, M. L. (2007). Coupling Genetic and Ecological-Niche Models to Examine How Past Population Distributions Contribute to Divergence. *Current Biology*, *17*(11), 940–946. https://doi.org/10.1016/j.cub.2007.04.033

Koch, P. L., Diffenbaugh, N. S., & Hoppe, K. A. (2004). The effects of late Quaternary climate and pCO2 change on C4 plant abundance in the south-central United States. *Palaeogeography, Palaeoclimatology, Palaeoecology*, *207*(3), 331–357. https://doi.org/10.1016/j.palaeo.2003.09.034

Kozak, K. H., Graham, C. H., & Wiens, J. J. (2008). Integrating GIS-based environmental data into evolutionary biology. *Trends in Ecology & Evolution*, *23*(3), 141–148. https://doi.org/10.1016/j.tree.2008.02.001

Küchler, A. W. (1970). A Biogeographical Boundary: The Tatschl Line. *Transactions of the Kansas Academy of Science (1903-)*, *73*(3), 298–301. https://doi.org/10.2307/3627174

Kunkel, K. E., Stevens, L. E., Stevens, S. E., & Sun, L. (n.d.). *Regional Climate Trends and Scenarios for the U.S. National Climate Assessment Part 4. Climate of the U.S. Great Plains*. 93.

Kurta, A. (1995). *Mammals of the Great Lakes Region* (3rd ed.). University of Michigan Press.

Lackey, J. A., Huckaby, D. G., & Ormiston, B. G. (1985). Peromyscus leucopus. *Mammalian Species*, *247*, 1–10. https://doi.org/10.2307/3503904

Lanier, H. C., Gunderson, A. M., Weksler, M., Fedorov, V. B., & Olson, L. E. (2015). Comparative Phylogeography Highlights the Double-Edged Sword of Climate Change Faced by Arctic- and Alpine-Adapted Mammals. *PLOS ONE*, *10*(3), e0118396. https://doi.org/10.1371/journal.pone.0118396

Lawing, A. M., & Polly, P. D. (2011). Pleistocene Climate, Phylogeny, and Climate Envelope Models: An Integrative Approach to Better Understand Species' Response to Climate Change. *PLOS ONE*, *6*(12), e28554. https://doi.org/10.1371/journal.pone.0028554

Le Roux, P. C., & McGeoch, M. A. (2008). Rapid range expansion and community reorganization in response to warming. *Global Change Biology*, *14*(12), 2950–2962. https://doi.org/10.1111/j.1365-2486.2008.01687.x

Liphardt, S. W., Kang, H. J., Arai, S., Gu, S. H., Cook, J. A., & Yanagihara, R. (2020). Reassortment Between Divergent Strains of Camp Ripley Virus (Hantaviridae) in the Northern Short-Tailed Shrew (Blarina brevicauda). *Frontiers in Cellular and Infection Microbiology*, *10*. https://www.frontiersin.org/article/10.3389/fcimb.2020.00460

Liu, C., Berry, P. M., Dawson, T. P., & Pearson, R. G. (2005). Selecting thresholds of occurrence in the prediction of species distributions. *Ecography*, *28*(3), 385–393. https://doi.org/10.1111/j.0906-7590.2005.03957.x

Long, A. D., Baldwin-Brown, J., Tao, Y., Cook, V. J., Balderrama-Gutierrez, G., Corbett-Detig, R., Mortazavi, A., & Barbour, A. G. (2019). The genome of Peromyscus leucopus, natural host for Lyme disease and other emerging infections. *Science Advances*, *5*(7), eaaw6441. https://doi.org/10.1126/sciadv.aaw6441

Lorenzen, E. D., Heller, R., & Siegismund, H. R. (2012). Comparative phylogeography of African savannah ungulates1. *Molecular Ecology*, *21*(15), 3656–3670. https://doi.org/10.1111/j.1365-294X.2012.05650.x

Loveless, A. M., Reding, D. M., Kapfer, P. M., & Papeş, M. (2016). Combining ecological niche modelling and morphology to assess the range-wide population genetic structure of bobcats (Lynx rufus). *Biological Journal of the Linnean Society*, *117*(4), 842–857. https://doi.org/10.1111/bij.12718

Lovette, I. (2005). Glacial cycles and the tempo of avian speciation. *Trends in Ecology & Evolution*, *20*(2), 57–59. https://doi.org/10.1016/j.tree.2004.11.011

Lurgi, M., López, B. C., & Montoya, J. M. (2012). Novel communities from climate change. *Philosophical Transactions of the Royal Society B: Biological Sciences*, *367*(1605), 2913–2922. https://doi.org/10.1098/rstb.2012.0238

Lyman, R. A., & Edwards, C. E. (2022). Revisiting the comparative phylogeography of unglaciated eastern North America: 15 years of patterns and progress. *Ecology and Evolution*, *12*(4), e8827. https://doi.org/10.1002/ece3.8827

Marbut: Soils of the United States, atlas of American... - Google Scholar. (n.d.). Retrieved May 9, 2022, from https://scholar.google.com/scholar_lookup?title=Soils%20of%20the%20United%20States%2C%20Atlas%20of%20American%20Agriculture%2C%20Part%20III&publication_year=1935&author=C.%20Marbut

Martin, L. D., & Hoffmann, R. S. (1987). *Pleistocene faunal provinces and Holocene biomes of the central Great Plains*. https://www.kgs.ku.edu/Publications/Bulletins/GB5/Martin2/

Martínez-Meyer, E., & Peterson, A. T. (2006). Conservatism of ecological niche characteristics in North American plant species over the Pleistocene-to-Recent transition. *Journal of Biogeography*, *33*(10), 1779–1789. https://doi.org/10.1111/j.1365-2699.2006.01482_33_10.x

Martínez-Meyer, E., Townsend Peterson, A., & Hargrove, W. W. (2004). Ecological niches as stable distributional constraints on mammal species, with implications for Pleistocene extinctions and climate change projections for biodiversity: Ecological niches as distributional constraints. *Global Ecology and Biogeography*, *13*(4), 305–314. https://doi.org/10.1111/j.1466-822X.2004.00107.x

McDonough, M., & Ferguson, A. (n.d.). *Phylogenomic systematics of the spotted skunks (Carnivora, Mephitidae, Spilogale): Additional species diversity and Pleistocene climate change as a major driver of diversification | bioRxiv*. Retrieved August 19, 2021, from https://www.biorxiv.org/content/10.1101/2020.10.23.353045v1.abstract

McDonough, M. M., Ferguson, A. W., Dowler, R. C., Gompper, M. E., & Maldonado, J. E. (2022). Phylogenomic systematics of the spotted skunks (Carnivora, Mephitidae, Spilogale): Additional species diversity and Pleistocene climate change as a major driver of diversification. *Molecular Phylogenetics and Evolution*, *167*, 107266. https://doi.org/10.1016/j.ympev.2021.107266

McGuire, J. L., & Davis, E. B. (2013). Using the palaeontological record of *Microtus* to test species distribution models and reveal responses to climate change. *Journal of Biogeography*, *40*(8), 1490–1500. https://doi.org/10.1111/jbi.12106

McKinney, M. L., & Lockwood, J. L. (1999). Biotic homogenization: A few winners replacing many losers in the next mass extinction. *Trends in Ecology & Evolution*, *14*(11), 450–453. https://doi.org/10.1016/S0169-5347(99)01679-1

Mengel, R. M. (1970). *The North American central plains as an isolating agent in bird speciation. Pag es 280-340 in Pleistocene and recent environ ments of the Central Great Plains (W Dort and J. K. Jones, Eds.)*. University of Kansas Press, Law rence.

Merow, C., Smith, M. J., & Silander Jr, J. A. (2013). A practical guide to MaxEnt for modeling species' distributions: What it does, and why inputs and settings matter. *Ecography*, *36*(10), 1058–1069. https://doi.org/10.1111/j.1600-0587.2013.07872.x

Miller, W. C. (1969). Ecological and Ethological Isolating Mechanisms Between Microtus pennsylvanicus and Microtus ochrogaster at Terre Haute, Indiana. *The American Midland Naturalist*, *82*(1), 140–148. https://doi.org/10.2307/2423824

Montoya, J. M., & Raffaelli, D. (2010). Climate change, biotic interactions and ecosystem services. *Philosophical Transactions of the Royal Society B: Biological Sciences*, *365*(1549), 2013–2018. https://doi.org/10.1098/rstb.2010.0114

Mooney, H. A. (1991). Biological Response to Climate Change: An Agenda for Research. *Ecological Applications*, *1*(2), 112–117. https://doi.org/10.2307/1941805

Morafka, D. J. (1977). The Physiography of the Chihuahuan Desert. In D. J. Morafka (Ed.), *A Biogeographical Analysis of the Chihuahuan Desert through its Herpetofauna* (pp. 27–38). Springer Netherlands. https://doi.org/10.1007/978-94-010-1318-5_4

Morrone, J. J., & Crisci, J. V. (1995). HISTORICAL BIOGEOGRAPHY: Introduction to Methods. *Annual Review of Ecology and Systematics*, *26*(1), 373–401. https://doi.org/10.1146/annurev.es.26.110195.002105

Nathan G. Swenson, D. J. H. (n.d.). *Clustering of Contact Zones, Hybrid Zones, and Phylogeographic Breaks in North America.* 11.

Nava-García, E., Guerrero-Enríquez, J. A., & Arellano, E. (2016). Molecular Phylogeography of Harvest Mice (Reithrodontomys megalotis) Based on Cytochrome b DNA Sequences. *Journal of Mammalian Evolution*, *23*(3), 297–307. https://doi.org/10.1007/s10914-015-9318-5

Newbold, T., Hudson, L. N., Arnell, A. P., Contu, S., De Palma, A., Ferrier, S., Hill, S. L. L., Hoskins, A. J., Lysenko, I., Phillips, H. R. P., Burton, V. J., Chng, C. W. T., Emerson, S., Gao, D., Pask-Hale, G., Hutton, J., Jung, M., Sanchez-Ortiz, K., Simmons, B. I., … Purvis, A. (2016). Has land use pushed terrestrial biodiversity beyond the planetary boundary? A global assessment. *Science*, *353*(6296), 288–291. https://doi.org/10.1126/science.aaf2201

Nordt, L., Von Fischer, J., Tieszen, L., & Tubbs, J. (2008). Coherent changes in relative C4 plant productivity and climate during the late Quaternary in the North American Great Plains. *Quaternary Science Reviews*, *27*(15), 1600–1611. https://doi.org/10.1016/j.quascirev.2008.05.008

Ottenburghs, J., Lavretsky, P., Peters, J. L., Kawakami, T., & Kraus, R. H. S. (2019). Population Genomics and Phylogeography. In R. H. S. Kraus (Ed.), *Avian Genomics in Ecology and Evolution: From the Lab into the Wild* (pp. 237–265). Springer International Publishing. https://doi.org/10.1007/978-3-030-16477-5_8

Palmer, E. (1957). Fieldbook of Mammals. *Journal of Mammalogy*, *39*(3), 461. E. P. Dutton & Co., Inc. https://doi.org/10.2307/1376182

Pandolfi, J. M. (1999). Response of Pleistocene Coral Reefs to Environmental Change Over Long Temporal Scales. *American Zoologist*, *39*(1), 113–130. https://doi.org/10.1093/icb/39.1.113

Parmesan, C. (2006). Ecological and Evolutionary Responses to Recent Climate Change. *Annual Review of Ecology, Evolution, and Systematics*, *37*(1), 637–669. https://doi.org/10.1146/annurev.ecolsys.37.091305.110100

Parmesan, C., & Yohe, G. (2003). A globally coherent fingerprint of climate change impacts across natural systems. *Nature*, *421*(6918), 37–42. https://doi.org/10.1038/nature01286

Peterson, A. T. (2009). perspective: Phylogeography is not enough: The need for multiple lines of evidence. *Frontiers of Biogeography*, *1*(1). https://doi.org/10.21425/F5FBG12232

Peterson, A. T. (2011). Ecological niche conservatism: A time-structured review of evidence. *Journal of Biogeography*, *38*(5), 817–827. https://doi.org/10.1111/j.1365-2699.2010.02456.x

Peterson, A. T., & Nyári, Á. S. (2008). Ecological Niche Conservatism and Pleistocene Refugia in the Thrush-Like Mourner, Schiffornis Sp., in the Neotropics. *Evolution*, *62*(1), 173–183. https://doi.org/10.1111/j.1558-5646.2007.00258.x

Peterson, A. T., Soberón, J., & Sánchez-Cordero, V. (1999). Conservatism of Ecological Niches in Evolutionary Time. *Science*, *285*(5431), 1265–1267. https://doi.org/10.1126/science.285.5431.1265

Peterson, G., Allen, C. R., & Holling, C. S. (n.d.). *Ecological Resilience, Biodiversity, and Scale*. 13.

Petit, J. R., Jouzel, J., Raynaud, D., Barkov, N. I., Barnola, J.-M., Basile, I., Bender, M., Chappellaz, J., Davis, M., Delaygue, G., Delmotte, M., Kotlyakov, V. M., Legrand, M.,

Lipenkov, V. Y., Lorius, C., PÉpin, L., Ritz, C., Saltzman, E., & Stievenard, M. (1999). Climate and atmospheric history of the past 420,000 years from the Vostok ice core, Antarctica. *Nature*, *399*(6735), 429–436. https://doi.org/10.1038/20859

Phillips, S. J., Anderson, R. P., Dudík, M., Schapire, R. E., & Blair, M. E. (2017). Opening the black box: An open-source release of Maxent. *Ecography*, *40*(7), 887–893. https://doi.org/10.1111/ecog.03049

Planz, J. V., Zimmerman, E. G., Spradling, T. A., & Akins, D. R. (1996). Molecular Phylogeny of the Neotoma floridana Species Group. *Journal of Mammalogy*, *77*(2), 519–535. https://doi.org/10.2307/1382826

Powell, J. W., Gilbert, G. K., Dutton, C. E., Drummond, W., & Thompson, A. H. (1879). *Report on the Lands of the Arid Region of the United States: With a More Detailed Account of the Lands of Utah: With Maps.* United States: U.S. Government Printing Office. https://www.google.com/books/edition/Report_on_the_Lands_of_the_Arid_Region_o/FcEQAAAAIAAJ?hl=en&gbpv=1&pg=PR1&printsec=frontcover

Provost, K. L., Myers, E. A., & Smith, B. T. (2021). Community phylogeographic patterns reveal how a barrier filters and structures taxa in North American warm deserts. *Journal of Biogeography*, *48*(6), 1267–1283. https://doi.org/10.1111/jbi.14115

Puckett, E. E., Etter, P. D., Johnson, E. A., & Eggert, L. S. (2015). Phylogeographic Analyses of American Black Bears (Ursus americanus) Suggest Four Glacial Refugia and Complex Patterns of Postglacial Admixture. *Molecular Biology and Evolution*, *32*(9), 2338–2350. https://doi.org/10.1093/molbev/msv114

Pyron, A. R., & Burbrink, F. T. (2010). Hard and soft allopatry: Physically and ecologically mediated modes of geographic speciation: Modes of allopatric speciation. *Journal of Biogeography*, no-no. https://doi.org/10.1111/j.1365-2699.2010.02336.x

R Core Team. (2021). *R: A language and environment for statistical computing*. R Foundation for Statistical Computing. https://www.R-project.org/

Radosavljevic, A., & Anderson, R. P. (2014). Making better Maxent models of species distributions: Complexity, overfitting and evaluation. *Journal of Biogeography*, *41*(4), 629–643. https://doi.org/10.1111/jbi.12227

Rambaut, A., & Drummond, A. (2012). FigTree: Tree figure drawing tool, v1. 4.2. *Institute of Evolutionary Biology, University of Edinburgh*.

Rambaut, A., & Drummond, A. J. (2020). *TreeAnnotator Version 1.10. 1. Computer Software and Manual. 2002–2018*.

Rambaut, A., Drummond, A. J., Xie, D., Baele, G., & Suchard, M. A. (2018). Posterior Summarization in Bayesian Phylogenetics Using Tracer 1.7. *Systematic Biology*, *67*(5), 901–904. https://doi.org/10.1093/sysbio/syy032

Ratajczak, Z., Nippert, J. B., Briggs, J. M., & Blair, J. M. (2014). Fire dynamics distinguish grasslands, shrublands and woodlands as alternative attractors in the Central Great Plains of North America. *Journal of Ecology, 102*(6), 1374–1385.

Real, R., Barbosa, A. M., & Vargas, J. M. (2006). Obtaining Environmental Favourability Functions from Logistic Regression. *Environmental and Ecological Statistics*, *13*(2), 237–245. https://doi.org/10.1007/s10651-005-0003-3

Reding, D. M., Bronikowski, A. M., Johnson, W. E., & Clark, W. R. (2012). Pleistocene and ecological effects on continental-scale genetic differentiation in the bobcat (Lynx rufus).

Molecular Ecology, *21*(12), 3078–3093. https://doi.org/10.1111/j.1365-294X.2012.05595.x

Reding, D. M., Castañeda-Rico, S., Shirazi, S., Hofman, C. A., Cancellare, I. A., Lance, S. L., Beringer, J., Clark, W. R., & Maldonado, J. E. (2021). Mitochondrial Genomes of the United States Distribution of Gray Fox (Urocyon cinereoargenteus) Reveal a Major Phylogeographic Break at the Great Plains Suture Zone. *Frontiers in Ecology and Evolution*, *9*, 666800. https://doi.org/10.3389/fevo.2021.666800

Reilly, S. M., Manning, R. W., Nice, C. C., & Forstner, M. R. J. (2005). Systematics of Isolated Populations of Short-Tailed Shrews (Soricidae: Blarina) in Texas. *Journal of Mammalogy*, *86*(5), 887–894. https://doi.org/10.1644/1545-1542(2005)86[887:SOIPOS]2.0.CO;2

Remington, C. L. (1968). Suture-Zones of Hybrid Interaction Between Recently Joined Biotas. In T. Dobzhansky, M. K. Hecht, & W. C. Steere (Eds.), *Evolutionary Biology* (pp. 321–428). Springer US. https://doi.org/10.1007/978-1-4684-8094-8_8

Richards, C. L., Carstens, B. C., & Knowles, L. L. (2007). Distribution modelling and statistical phylogeography: An integrative framework for generating and testing alternative biogeographical hypotheses. *Journal of Biogeography*, *34*(11), 1833–1845. https://doi.org/10.1111/j.1365-2699.2007.01814.x

Ricketts, T. H., Dinerstein, E., Olson, D. M., Eichbaum, W., Loucks, C. J., DellaSala, D. A., Kavanagh, K., Hedao, P., Hurley, P., Carney, K., Abell, R., & Walters, S. (1999). *Terrestrial Ecoregions of North America: A Conservation Assessment*. Island Press.

Ricklefs, R. E. (1987). Community Diversity: Relative Roles of Local and Regional Processes. *Science*, *235*(4785), 167–171.

Ricklefs, R. E., & Jenkins, D. G. (2011). Biogeography and ecology: Towards the integration of two disciplines. *Philosophical Transactions of the Royal Society B: Biological Sciences*, *366*(1576), 2438–2448. https://doi.org/10.1098/rstb.2011.0066

Riddle, B. R., & Hafner, D. J. (2006). A step-wise approach to integrating phylogeographic and phylogenetic biogeographic perspectives on the history of a core North American warm deserts biota. *Journal of Arid Environments*, *66*(3), 435–461. https://doi.org/10.1016/j.jaridenv.2006.01.014

Riddle, B. R., & Jezkova, T. (2019). How is phylogeography shaping our understanding of the geography of diversity, diversification, and range dynamics in mammals? *Journal of Mammalogy*, *100*(3), 872–893. https://doi.org/10.1093/jmammal/gyz027

Rising, J. D. (1969). A comparison of metabolism and evaporative water loss of baltimore and bullock orioles. *Comparative Biochemistry and Physiology*, *31*(6), 915–925. https://doi.org/10.1016/0010-406X(69)91801-5

Rising, J. D. (1970). Morphological Variation and Evolution in Some North American Orioles. *Systematic Zoology*, *19*(4), 315. https://doi.org/10.2307/2412275

Rising, J. D. (1983). The Great Plains Hybrid Zones. In R. F. Johnston (Ed.), *Current Ornithology* (pp. 131–157). Springer US. https://doi.org/10.1007/978-1-4615-6781-3_5

Rissler, L. J., & Smith, W. H. (2010). Mapping amphibian contact zones and phylogeographical break hotspots across the United States. *Molecular Ecology*, *19*(24), 5404–5416. https://doi.org/10.1111/j.1365-294X.2010.04879.x

Rittenour, T. M., Blum, M. D., & Goble, R. J. (2007). Fluvial evolution of the lower Mississippi River valley during the last 100 k.y. glacial cycle: Response to glaciation and sea-level

change. *Geological Society of America Bulletin*, *119*(5–6), 586–608. https://doi.org/10.1130/B25934.1

Roberts, D. R., Bahn, V., Ciuti, S., Boyce, M. S., Elith, J., Guillera-Arroita, G., Hauenstein, S., Lahoz-Monfort, J. J., Schröder, B., Thuiller, W., Warton, D. I., Wintle, B. A., Hartig, F., & Dormann, C. F. (2017). Cross-validation strategies for data with temporal, spatial, hierarchical, or phylogenetic structure. *Ecography*, *40*(8), 913–929. https://doi.org/10.1111/ecog.02881

Root, T. L., Holmgren, M. A., & Andrews, R. W. (1981). Winter Abundance Patterns of Some Songbirds near the 100th Meridian in the Southern United States. *The Southwestern Naturalist*, *26*(2), 95. https://doi.org/10.2307/3671104

Rosenberg, N. J. (1987). Climate of the Great Plains Region of The United States. *Great Plains Quarterly*, *344*, 12.

Rosenzweig, C., Casassa, G., Karoly, D. J., Imeson, A., Liu, C., Menzel, A., Rawlins, S., Root, T. L., Seguin, B., & Tryjanowski, P. (2007). *Assessment of observed changes and responses in natural and managed systems*. https://doi.org/10.5167/UZH-33180

Rowe, K. C., Heske, E. J., & Paige, K. N. (2006). Comparative phylogeography of eastern chipmunks and white-footed mice in relation to the individualistic nature of species: COMPARATIVE PHYLOGEOGRAPHY OF CHIPMUNKS AND MICE. *Molecular Ecology*, *15*(13), 4003–4020. https://doi.org/10.1111/j.1365-294X.2006.03063.x

Roy-Dufresne, E., Logan, T., Simon, J. A., Chmura, G. L., & Millien, V. (2013). Poleward Expansion of the White-Footed Mouse (Peromyscus leucopus) under Climate Change: Implications for the Spread of Lyme Disease. *PLOS ONE*, *8*(11), e80724. https://doi.org/10.1371/journal.pone.0080724

Sacks, B. N., Mitchell, K. J., Quinn, C. B., Hennelly, L. M., Sinding, M. S., Statham, M. J., Preckler-Quisquater, S., Fain, S. R., Kistler, L., Vanderzwan, S. L., Meachen, J. A., Ostrander, E. A., & Frantz, L. A. F. (2021). Pleistocene origins, western ghost lineages, and the emerging phylogeographic history of the red wolf and coyote. *Molecular Ecology*, *30*(17), 4292–4304. https://doi.org/10.1111/mec.16048

Salley, S. W., Sleezer, R. O., Bergstrom, R. M., Martin, P. H., & Kelly, E. F. (2016a). A long-term analysis of the historical dry boundary for the Great Plains of North America: Implications of climatic variability and climatic change on temporal and spatial patterns in soil moisture. *Geoderma*, *274*, 104–113. https://doi.org/10.1016/j.geoderma.2016.03.020

Salley, S. W., Sleezer, R. O., Bergstrom, R. M., Martin, P. H., & Kelly, E. F. (2016b). A long-term analysis of the historical dry boundary for the Great Plains of North America: Implications of climatic variability and climatic change on temporal and spatial patterns in soil moisture. *Geoderma*, *274*, 104–113. https://doi.org/10.1016/j.geoderma.2016.03.020

Schmidly, D. J., & Bradley, R. D. (2016). *The Mammals of Texas*. University of Texas Press.

Schmitt, T. (2007). Molecular biogeography of Europe: Pleistocene cycles and postglacial trends. *Frontiers in Zoology*, *4*(1), 11. https://doi.org/10.1186/1742-9994-4-11

Schmitz, O. J., Post, E., Burns, C. E., & Johnston, K. M. (2003). Ecosystem Responses to Global Climate Change: Moving Beyond Color Mapping. *BioScience*, *53*(12), 1199–1205. https://doi.org/10.1641/0006-3568(2003)053[1199:ERTGCC]2.0.CO;2

Schwartz, C., & Schwartz, E. (1981). The Wild Mammals of Missouri. *Columbia & London: University of Missouri Press and Missouri Department of Conservation*.

Seager, R., Lis, N., Feldman, J., Ting, M., Williams, A. P., Nakamura, J., Liu, H., & Henderson, N. (2018). Whither the 100th Meridian? The Once and Future Physical and Human Geography of America's Arid–Humid Divide. Part I: The Story So Far. *Earth Interactions*, *22*(5), 1–22. https://doi.org/10.1175/EI-D-17-0011.1

Seersholm, F. V., Werndly, D. J., Grealy, A., Johnson, T., Keenan Early, E. M., Lundelius, E. L., Winsborough, B., Farr, G. E., Toomey, R., Hansen, A. J., Shapiro, B., Waters, M. R., McDonald, G., Linderholm, A., Stafford, T. W., & Bunce, M. (2020). Rapid range shifts and megafaunal extinctions associated with late Pleistocene climate change. *Nature Communications*, *11*(1), 2770. https://doi.org/10.1038/s41467-020-16502-3

Shaffer, A. A., Dowler, R. C., Perkins, J. C., Ferguson, A. W., McDonough, M. M., & Ammerman, L. K. (2018). Genetic variation in the eastern spotted skunk (Spilogale putorius) with emphasis on the plains spotted skunk (S. p. Interrupta). *Journal of Mammalogy*, *99*(5), 1237–1248. https://doi.org/10.1093/jmammal/gyy098

Sikes, R. S., & Animal Care and Use Committee of the American Society of Mammalogists. (2016). Sikes, R.S. and Animal Care and Use Guidelines of the American Society of Mammalogists for the use of wild mammals in research and education. *Journal of Mammalogy*, *97*(3), 663–688.

Smith, M. F., & Patton, J. L. (1993). The diversification of South American murid rodents: Evidence from mitochondrial DNA sequence data for the akodontine tribe. *Biological Journal of the Linnean Society*, *50*(3), 149–177. https://doi.org/10.1111/j.1095-8312.1993.tb00924.x

Soberón, J. (2007). Grinnellian and Eltonian niches and geographic distributions of species. *Ecology Letters*, *10*(12), 1115–1123. https://doi.org/10.1111/j.1461-0248.2007.01107.x

Soberón, J. M. (2010). Niche and area of distribution modeling: A population ecology perspective. *Ecography*, *33*(1), 159–167. https://doi.org/10.1111/j.1600-0587.2009.06074.x

Soberón, J., & Peterson, T. (2004). Biodiversity informatics: Managing and applying primary biodiversity data. *Philosophical Transactions of the Royal Society of London. Series B: Biological Sciences*, *359*(1444), 689–698. https://doi.org/10.1098/rstb.2003.1439

Soltis, D. E., Morris, A. B., McLACHLAN, J. S., Manos, P. S., & Soltis, P. S. (2006). Comparative phylogeography of unglaciated eastern North America. *Molecular Ecology*, *15*(14), 4261–4293. https://doi.org/10.1111/j.1365-294X.2006.03061.x

Spencer, S. R., & Cameron, G. N. (1982). Reithrodontomys fulvescens. *Mammalian Species*, *174*, 1–7. https://doi.org/10.2307/3503795

Stalling, D. T. (1990). Microtus ochrogaster. *Mammalian Species*, *355*, 1–9. https://doi.org/10.2307/3504103

Still, C. J., Cotton, J. M., & Griffith, D. M. (2019). Assessing earth system model predictions of C4 grass cover in North America: From the glacial era to the end of this century. *Global Ecology and Biogeography*, *28*(2), 145–157. https://doi.org/10.1111/geb.12830

Svenning, J.-C., & Skov, F. (2004). Limited filling of the potential range in European tree species. *Ecology Letters*, *7*(7), 565–573. https://doi.org/10.1111/j.1461-0248.2004.00614.x

Swenson, N. (2013). Suture zones and phylogeographic concordance: Are they the same and how should we test for their existence? *Phylogeography: Concepts, Intraspecific Patterns and Speciation Processes*, 105–116.

Swenson, N. G. (2006). Gis-based niche models reveal unifying climatic mechanisms that maintain the location of avian hybrid zones in a North American suture zone. *Journal of Evolutionary Biology*, *19*(3), 717–725. https://doi.org/10.1111/j.1420-9101.2005.01066.x

Swenson, N. G., & Howard, D. J. (2004). Do Suture Zones Exist? *Evolution*, *58*(11), 2391–2397. https://doi.org/10.1111/j.0014-3820.2004.tb00869.x

Swenson, N. G., & Howard, D. J. (2005). Clustering of Contact Zones, Hybrid Zones, and Phylogeographic Breaks in North America. *The American Naturalist*, *166*(5), 581–591. https://doi.org/10.1086/491688

Swihart, R. K., & Slade, N. A. (1990). Long-term Dynamics of an Early Successional Small Mammal Community. *The American Midland Naturalist*, *123*(2), 372–382. https://doi.org/10.2307/2426565

Symstad, A. J., & Leis, S. A. (2017). Woody Encroachment in Northern Great Plains Grasslands: Perceptions, Actions, and Needs. *Natural Areas Journal*, *37*(1), 118–127. https://doi.org/10.3375/043.037.0114

Szijj, L. J. (1966). Hybridization and the Nature of the Isolating Mechanism in Sympatric Populations of Meadowlarks (Sturnella) in Ontario. *Zeitschrift Für Tierpsychologie*, *23*(6), 677–690. https://doi.org/10.1111/j.1439-0310.1966.tb01705.x

Thompson, C. W., Choate, J. R., Genoways, H. H., & Finck, E. J. (2011). Blarina hylophaga (Soricomorpha: Soricidae). *Mammalian Species*, *43*, 94–103. https://doi.org/10.1644/878.1

Toews, D. P. L., & Brelsford, A. (2012). The biogeography of mitochondrial and nuclear discordance in animals. *Molecular Ecology*, *21*(16), 3907–3930. https://doi.org/10.1111/j.1365-294X.2012.05664.x

Tufts, D. M., & Diuk-Wasser, M. A. (2018). Transplacental transmission of tick-borne Babesia microti in its natural host Peromyscus leucopus. *Parasites & Vectors*, *11*(1), 286. https://doi.org/10.1186/s13071-018-2875-8

Tylianakis, J. M., Didham, R. K., Bascompte, J., & Wardle, D. A. (2008). Global change and species interactions in terrestrial ecosystems. *Ecology Letters*, *11*(12), 1351–1363. https://doi.org/10.1111/j.1461-0248.2008.01250.x

Udvardy, M. D. F., & Papp, C. S. (1969). *Dynamic zoogeography*. Van Nostrand Reinhold.

Varela, S., Lima-Ribeiro, M. S., & Terribile, L. C. (2015). A Short Guide to the Climatic Variables of the Last Glacial Maximum for Biogeographers. *PLOS ONE*, *10*(6), e0129037. https://doi.org/10.1371/journal.pone.0129037

Violle, C., Reich, P. B., Pacala, S. W., Enquist, B. J., & Kattge, J. (2014). The emergence and promise of functional biogeography. *Proceedings of the National Academy of Sciences*, *111*(38), 13690–13696. https://doi.org/10.1073/pnas.1415442111

Vuilleumier, B. S. (1971). Pleistocene Changes in the Fauna and Flora of South America. *Science*, *173*(3999), 771–780.

Waltari, E., & Guralnick, R. P. (2009). Ecological niche modelling of montane mammals in the Great Basin, North America: Examining past and present connectivity of species across basins and ranges. *Journal of Biogeography*, *36*(1), 148–161. https://doi.org/10.1111/j.1365-2699.2008.01959.x

Waltari, E., Hijmans, R. J., Peterson, A. T., Nyári, Á. S., Perkins, S. L., & Guralnick, R. P. (2007). Locating Pleistocene Refugia: Comparing Phylogeographic and Ecological Niche Model Predictions. *PLOS ONE*, *2*(7), e563. https://doi.org/10.1371/journal.pone.0000563

Walther, G.-R., Post, E., Convey, P., Menzel, A., Parmesan, C., Hoegh-Guldberg, O., & Bairlein, F. (2002). *Ecological responses to recent climate change*. *416*, 7.

Wang, C., Hunt, E. R., Zhang, L., & Guo, H. (2013). Phenology-assisted classification of C3 and C4 grasses in the U.S. Great Plains and their climate dependency with MODIS time series. *Remote Sensing of Environment*, *138*, 90–101. https://doi.org/10.1016/j.rse.2013.07.025

Warren, D. L. (2012). In defense of 'niche modeling.' *Trends in Ecology & Evolution*, *27*(9), 497–500. https://doi.org/10.1016/j.tree.2012.03.010

Webster, W., Parnell, J., & Biggs, W. (1985). *Mammals of the Carolinas, Virginia, and Maryland*. Chapel Hill: The University of North Carolina Press.

Wiens, J. J., & Donoghue, M. J. (2004). Historical biogeography, ecology and species richness. *Trends in Ecology & Evolution*, *19*(12), 639–644. https://doi.org/10.1016/j.tree.2004.09.011

Wiley, R. (1980). *Neotoma floridana* (Vols. 1–7).

Williams, J. W., & Jackson, S. T. (2007). Novel climates, no-analog communities, and ecological surprises. *Frontiers in Ecology and the Environment*, *5*(9), 475–482. https://doi.org/10.1890/070037

Williams, J. W., Kharouba, H. M., Veloz, S., Vellend, M., McLachlan, J., Liu, Z., Otto-Bliesner, B., & He, F. (2013). The ice age ecologist: Testing methods for reserve prioritization during the last global warming: Reserve selection and the ice age ecologist. *Global Ecology and Biogeography*, *22*(3), 289–301. https://doi.org/10.1111/j.1466-8238.2012.00760.x

Willis, K. J., & Whittaker, R. J. (2002). Species Diversity—Scale Matters. *Science*, *295*(5558), 1245–1248. https://doi.org/10.1126/science.1067335

Wilson, D., & Ruff, S. (1999). *The Smithsonian Book of North American Mammals*. Smithsonian Institution Press.

Wooding, S., & Ward, R. (1997). Phylogeography and pleistocene evolution in the North American black bear. *Molecular Biology and Evolution*, *14*(11), 1096–1105. https://doi.org/10.1093/oxfordjournals.molbev.a025719

Woolhouse, M. E. J., Haydon, D. T., & Antia, R. (2005). Emerging pathogens: The epidemiology and evolution of species jumps. *Trends in Ecology & Evolution*, *20*(5), 238–244. https://doi.org/10.1016/j.tree.2005.02.009

Zink, R. M. (2002). Methods in Comparative Phylogeography, and Their Application to Studying Evolution in the North American Aridlands1. *Integrative and Comparative Biology*, *42*(5), 953–959. https://doi.org/10.1093/icb/42.5.953

Supplementary Material

Supplementary Figures

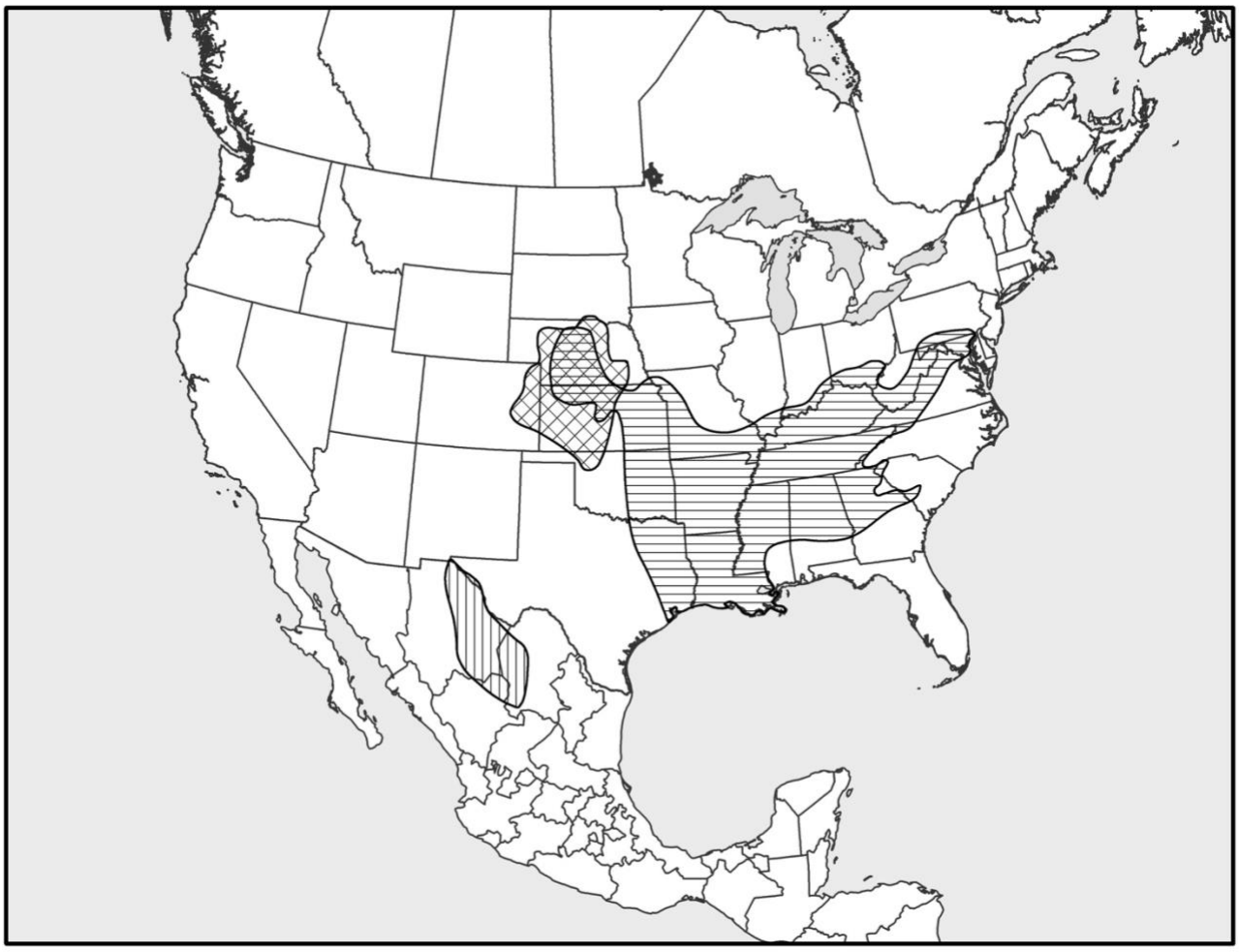

Figure S1.
Faunal element assemblage core transcribed from Armstrong, 1972. Vertical lines represent Chihuahuan faunal element. Crosshatch lines represent Campestrian faunal element. Vertical lines represent Eastern faunal element.

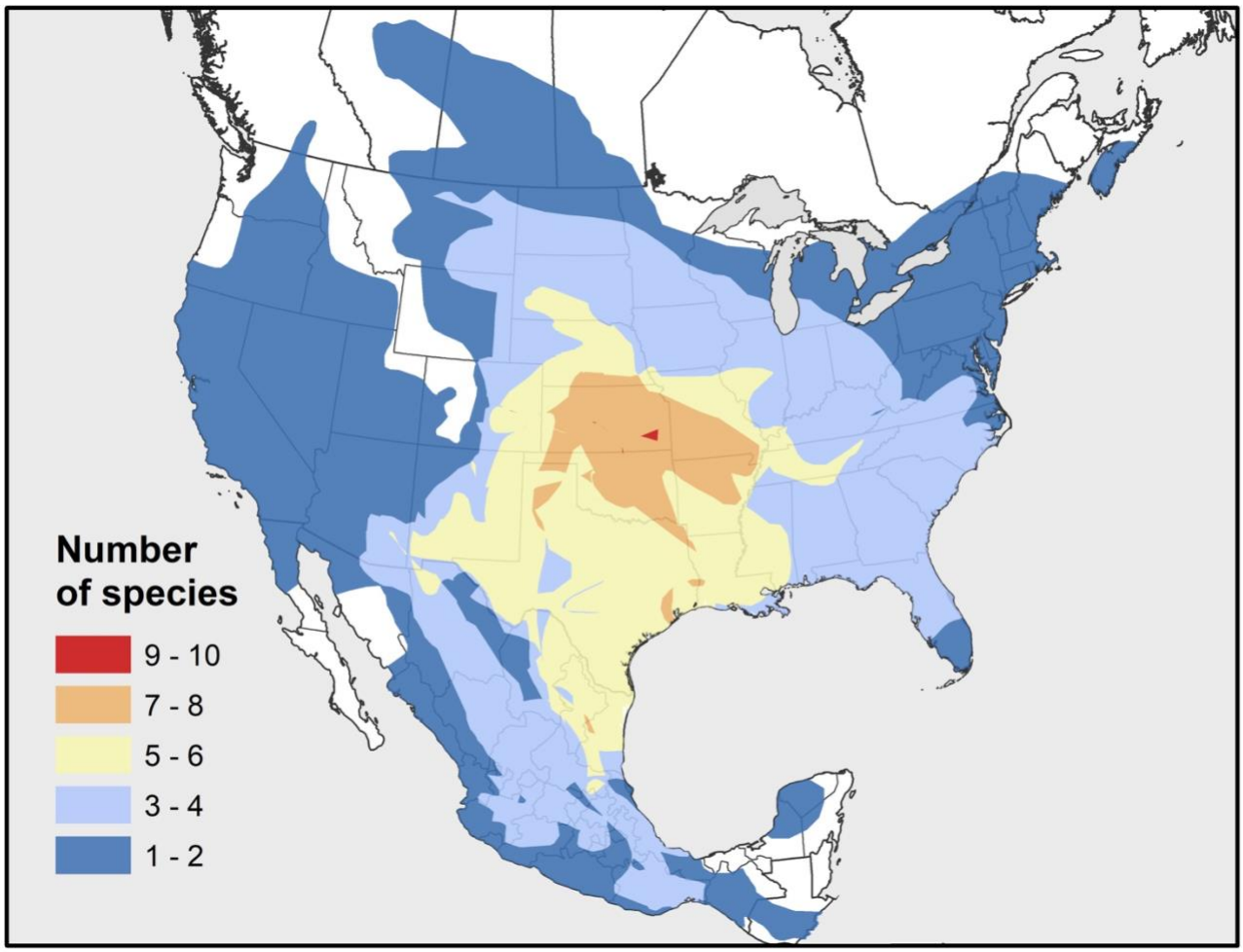

Figure S2.
Overlapping IUCN distributions for all ten species. Colors represent the number of overlapping species.

Appendix A - Supplementary Table

Table A1. *Cytb* and museum specimen appendix

List of 10 species examined and ENM metrics, including number of occurrence points, point buffer-radius used for study area (km), selected model (regularization parameter and feature class), and model selection criteria.

Species	Genbank	Museum Catalog	Tissue Identifier
Blarina hylophaga	AF395475		
Blarina hylophaga	AF395476		
Blarina hylophaga	AF395477		
Blarina hylophaga	AF395478		
Blarina hylophaga	AF395479		
Blarina hylophaga	AF395480		
Blarina hylophaga	AY546660		
Blarina hylophaga	AY546661		
Blarina hylophaga	AY546662		
Blarina hylophaga	AY546663		
Blarina hylophaga	AY546664		
Blarina hylophaga	AY546665		
Blarina hylophaga	AY546666		
Blarina hylophaga	AY546667		
Blarina hylophaga	AY546668		
Blarina hylophaga	AY546669		
Blarina hylophaga	AY546670		
Blarina hylophaga	AY546671		
Blarina hylophaga	AY546672		
Blarina hylophaga	AY546673		
Blarina hylophaga	AY546674		
Blarina hylophaga	AY546675		
Blarina hylophaga	AY546676		
Blarina hylophaga	AY546677		
Blarina hylophaga	AY546678		
Blarina hylophaga	AY546679		
Blarina hylophaga	AY546680		
Blarina hylophaga	AY546681		
Blarina hylophaga	JF912177		
Blarina hylophaga	JF912178		
Blarina hylophaga	KF735662		
Blarina hylophaga	MH801939		
Blarina hylophaga	NC_042694		
Blarina hylophaga		MSB	NK269690

Blarina hylophaga		MSB	NK306506
Chaetodipus hispidus	AF172832		
Chaetodipus hispidus	AY009247		
Chaetodipus hispidus	AY926391		
Chaetodipus hispidus	JQ411944		
Chaetodipus hispidus	JQ411945		
Chaetodipus hispidus	JQ411946		
Chaetodipus hispidus	JQ411947		
Chaetodipus hispidus	JQ411948		
Chaetodipus hispidus	JQ411949		
Chaetodipus hispidus	JQ411950		
Chaetodipus hispidus	JQ411951		
Chaetodipus hispidus	JQ411952		
Chaetodipus hispidus	JQ411953		
Chaetodipus hispidus	JQ411954		
Chaetodipus hispidus	JQ411955		
Chaetodipus hispidus	JQ411956		
Chaetodipus hispidus	JQ411957		
Chaetodipus hispidus	JQ411958		
Chaetodipus hispidus	JQ411959		
Chaetodipus hispidus	JQ411960		
Chaetodipus hispidus	JQ411961		
Chaetodipus hispidus	JQ411962		
Chaetodipus hispidus	JQ411963		
Chaetodipus hispidus	JQ411964		
Chaetodipus hispidus	JQ411965		
Chaetodipus hispidus	JQ411966		
Chaetodipus hispidus	JQ411967		
Chaetodipus hispidus	JQ411968		
Chaetodipus hispidus	JQ411969		
Chaetodipus hispidus	JQ411970		
Chaetodipus hispidus	JQ411971		
Chaetodipus hispidus	JQ411972		
Chaetodipus hispidus	JQ411973		
Chaetodipus hispidus	JQ411974		
Chaetodipus hispidus	JQ411975		
Chaetodipus hispidus	JQ411976		
Chaetodipus hispidus	JQ411977		
Chaetodipus hispidus	JQ411978		
Chaetodipus hispidus	JQ411979		
Chaetodipus hispidus	JQ411980		

Chaetodipus hispidus	JQ411981		
Chaetodipus hispidus	JQ411982		
Chaetodipus hispidus	JQ411983		
Chaetodipus hispidus	JQ411984		
Chaetodipus hispidus	JQ411985		
Chaetodipus hispidus	JQ411986		
Chaetodipus hispidus	JQ411987		
Chaetodipus hispidus	JQ411988		
Chaetodipus hispidus	JQ411989		
Chaetodipus hispidus	JQ411990		
Chaetodipus hispidus	JQ411992		
Chaetodipus hispidus	JQ411994		
Chaetodipus hispidus	JQ412000		
Chaetodipus hispidus	JQ412003		
Chaetodipus hispidus		MSB	NK306049
Chaetodipus hispidus		MSB	NK306161
Cryptotis berlandieri		ASNHC:Mamm:13679	
Cryptotis berlandieri		MSB	NK305214
Cryptotis parvus	AB175135		
Cryptotis parvus	AF395483		
Cryptotis parvus	AF395484		
Cryptotis parvus		ASNHC:Mamm:11116	
Cryptotis parvus		ASNHC:Mamm:12494	
Cryptotis parvus		ASNHC:Mamm:13501	
Cryptotis parvus		ASNHC:Mamm:13502	
Cryptotis parvus		ASNHC:Mamm:14356	
Cryptotis parvus		ASNHC:Mamm:8191	
Cryptotis parvus		ASNHC:Mamm:8192	
Cryptotis parvus		DMNS:Mamm:16603	
Cryptotis parvus		DMNS:Mamm:19752	
Cryptotis parvus		DMNS:Mamm:9689	
Cryptotis parvus		MSB:Mamm:329914	ET203
Cryptotis parvus		MSB:Mamm:329915	ET207
Cryptotis parvus		MSB	ET460
Cryptotis parvus		MSB:Mamm:329916	ET465
Cryptotis parvus		MSB:Mamm:329884	FT640
Cryptotis parvus		MSB:Mamm:329885	FT641
Cryptotis parvus		MSB:Mamm:329886	FT642
Cryptotis parvus		MSB:Mamm:329888	FT644
Cryptotis parvus		MSB:Mamm:329889	FT645
Cryptotis parvus		MSB:Mamm:329890	FT646

Cryptotis parvus		MSB:Mamm:329891	FT647
Cryptotis parvus		MSB:Mamm:329892	FT648
Cryptotis parvus		MSB:Mamm:329894	FT650
Cryptotis parvus		MSB:Mamm:329896	FT652
Cryptotis parvus		MSB:Mamm:329898	FT654
Cryptotis parvus		MSB:Mamm:329904	FT660
Cryptotis parvus	KT876866		
Cryptotis parvus	KT876867		
Cryptotis parvus	KT876868		
Cryptotis parvus	KT876869		
Cryptotis parvus		LSUMZ:Mamm:25419	
Cryptotis parvus		LSUMZ:Mamm:28942	
Cryptotis parvus		LSUMZ:Mamm:29128	
Cryptotis parvus		LSUMZ:Mamm:29129	
Cryptotis parvus	MF158114		
Cryptotis parvus		MSB:Mamm:196185	
Cryptotis parvus		MSB:Mamm:271238	
Cryptotis parvus		MSB:Mamm:271289	
Cryptotis parvus		MSB:Mamm:271290	
Cryptotis parvus		MSB:Mamm:271323	
Cryptotis parvus		MSB:Mamm:271324	
Cryptotis parvus		MSB:Mamm:271654	
Cryptotis parvus		MSB:Mamm:271655	
Cryptotis parvus		MSB:Mamm:305705	
Cryptotis parvus		MSB:Mamm:305706	
Cryptotis parvus		MSB:Mamm:305710	
Cryptotis parvus		MSB:Mamm:310263	
Cryptotis parvus		TCWC:Mamm:63771	
Cryptotis parvus		MSB	NK296148
Cryptotis parvus		MSB	NK296149
Cryptotis parvus		MSB	NK296152
Cryptotis parvus		MSB	NK305195
Cryptotis parvus		MSB	NK305196
Cryptotis parvus		MSB	NK305197
Cryptotis parvus		MSB	NK305198
Cryptotis parvus		MSB	NK305199
Cryptotis parvus		MSB	NK305200
Cryptotis parvus		MSB	NK305202
Cryptotis parvus		MSB	NK305204
Cryptotis parvus		MSB	NK305205
Cryptotis parvus		MSB	NK305206

Cryptotis parvus		MSB	NK305207
Cryptotis parvus		MSB	NK305208
Cryptotis parvus		MSB	NK305209
Cryptotis parvus		MSB	NK305210
Cryptotis parvus		MSB	NK305211
Cryptotis parvus		MSB	NK305213
Cryptotis parvus		MSB	NK306132
Cryptotis parvus		MSB	NK306133
Cryptotis parvus		MSB	NK306166
Cryptotis parvus		MSB	NK306167
Cryptotis parvus		MSB	NK306540
Cryptotis parvus		MSB	NK306951
Cryptotis parvus		MSB	NK306952
Cryptotis parvus		MSB	NK306953
Cryptotis parvus		MSB	NK306954
Cryptotis parvus		MSB	NK306956
Cryptotis parvus		MSB	NK306957
Cryptotis parvus		MSB	NK306958
Cryptotis parvus		MSB	NK306959
Cryptotis parvus		MSB	NK306960
Cryptotis parvus		MSB	NK307135
Cryptotis parvus floridanus		UF:Mamm:31133	
Cryptotis parvus floridanus		UF:Mamm:31353	
Cryptotis parvus floridanus		UF:Mamm:31660	
Cryptotis parvus floridanus		UF:Mamm:31663	
Cryptotis parvus floridanus		UF:Mamm:33456	
Cryptotis parvus floridanus		UF:Mamm:33459	
Cryptotis parvus floridanus		UF:Mamm:33466	
Cryptotis parvus floridanus		UF:Mamm:33470	
Cryptotis parvus floridanus		UF:Mamm:33471	
Cryptotis parvus floridanus		UF:Mamm:33476	
Cryptotis parvus floridanus		UF:Mamm:33519	
Microtus ochrogaster	AF163901		
Microtus ochrogaster	DQ432006		
Microtus ochrogaster	DQ432008		
Microtus ochrogaster	KY754041		
Microtus ochrogaster	MT259132		
Microtus ochrogaster	MT259134		
Microtus ochrogaster	MT259135		
Microtus ochrogaster	MT259136		
Microtus ochrogaster	MT259137		

Microtus ochrogaster	MT259138		
Microtus ochrogaster	MT259139		
Microtus ochrogaster	MT259140		
Microtus ochrogaster	MT259142		
Microtus ochrogaster	MT259143		
Microtus ochrogaster	MT259147		
Microtus ochrogaster	MT259148		
Microtus ochrogaster	MT259149		
Microtus ochrogaster		MSB	NK234472
Microtus ochrogaster		MSB	NK269952
Microtus ochrogaster		MSB	NK269956
Microtus ochrogaster		MSB	NK304845
Microtus ochrogaster		MSB	NK306231
Microtus ochrogaster		MSB	NK306232
Microtus ochrogaster		MSB	NK306247
Neotoma floridana	AF186818		
Neotoma floridana	AF186819		
Neotoma floridana	AF294333		
Neotoma floridana	AF294334		
Neotoma floridana	AF294335		
Neotoma floridana	AF294339		
Neotoma floridana	AF294340		
Neotoma floridana	AF294343		
Neotoma floridana	AF294344		
Neotoma floridana	DQ179819		
Neotoma floridana	DQ179820		
Neotoma floridana	DQ179821		
Neotoma floridana	DQ179854		
Neotoma floridana	KY754059		
Neotoma floridana		MSB	NK269965
Neotoma floridana		MSB	NK296264
Neotoma floridana		MSB	NK306007
Neotoma floridana		MSB	NK306008
Neotoma floridana		MSB	NK306015
Neotoma floridana		MSB	NK306214
Neotoma floridana		MSB	NK306532
Neotoma floridana		MSB	NK306547
Neotoma floridana		MSB	NK306576
Neotoma floridana		MSB	NK306725
Neotoma micropus	AF186822		
Neotoma micropus	AF186825		

Neotoma micropus	AF186826		
Neotoma micropus	AF298845		
Neotoma micropus	AF376473		
Neotoma micropus	AF376474		
Neotoma micropus	DQ179818		
Neotoma micropus	DQ179848		
Neotoma micropus	DQ179849		
Neotoma micropus	DQ179850		
Neotoma micropus	EF989952		
Neotoma micropus	EF989953		
Neotoma micropus	EU286808		
Neotoma micropus	FJ716217		
Neotoma micropus	FJ716220		
Neotoma micropus	FJ716221		
Neotoma micropus	KC153472		
Neotoma micropus	KC153473		
Neotoma micropus	KC153474		
Neotoma micropus	KC153475		
Neotoma micropus	KC153476		
Neotoma micropus	KC153477		
Neotoma micropus	KC153478		
Neotoma micropus	KC153479		
Neotoma micropus	KC153480		
Neotoma micropus	KC153481		
Neotoma micropus	KC153482		
Neotoma micropus	KC153485		
Neotoma micropus	KC153486		
Neotoma micropus	KC153487		
Neotoma micropus	KC153488		
Neotoma micropus	KC812730		
Neotoma micropus	KY754063		
Neotoma micropus	MK253562		
Neotoma micropus	MK253563		
Neotoma micropus	MK253566		
Neotoma micropus		MSB	NK305240
Neotoma micropus		MSB	NK306111
Neotoma micropus		MSB	NK306162
Neotoma micropus		MSB	NK306163
Neotoma micropus		MSB	NK307103
Peromyscus leucopus	AF131926		
Peromyscus leucopus	AY041198		

Peromyscus leucopus	AY263615
Peromyscus leucopus	AY859474
Peromyscus leucopus	BK010700
Peromyscus leucopus	DQ000483
Peromyscus leucopus	DQ861376
Peromyscus leucopus	DQ973104
Peromyscus leucopus	EF989979
Peromyscus leucopus	KJ810666
Peromyscus leucopus	KX784130
Peromyscus leucopus	KX784131
Peromyscus leucopus	KX784132
Peromyscus leucopus	KX784133
Peromyscus leucopus	KX784134
Peromyscus leucopus	KX784135
Peromyscus leucopus	KX784136
Peromyscus leucopus	KX784137
Peromyscus leucopus	KX784138
Peromyscus leucopus	KX784139
Peromyscus leucopus	KX784140
Peromyscus leucopus	KX784141
Peromyscus leucopus	KX784142
Peromyscus leucopus	KX784143
Peromyscus leucopus	KX784144
Peromyscus leucopus	KX784145
Peromyscus leucopus	KX784146
Peromyscus leucopus	KX784147
Peromyscus leucopus	KX784148
Peromyscus leucopus	KX784149
Peromyscus leucopus	KX784150
Peromyscus leucopus	KX784151
Peromyscus leucopus	KX784152
Peromyscus leucopus	KX784153
Peromyscus leucopus	KX784154
Peromyscus leucopus	KX784155
Peromyscus leucopus	KX784156
Peromyscus leucopus	KX784157
Peromyscus leucopus	KX784158
Peromyscus leucopus	KX784159
Peromyscus leucopus	KX784160
Peromyscus leucopus	KX784161
Peromyscus leucopus	KX784162

Peromyscus leucopus	KX784163		
Peromyscus leucopus	KX784164		
Peromyscus leucopus	KX784165		
Peromyscus leucopus	KX784166		
Peromyscus leucopus	KY064165		
Peromyscus leucopus	KY064166		
Peromyscus leucopus	KY754106		
Peromyscus leucopus	MF589853		
Peromyscus leucopus	MG674646		
Peromyscus leucopus	MG674647		
Peromyscus leucopus	MG674648		
Peromyscus leucopus	MH256659		
Peromyscus leucopus	MK410314		
Peromyscus leucopus	MN124383		
Peromyscus leucopus	X89790		
Peromyscus leucopus		MSB	NK296346
Peromyscus leucopus		MSB	NK296414
Peromyscus leucopus		MSB	NK305068
Peromyscus leucopus		MSB	NK305999
Peromyscus leucopus		MSB	NK306036
Peromyscus leucopus		MSB	NK306136
Peromyscus leucopus		MSB	NK306178
Peromyscus leucopus		MSB	NK306193
Peromyscus leucopus		MSB	NK306194
Peromyscus leucopus		MSB	NK306205
Peromyscus leucopus		MSB	NK306250
Peromyscus leucopus		MSB	NK306543
Peromyscus leucopus		MSB	NK306544
Peromyscus leucopus		MSB	NK306564
Peromyscus leucopus		MSB	NK306565
Peromyscus leucopus		MSB	NK306709
Peromyscus leucopus		MSB	NK306713
Peromyscus leucopus		MSB	NK306737
Reithrodontomys fulvescens	AY294626		
Reithrodontomys fulvescens	EF990001		
Reithrodontomys fulvescens	EF990002		
Reithrodontomys fulvescens	EF990003		
Reithrodontomys fulvescens	KF303328		
Reithrodontomys fulvescens	KF303329		
Reithrodontomys fulvescens	KF303330		
Reithrodontomys fulvescens	KF303331		

Reithrodontomys fulvescens	KF303332		
Reithrodontomys fulvescens	KF303333		
Reithrodontomys fulvescens	KF303334		
Reithrodontomys fulvescens	KF303335		
Reithrodontomys fulvescens	KF303336		
Reithrodontomys fulvescens	KF303337		
Reithrodontomys fulvescens		MSB	NK306662
Reithrodontomys fulvescens		MSB	NK306688
Reithrodontomys fulvescens		MSB	NK306689
Reithrodontomys fulvescens		MSB	NK306720
Reithrodontomys megalotis	AB618724		
Reithrodontomys megalotis	AB618725		
Reithrodontomys megalotis	AF108707		
Reithrodontomys megalotis	AF176248		
Reithrodontomys megalotis	AF176249		
Reithrodontomys megalotis	AY859468		
Reithrodontomys megalotis	EF990008		
Reithrodontomys megalotis	EF990009		
Reithrodontomys megalotis	HQ269731		
Reithrodontomys megalotis	HQ269732		
Reithrodontomys megalotis	KP788717		
Reithrodontomys megalotis	KP788718		
Reithrodontomys megalotis	KP788719		
Reithrodontomys megalotis	KP788720		
Reithrodontomys megalotis	KP788721		
Reithrodontomys megalotis	KP788722		
Reithrodontomys megalotis	KP788723		
Reithrodontomys megalotis	KP788724		
Reithrodontomys megalotis	KP788725		
Reithrodontomys megalotis	KP788726		
Reithrodontomys megalotis	KP788727		
Reithrodontomys megalotis	KP788728		
Reithrodontomys megalotis	KP788729		
Reithrodontomys megalotis	KP788730		
Reithrodontomys megalotis	KP788731		
Reithrodontomys megalotis	KP788732		
Reithrodontomys megalotis	KP788733		
Reithrodontomys megalotis	KP788734		
Reithrodontomys megalotis	KP788735		
Reithrodontomys megalotis	KP788736		
Reithrodontomys megalotis	KP788737		

Reithrodontomys megalotis	KP788738
Reithrodontomys megalotis	KP788739
Reithrodontomys megalotis	KP788740
Reithrodontomys megalotis	KP788741
Reithrodontomys megalotis	KP788742
Reithrodontomys megalotis	KP788743
Reithrodontomys megalotis	KP788744
Reithrodontomys megalotis	KP788745
Reithrodontomys megalotis	KP788746
Reithrodontomys megalotis	KP788747
Reithrodontomys megalotis	KP788748
Reithrodontomys megalotis	KP788749
Reithrodontomys megalotis	KP788750
Reithrodontomys megalotis	KP788751
Reithrodontomys megalotis	KP788752
Reithrodontomys megalotis	KP788753
Reithrodontomys megalotis	KP788754
Reithrodontomys megalotis	KP788755
Reithrodontomys megalotis	KP788756
Reithrodontomys megalotis	KP788757
Reithrodontomys megalotis	KP788758
Reithrodontomys megalotis	KP788759
Reithrodontomys megalotis	KR611927
Reithrodontomys megalotis	KR611928
Reithrodontomys megalotis	KR611929
Reithrodontomys megalotis	KR611930
Reithrodontomys megalotis	KR611931
Reithrodontomys megalotis	KR611932
Reithrodontomys megalotis	KR611933
Reithrodontomys megalotis	KR611934
Reithrodontomys megalotis	KR611935
Reithrodontomys megalotis	KR611936
Reithrodontomys megalotis	KR611937
Reithrodontomys megalotis	KR611938
Reithrodontomys megalotis	KR611939
Reithrodontomys megalotis	KR611940
Reithrodontomys megalotis	KR611941
Reithrodontomys megalotis	KR611942
Reithrodontomys megalotis	KR611943
Reithrodontomys megalotis	KR611944
Reithrodontomys megalotis	KR611945

Reithrodontomys megalotis	KU532163		
Reithrodontomys megalotis	KU532164		
Reithrodontomys megalotis	KU532165		
Reithrodontomys megalotis	KU532166		
Reithrodontomys megalotis	KU532167		
Reithrodontomys megalotis	KU532168		
Reithrodontomys megalotis	KU532169		
Reithrodontomys megalotis	KU532170		
Reithrodontomys megalotis	KU532171		
Reithrodontomys megalotis	KU532172		
Reithrodontomys megalotis	KU532173		
Reithrodontomys megalotis	KY754136		
Reithrodontomys megalotis		MSB	NK305178
Reithrodontomys megalotis		MSB	NK306011
Reithrodontomys megalotis		MSB	NK306035
Reithrodontomys megalotis		MSB	NK306044
Reithrodontomys megalotis		MSB	NK306052
Reithrodontomys megalotis		MSB	NK306150
Reithrodontomys megalotis		MSB	NK306168
Sigmodon hispidus	AF155414		
Sigmodon hispidus	AF155415		
Sigmodon hispidus	AF155420		
Sigmodon hispidus	AF155421		
Sigmodon hispidus	AF188198		
Sigmodon hispidus	AF425199		
Sigmodon hispidus	AF425201		
Sigmodon hispidus	AF425202		
Sigmodon hispidus	AF425203		
Sigmodon hispidus	AF425204		
Sigmodon hispidus	AF425205		
Sigmodon hispidus	AF425206		
Sigmodon hispidus	AF425207		
Sigmodon hispidus	AF425208		
Sigmodon hispidus	AF425209		
Sigmodon hispidus	AF425210		
Sigmodon hispidus	AF425211		
Sigmodon hispidus	AF425212		
Sigmodon hispidus	AF425213		
Sigmodon hispidus	AF425214		
Sigmodon hispidus	AF425227		
Sigmodon hispidus	AF435110		

Sigmodon hispidus	AY041202
Sigmodon hispidus	DQ644040
Sigmodon hispidus	DQ644044
Sigmodon hispidus	DQ644045
Sigmodon hispidus	DQ644047
Sigmodon hispidus	DQ644048
Sigmodon hispidus	DQ644049
Sigmodon hispidus	DQ644051
Sigmodon hispidus	DQ644052
Sigmodon hispidus	DQ644053
Sigmodon hispidus	DQ644054
Sigmodon hispidus	DQ644056
Sigmodon hispidus	DQ644059
Sigmodon hispidus	DQ644060
Sigmodon hispidus	DQ644061
Sigmodon hispidus	DQ644062
Sigmodon hispidus	DQ644063
Sigmodon hispidus	DQ644064
Sigmodon hispidus	DQ644065
Sigmodon hispidus	DQ644066
Sigmodon hispidus	DQ644067
Sigmodon hispidus	DQ644068
Sigmodon hispidus	DQ644070
Sigmodon hispidus	DQ644072
Sigmodon hispidus	DQ644074
Sigmodon hispidus	DQ644076
Sigmodon hispidus	DQ644077
Sigmodon hispidus	DQ644078
Sigmodon hispidus	DQ644079
Sigmodon hispidus	DQ644080
Sigmodon hispidus	DQ644081
Sigmodon hispidus	DQ644082
Sigmodon hispidus	DQ644083
Sigmodon hispidus	DQ644084
Sigmodon hispidus	DQ644085
Sigmodon hispidus	DQ644086
Sigmodon hispidus	DQ644087
Sigmodon hispidus	DQ644088
Sigmodon hispidus	DQ644089
Sigmodon hispidus	DQ644090
Sigmodon hispidus	DQ644091

Sigmodon hispidus	DQ644092
Sigmodon hispidus	DQ644093
Sigmodon hispidus	DQ644094
Sigmodon hispidus	DQ644096
Sigmodon hispidus	DQ644097
Sigmodon hispidus	DQ644098
Sigmodon hispidus	DQ644099
Sigmodon hispidus	DQ644101
Sigmodon hispidus	DQ644104
Sigmodon hispidus	DQ644105
Sigmodon hispidus	DQ644106
Sigmodon hispidus	DQ644110
Sigmodon hispidus	DQ644111
Sigmodon hispidus	DQ644114
Sigmodon hispidus	DQ644117
Sigmodon hispidus	DQ644121
Sigmodon hispidus	DQ644123
Sigmodon hispidus	DQ644124
Sigmodon hispidus	DQ644127
Sigmodon hispidus	EU073177
Sigmodon hispidus	EU293740
Sigmodon hispidus	EU293741
Sigmodon hispidus	EU293742
Sigmodon hispidus	EU293743
Sigmodon hispidus	EU293744
Sigmodon hispidus	EU293748
Sigmodon hispidus	EU293749
Sigmodon hispidus	EU293755
Sigmodon hispidus	EU293756
Sigmodon hispidus	FJ232944
Sigmodon hispidus	FJ232945
Sigmodon hispidus	HQ290325
Sigmodon hispidus	HQ290329
Sigmodon hispidus	HQ290334
Sigmodon hispidus	HQ290335
Sigmodon hispidus	HQ290336
Sigmodon hispidus	HQ290341
Sigmodon hispidus	HQ290342
Sigmodon hispidus	HQ290345
Sigmodon hispidus	HQ290347
Sigmodon hispidus	HQ290348

Sigmodon hispidus	HQ326702		
Sigmodon hispidus	HQ326705		
Sigmodon hispidus	HQ326707		
Sigmodon hispidus	HQ326711		
Sigmodon hispidus	HQ326712		
Sigmodon hispidus	JX133806		
Sigmodon hispidus	JX133807		
Sigmodon hispidus	JX133808		
Sigmodon hispidus	JX133810		
Sigmodon hispidus	JX133811		
Sigmodon hispidus	JX133812		
Sigmodon hispidus	JX133813		
Sigmodon hispidus	JX133814		
Sigmodon hispidus	JX133815		
Sigmodon hispidus	JX133816		
Sigmodon hispidus	JX133817		
Sigmodon hispidus	KX866980		
Sigmodon hispidus	KX866981		
Sigmodon hispidus	KY707311		
Sigmodon hispidus		MSB	NK234469
Sigmodon hispidus		MSB	NK234470
Sigmodon hispidus		MSB	NK269903
Sigmodon hispidus		MSB	NK306014
Sigmodon hispidus		MSB	NK306098
Sigmodon hispidus		MSB	NK306112
Sigmodon hispidus		MSB	NK306115
Sigmodon hispidus		MSB	NK306183
Sigmodon hispidus		MSB	NK306548
Sigmodon hispidus		MSB	NK306573
Sigmodon hispidus		MSB	NK306577
Sigmodon hispidus		MSB	NK306707
Sigmodon hispidus		MSB	NK306721
Sigmodon hispidus		MSB	NK306727
Sigmodon hispidus		MSB	NK306735
Sigmodon hispidus		MSB	NK306751
Sigmodon hispidus		MSB	NK306753
Sigmodon hispidus		MSB	NK306764